



UNIVERSITAT ROVIRA I VIRGILI  
Departament de Química Analítica  
i Química Orgànica

## **RESINAS EPOXI Y BENZOXAZINAS FOSFORADAS Y SILILADAS RETARDANTES A LA LLAMA**



*Memoria presentada por Marisa Elisabet Spontón para optar al grado de  
Doctor por la Universitat Rovira i Virgili*

*Tarragona, Octubre 2008*

UNIVERSITAT ROVIRA I VIRGILI  
RESINAS EPOXI Y BENZOXAZINAS FOSFORADAS Y SILILADAS RETARDANTES A LA LLAMA  
Marisa Elisabet Spontón  
ISBN:978-84-691-9480-5/DL:T-22-2009



Virginia Cádiz Deleito, Catedrática de Universidad, y Marina Galià Clua, Profesora Titular de Universidad, del Departament de Química Analítica i Química Orgànica de la Facultat de Química de la Universitat Rovira i Virgili.

Hacen constar:

Que la presente tesis doctoral, titulada “Resinas epoxi y benzoxazinas fosforadas y sililadas retardantes a la llama” presentada por Marisa Elisabet Spontón para optar el grado de doctor por la Universitat Rovira i Virgili ha sido realizada bajo nuestra dirección, en el área de Química Orgànica del Departament de Química Analítica i Química Orgànica, y que todos los resultados obtenidos son fruto de las experiencias realizadas por la mencionada doctoranda.

Tarragona, Octubre 2008.

Virginia Cádiz Deleito

Marina Galià Clua

UNIVERSITAT ROVIRA I VIRGILI  
RESINAS EPOXI Y BENZOXAZINAS FOSFORADAS Y SILILADAS RETARDANTES A LA LLAMA  
Marisa Elisabet Spontón  
ISBN:978-84-691-9480-5/DL:T-22-2009

*Me gustaría expresar mis sinceros agradecimientos a las personas que contribuyeron a esta tesis:*

*En primer lugar quiero agradecer a las Dras Virginia Cádiz y Marina Galà por ser mi mayor soporte en esta tesis: por su paciencia, comprensión, ánimo, consejos, dedicación, y el aporte de soluciones durante estos cuatro años. Y también mi gratitud al Dr Juan Carlos Ronda por su disponibilidad incondicional de ayudar y aconsejar.*

*Mi gratitud al resto de los Dres del área: Àngels Serra, Toni Reina, Ana Mantecón, Sergio Castellón, Yolanda Díaz y Maribel Matheu por su disponibilidad.*

*Enrique (Quike), Lucas, David, Mercè, Silvana, Vanessa y Mireia. Gracias por todos los momentos compartidos y por brindarme su amistad. También mi gratitud a Gerard, Luis Adolfo, David, Omar, Miguel, Roser, Nuria y Andrea, por su ayuda y apoyo en mis primeros años de tesis. Sobre todo quiero agradecer especialmente a dos personas, en primer lugar a Marta por todos los momentos que hemos vivido durante estos años llenos de sentimientos y pensamientos compartidos, sueños, risas y lágrimas, y sobre todo, amistad. A Robert por su disponibilidad, por compartir sus conocimientos y también por su amistad. Cada apreciado segundo quedará atesorado en mi corazón.*

*Pablo, gracias por tu espera y confianza, por demostrar tu preocupación por mí, escuchar mis problemas y ayudarme a buscarles solución y sobre todo por mostrar tu amor e iluminar mi vida.*

*Finalmente a mis padres y hermanos por su apoyo incondicional y afecto que me han dado fuerzas para recorrer este camino. También mi gratitud a Rubén y Estela por su apoyo constante y por sus consejos.*

UNIVERSITAT ROVIRA I VIRGILI  
RESINAS EPOXI Y BENZOXAZINAS FOSFORADAS Y SILILADAS RETARDANTES A LA LLAMA  
Marisa Elisabet Spontón  
ISBN:978-84-691-9480-5/DL:T-22-2009

## CAPÍTULO 1- Introducción

|                                   |    |
|-----------------------------------|----|
| 1.1 Materiales poliméricos        | 3  |
| 1.2 Combustión de los polímeros   | 5  |
| 1.3 Retardantes a la llama        | 7  |
| 1.4 Tests de retardancia al fuego | 15 |
| 1.5 Objetivo general              | 17 |

## CAPÍTULO 2- Síntesis y caracterización de resinas epoxi fosforadas y/o sililadas

|   |    |
|---|----|
| 2.1 Resinas epoxi retardantes a la llama  | 21 |
| 2.2 Objetivos   | 30 |
| 2.3 Parte experimental y resultados   | 30 |
| 2.3.1 Flame retardant epoxy resins based on diglycidyl ether of (2,5-dihydroxyphenyl)diphenyl phosphine oxide | 35 |
| 2.3.2 Preparation, thermal properties and flame retardancy of phosphorus- and silicon-containing epoxy resins | 57 |

## CAPÍTULO 3- Síntesis y caracterización de sistemas benzoxazina y benzoxazina-epoxi fosforados o sililados

|   |    |
|---|----|
| 3.1 Polibenzoxazinas                        | 83 |
| 3.2 Benzoxazinas polifuncionales            | 91 |
| 3.3 Copolimerización de benzoxazinas        | 93 |
| 3.4 Polibenzoxazinas retardantes a la llama | 94 |
| 3.5 Degradación térmica de polibenzoxazinas | 96 |

|  |     |
|--|-----|
| 3.6 Objetivos  | 98  |
| 3.7 Parte experimental y resultados  | 98  |
| 3.7.1 Synthesis and study of the thermal crosslinking of<br>Bis (m-aminophenyl) methylphosphine oxide based benzoxazine  | 103 |
| 3.7.2 Studies on thermal and flame retardant behaviour of<br>mixtures of bis (m-aminophenyl)methylphosphine oxide based<br>benzoxazine and glycidylether or benzoxazine of bisphenol A | 129 |
| 3.7.3 Development of flame retardant phosphorus- and<br>silicon- containing polybenzoxazines   | 153 |

## CAPÍTULO 4- Estudio de retardancia a la llama de sistemas benzoxazina-epoxi fosforados y sililados mediante calorimetría de cono

|  |     |
|--|-----|
| 4.1 Introducción   | 177 |
| 4.2 Objetivos  | 181 |
| 4.3 Parte experimental y resultados  | 181 |
| 4.3.1 Cone calorimetry studies of benzoxazine-epoxy systems<br>flame retarded by chemically bonded phosphorus or silicon | 185 |

|              |     |
|--------------|-----|
| CONCLUSIONES | 201 |
|--------------|-----|

## APÉNDICE A

|              |     |
|--------------|-----|
| Abreviaturas | 203 |
|--------------|-----|

## APÉNDICE B

|                        |     |
|------------------------|-----|
| Lista de publicaciones | 205 |
|------------------------|-----|



# CAPÍTULO 1

## Introducción

---

*Los materiales poliméricos sintéticos y/o naturales aportan numerosas ventajas a la sociedad en la vida cotidiana, pero la mayoría de ellos en presencia de una fuente de calor y de oxígeno se queman fácil y rápidamente. Este trabajo plantea el estudio de nuevos sistemas poliméricos termoestables resistentes al fuego. En este capítulo se enmarca su interés y se exponen los objetivos concretos del trabajo.*

---

- 1.1 Materiales poliméricos
- 1.2 Combustión de los polímeros
- 1.3 Retardantes a la llama
- 1.4 Tests de retardancia al fuego
- 1.5 Objetivos generales

UNIVERSITAT ROVIRA I VIRGILI  
RESINAS EPOXI Y BENZOXAZINAS FOSFORADAS Y SILILADAS RETARDANTES A LA LLAMA  
Marisa Elisabet Spontón  
ISBN:978-84-691-9480-5/DL:T-22-2009

## 1.1

### Materiales poliméricos

Los polímeros sintéticos pueden ser considerados como los materiales del siglo XX. Desde la segunda guerra mundial han experimentado un continuo desarrollo y el volumen de producción desde entonces se ha incrementado hasta alcanzar en la actualidad una producción anual mayor de 120 millones de toneladas (figura 1.1)<sup>1,2</sup>. Asimismo, el consumo per cápita también ha aumentado una media mundial de aproximadamente 20 Kg por año.

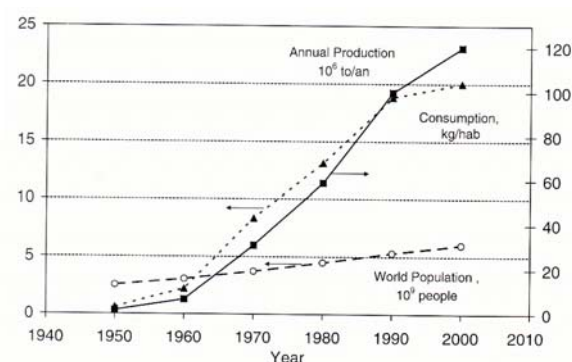


**Figura 1.1** Producción de polímeros y evolución de la población desde 1940.

El gran crecimiento de los polímeros sintéticos se basa en las buenas propiedades que poseen, lo que les permite cubrir un amplio campo de aplicaciones. Junto con las numerosas ventajas que aportan los materiales poliméricos sintéticos a la sociedad en la vida cotidiana, presentan en general, la desventaja de su alta inflamabilidad, ya que en presencia de una

<sup>1</sup> Association of Plastics Manufacturers in Europe, report, 2002.

<sup>2</sup> Handbook of Polymer Reaction Engineering . Vol 1. Ed: Meyer T, Keurentjes J. Wiley-VCH. Weinheim, 2005.

fuelle de calor y de oxígeno se queman fácil y rápidamente<sup>3</sup>. Evidentemente, el problema que se plantea no es únicamente la pérdida de propiedades del material, sino que el humo y los gases tóxicos que se desprenden son los principales responsables del peligro que supone un incendio.

Por lo tanto, los materiales retardantes a la llama son imprescindibles para aquellas aplicaciones que suponen un cambio significativo de las propiedades del material al ser expuestos a una fuente de calor. Estas aplicaciones abarcan campos tan diversos como la industria eléctrica, electrónica y aeroespacial, siendo de especial relevancia para aquellas aplicaciones en que la propagación rápida del fuego puede causar serios problemas, como los asociados con materiales de construcción y transporte. Es por esta razón que actualmente se está realizando un gran esfuerzo por parte de los investigadores para conocer el comportamiento de los polímeros frente al fuego.

Entre los principales mercados en los que se requieren materiales resistentes a la llama los componentes eléctricos y electrónicos destacan por su importancia. En general, para la fabricación de laminados de aplicaciones en electrónica se usan dos tipos de polímeros termoestables retardantes a la llama: resinas epoxi bromadas y resinas fenólicas, aunque ambos tipos presentan importantes desventajas. Las propiedades mecánicas y eléctricas de las resinas epoxi bromadas son excelentes pero en caso de incendio pueden desprender gases altamente tóxicos y corrosivos, a pesar de su naturaleza autoextinguible. Las resinas fenólicas son menos inflamables pero sus propiedades son inferiores a las de las resinas epoxi, además de

---

<sup>3</sup> Ebdon JR, Jones MS. Flame Retardants. Polymeric Materials Science Encyclopedia. Vol 3, p 2397. Ed: Salomone JC. CRC Press: Boca Raton, 1996.

generar agua como subproducto en el proceso de curado. Existe una nueva clase de resinas termoestables que combina las ventajas de estos dos tipos y que no presenta sus inconvenientes, basada químicamente en 3,4-dihidro-2H-1,3-benzoxazinas.

## 1.2

### **Combustión de los polímeros**

La combustión de los materiales poliméricos es un proceso complejo, que implica una serie de etapas interrelacionadas y/o independientes, que ocurren en la fase condensada, gaseosa o bien en la interfase entre ambas (figura 1.2)<sup>3</sup>. En la primera etapa, el calor, proveniente de una fuente externa o de la combustión del propio material, provoca su descomposición dando lugar a fragmentos volátiles e inflamables. En una segunda etapa, estos volátiles se oxidan en fase gas por efecto del oxígeno y del calor y forman los productos de combustión: humo, gases y calor. También puede producirse una combustión lenta cuando la segunda etapa supone una oxidación en estado sólido del resto carbonado producido en la descomposición. Las reacciones específicas que constituyen el proceso global dependen de la naturaleza de los gases y del medio ambiente de la combustión, siendo las reacciones que transcurren por radicales libres las más críticas para la propagación de la llama.

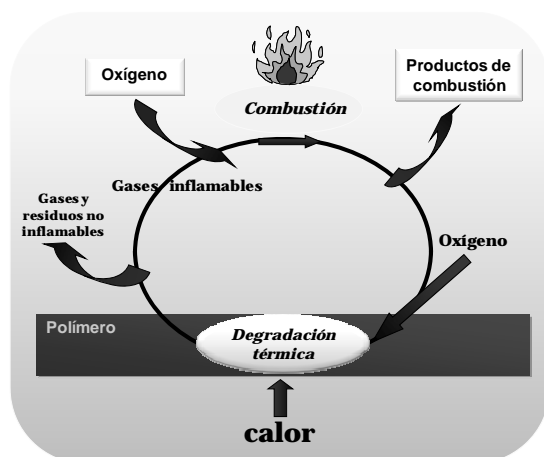


**Figura 1.2** Representación esquemática del proceso de combustión de un polímero.

En general los polímeros con grupos aromáticos o heterociclos en la cadena principal son menos combustibles que los polímeros con cadenas alifáticas<sup>4</sup>. Los polímeros con anillos aromáticos unidos por enlaces cortos y flexibles tienden a entrecruzarse formando un elevado resto carbonado, siendo térmicamente estables y mostrando una relativa buena retardancia a la llama. Ejemplos de este tipo de polímeros son los policarbonatos basados en bisfenol A, las resinas fenol formaldehído y las poliimidas. Todos ellos tuvieron un especial desarrollo en la década de los 60 por la necesidad de obtener materiales térmicamente estables para la industria aeroespacial. Los polímeros con enlaces relativamente largos y flexibles como las cadenas alifáticas son combustibles a pesar de que puedan contener grupos aromáticos. Ejemplos de este tipo son: polipropileno, poliestireno, poliuretano, polietileno tereftalato y resinas epoxi basadas en bisfenol A. Todos ellos son de gran interés para la industria de polímeros y en

<sup>4</sup> Levchik SV. Introduction to Flame Retardancy and Polymer Flammability. Flame Retardant Polymer Nanocomposites. p 1. Ed: Morgan AB, Wilkie CA. Wiley Interscience. Hoboken NJ, 2007.

particular las resinas epoxi por sus especiales propiedades, aunque su inflamabilidad es una seria limitación en aplicaciones en las que se requiere alta retardancia a la llama.

### 1.3

#### Retardantes a la llama

Un retardante a la llama puede definirse como una sustancia incorporada en, o tratamiento aplicado a, un material, que suprime o retrasa la combustión del mismo bajo condiciones específicas<sup>5</sup>. Esta definición cubre todas las características de la combustión, es decir, ignición, combustión lenta y propagación de la llama, liberación de calor, de humo y de gases tóxicos y en consecuencia incluye acepciones más limitadas como retardante de la llama o supresor de humos. La mayoría de ellos son únicamente retardantes a la llama que en la práctica reducen la ignición y la propagación de la llama.

Las primeras referencias de retardantes a la llama datan del siglo V a.c, en que los egipcios impregnaban los materiales de construcción con sulfato de aluminio y potasio para reducir su inflamabilidad<sup>6</sup>. Todos los intentos posteriores se basaron en estrategias similares de impregnación o recubrimientos de materiales naturales. Un ejemplo de las primeras investigaciones básicas de los retardantes a la llama en materiales textiles es la utilización de fosfato de amonio, cloruro de amonio y bórax, que fue

---

<sup>5</sup> Ramsay GC, Dowling VP. *Materials Forum*. 1995;19:163.

<sup>6</sup> Hindersinn RR. *Fire and Polymers: Hazards, Identification and Prevention*. p 91. ACS Symposium Series 425. Ed Nelson GL. American Chemical Society, 1990.

desarrollada por Gay-Lussac a finales del siglo XVIII y principios del XIX. Este sistema aún hoy en día se aplica a materiales celulósicos<sup>7</sup>.

A pesar de que los mecanismos de retardancia a la llama fueron establecidos a principios del siglo XX por Perkin<sup>7</sup>, fue el desarrollo de los polímeros sintéticos durante la segunda guerra mundial lo que estimuló el progreso de la amplia variedad de retardantes a la llama y la diversidad de estrategias de las que se dispone actualmente.

Las estrategias para reducir la inflamabilidad de los materiales poliméricos suponen interrumpir alguna de las etapas complejas del proceso de combustión reduciendo la velocidad y/o modificando el mecanismo de combustión<sup>8-10</sup>. Los compuestos químicos empleados (retardantes a la llama) para interrumpir la combustión pueden estar mezclados con el sustrato polimérico (aditivos), o estar químicamente incorporados en la matriz del polímero (reactivos). Los retardantes a la llama interfieren en el proceso de combustión actuando física o químicamente en la liberación de calor, descomposición, o propagación de la llama del polímero. Pueden presentar más de un modo de actuación que puede variar dependiendo de la naturaleza química del material, por lo que resulta difícil asegurar su forma de operar.

Actualmente, alrededor del 90% de los compuestos comerciales retardantes a la llama que se emplean son: trihidróxido de aluminio, óxidos

---

<sup>7</sup> International Plastics Flammability Handbook, 3<sup>a</sup> ed. Ed: Troitzsch JH. Hanser. Munich, 2004.

<sup>8</sup> Levchik SV, Camino G, Luda MP, Costa L, Muller G, Costes B. Polym Degrad Stab. 1998;60:169.

<sup>9</sup> Liu YL, Hsiue GH, Lan CW, Chiu YS. Polym Degrad Stab. 1997;56:291.

<sup>10</sup> Levchik SV, Camino G, Luda MP, Costa L, Costes B, Henry Y, Muller G, Morel E. Polym Degrad Stab. 1995;48:359.



de antimonio, melanina, boratos y compuestos organoclorados, organobromados, fosforados, y fósforo-halogenados<sup>11</sup> (figura 1.3). Otros compuestos retardantes a la llama de menor aplicación pero que han resultado también eficaces son los de silicio.

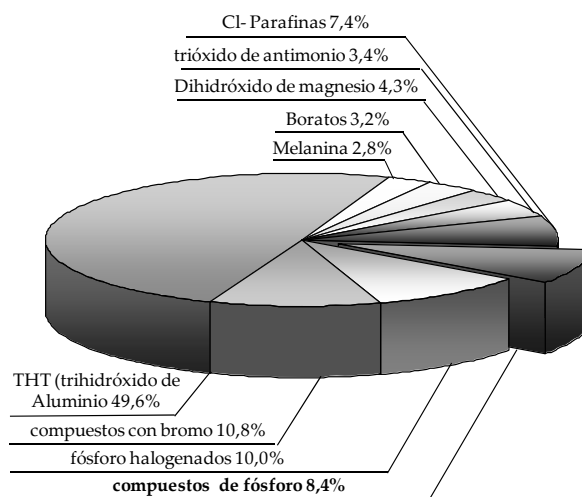


**Figura 1.3** Retardantes a la llama utilizados en el mercado. Datos aportados por la Asociación de Retardantes a la Llama Europea (EFRA).

Básicamente hay dos modos fundamentales de actuación para los compuestos retardantes a la llama: en la fase gaseosa y en la fase condensada<sup>7,12</sup>. En la fase gaseosa los retardantes actúan reaccionando con los radicales libres y produciendo especies menos reactivas. Como resultado, las reacciones exotérmicas disminuyen, el sistema se enfría y se dispone de menos calor para continuar el proceso de combustión. Los

<sup>11</sup> EFRA (The European Flame Retardants Association)-january 2007.

<sup>12</sup> Lewin M, Weil ED. Mechanisms and Modes of Action in Flame Retardancy of Polymers. Fire Retardant Materials. p 31. Ed: Horrocks AR, Price D. CRC Press. Boca Raton, 2001.

compuestos orgánicos que contienen halógenos o fósforo y halógeno<sup>13-17</sup> son buenos ejemplos de este tipo.

En la fase sólida, el retardante altera las reacciones de descomposición favoreciendo la formación de volátiles menos inflamables, y produce o acelera la formación de restos carbonados. Estos restos protegen al material formando una capa o barrera de sólido entre el material y los productos volátiles de la combustión. Típicas barreras sólidas son los residuos formados por recubrimientos intumescentes derivados de la descomposición del sustrato, y recubrimientos vítreos formados por el retardante. La barrera (figura 1.4) impide la transferencia de calor hacia el material sin quemar, reduciendo de esta manera la descomposición y la producción de nuevos volátiles. Otro mecanismo de actuación del retardante es una descomposición endotérmica que produce el enfriamiento de la zona de pirólisis, eliminando calor del sistema y reduciendo la descomposición y producción de volátiles. También puede actuar “diluyendo” la fase sólida o la gaseosa. En el primer caso, el retardante, una carga inerte, compite por el calor con el material en combustión. En el segundo caso, el retardante desprende gases inertes, los cuales diluyen los volátiles que se producen. El trihidróxido de aluminio es un buen ejemplo de descomposición endotérmica y desprendimiento de vapor de agua diluyendo así la fase gaseosa.

---

<sup>13</sup> Pitts JJ. Flame Retardancy of Polymeric Materials. Vol 1, p 162. Ed: Kuryla WC, Papa AJ. Marcel Dekker Inc New York, 1973.

<sup>14</sup> Troitzsch J. Makromol Chem Makromol Symp. 1993;74:125.

<sup>15</sup> The Combustión of Organic Polymers. Ed: Cullis CF, Hirschler MM. Oxford, 1981.

<sup>16</sup> Lyons JW. J Fire Flammability. 1970;1:302.

<sup>17</sup> Flammability Handbook for Plastics, 5<sup>th</sup>. Ed: Hilado CJ. Technomic Publishing Co. Inc. Lancaster, 1998.

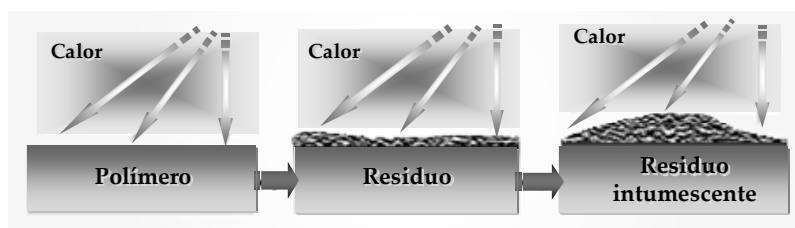


**Figura 1.4** Formación de una capa intumescente durante la descomposición.

Los retardantes a la llama aditivos se encuentran mezclados con el sustrato polimérico y pueden ser añadidos en cualquier etapa de la producción y el procesado. Su utilización presenta algunos inconvenientes, tales como poder ser extraídos con facilidad con agua, detergentes o disolventes y poder migrar alterando las propiedades físicas y químicas del material<sup>18</sup>. A pesar de sus inconvenientes, son de utilización generalizada debido a su bajo coste y amplia aplicación. Despierta un especial interés el sinergismo derivado de la aplicación de mezclas de aditivos retardantes a la llama, que con frecuencia presentan distintos mecanismos de actuación<sup>19</sup>. El caso más clásico es la utilización de mezclas de óxido de antimonio y compuestos halogenados en las que el óxido de antimonio actúa como catalizador facilitando la descomposición de los retardantes halogenados.

Un método alternativo al uso de los retardantes a la llama aditivos es la incorporación del retardante a la matriz polimérica mediante enlace químico. Estos retardantes reactivos presentan la ventaja sobre los aditivos de estar permanentemente unidos al sustrato. Además bajos niveles de modificación de los polímeros, o cantidades relativamente bajas de retardante, pueden tener efectos comparables a los conseguidos con cargas relativamente altas de aditivos. Por el contrario, la obtención de sistemas reactivos es más costoso y consume más tiempo, ya que los reactivos

<sup>18</sup> Combustion of Polymeric Material. Ed: Aseeva RM, Zaikov GH. Hanser, Munich, 1981.

<sup>19</sup>Liu YL, Hsiue GH, Chiu YS, Jeng RJ, Perng LH. J Appl Polym Sci. 1996:61:613.

requieren el desarrollo de un nuevo polímero con propiedades químicas y físicas específicas.

Desde hace varias décadas, la industria de los polímeros utiliza halógenos (Cl y Br) enlazados al sustrato polimérico como retardantes a la llama. Los compuestos de bromo son generalmente más efectivos que los clorados, pero son más caros y menos estables térmicamente por el enlace más débil C-Br<sup>3</sup>. Los compuestos halogenados actúan de manera efectiva durante la combustión eliminando los radicales H• y OH• en la fase gaseosa. Esta acción reduce considerablemente o evita el proceso de quemado, reduciendo la generación de calor y por tanto la producción de material gaseoso inflamable.

El uso de compuestos halogenados tiene el inconveniente de incrementar las cantidades de humos y productos de descomposición tóxicos que se desprenden durante la combustión del polímero. Además, dan lugar también al riesgo adicional de formación de gases fuertemente ácidos, por ejemplo HCl y HBr, que son liberados durante la combustión. Muchos compuestos bromados, principalmente aromáticos, durante su combustión además desprenden dibenzofuranos y dibenzodioxinas<sup>20</sup>. Por tanto, los compuestos halogenados representan un peligro de contaminación ambiental que está siendo considerado, sobre todo en estos últimos años. El concepto de desarrollo sostenible requiere la utilización de tecnologías de retardantes a la llama con un mínimo impacto en el medio ambiente. Así, la incorporación de fósforo o silicio en la estructura polimérica está descrito como uno de los caminos más eficientes para obtener un sistema retardante a la llama respetuoso con el medio ambiente<sup>21</sup>.

---

<sup>20</sup> Ashizuka A. Mol Nutr Food Res. 2008;52:273.

<sup>21</sup> Lu SY, Hamerton I. Prog Polym Sci. 2002;27:1661.

El uso de fósforo como retardante a la llama particularmente en resinas epoxi ha sido ampliamente estudiado<sup>3,22</sup>. Los retardantes a la llama basados en fósforo pueden ser activos en la fase vapor o en la fase condensada, u operar simultáneamente mediante ambos mecanismos. Principalmente los compuestos fosforados actúan en la fase condensada y se descomponen para producir ácido fosfórico polimérico que reacciona con grupos hidroxilo del material produciendo deshidratación<sup>3,23</sup>. Los materiales insaturados que se forman generan restos carbonados relativamente incombustibles (figura 1.5), que funcionan como una barrera que inhibe la degradación y protege al material de la pirolisis.

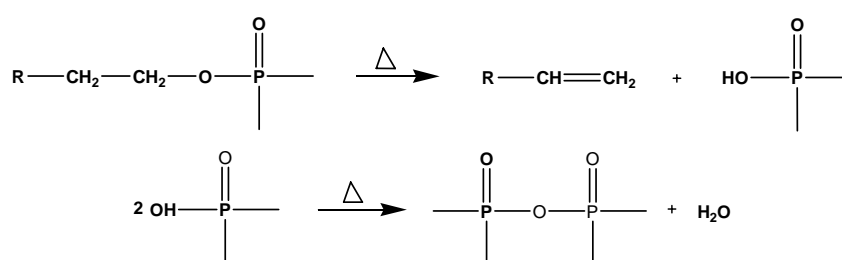


**Figura 1.5** Esquema de la degradación térmica de un compuesto organofosforado.

Los compuestos volátiles de fósforo se encuentran entre los inhibidores de la combustión más efectivos. Un estudio reciente<sup>24</sup> demuestra que el fósforo a igual concentración molar es más efectivo que el bromo y cloro. En determinadas condiciones las moléculas que contienen fósforo pueden volatilizarse y oxidarse produciendo radicales fosforados como  $\text{HPO}_2^\bullet$ ,  $\text{PO}^\bullet$ ,

<sup>22</sup> Von Gentzkow W, Huber J, Kapitza H, Rogler J. Vinyl & Additives Technology 1997;3:175.

<sup>23</sup> Hörold S. Polym Degrad Stab. 1999;64:427.

<sup>24</sup> Babushok V, Tsang W. Combust Flame. 2000;123:488.

$\text{PO}_2^\bullet$  y  $\text{HPO}^\bullet$  los cuales actúan de manera efectiva durante la combustión eliminando los radicales  $\text{H}^\bullet$  y  $\text{HO}^\bullet$ <sup>25</sup>.

Para la acción retardante a la llama de los compuestos que contienen silicio se propone, en general, un mecanismo en fase condensada que supone la formación de una capa protectora basada en este heteroelemento<sup>3,26</sup>. Sin embargo, la mayoría de estos sistemas no actúan aumentando los restos carbonados, por eso son considerados como un nuevo tipo de retardantes a la llama en los que el resto que se forma al calentar se comporta como aislante térmico y como barrera al transporte de masa, sin retener carbono de forma adicional en la fase condensada.

Recientemente, está despertando especial interés el sinergismo obtenido al aplicar mezclas de aditivos retardantes a la llama, que con frecuencia presentan distintos mecanismos de actuación. El caso más clásico es la interacción de óxido de antimonio con compuestos halogenados aunque existen otros ejemplos como los compuestos de fósforo y nitrógeno<sup>27-30</sup> halógenos y peróxidos, halógenos y fósforo y fósforo y silicio<sup>21,31,32</sup>.

---

<sup>25</sup> Hastie JW, Bonnell DW. Molecular Basis of Inhibited Combustion Systems. NBS. 80-2169. Research Report NBSIR. National Bureau of Standards, Gaithersburg. MD, 1980.

<sup>26</sup> Kashiwagi T, Gilman JW. Fire Retardancy of Polymeric Materials. Ed. Grand AF, Wilkie CA. Marcel Dekker, New York 2000.

<sup>27</sup> Wang Q, Shi W. Polym Degrad Stab. 2006;91:1747.

<sup>28</sup> Liu Y, Wang Q. Polym Degrad Stab. 2006;91:3103.

<sup>29</sup> Gaan S, Sun G. J Anal Appl Pyrolysis. 2007;78:371.

<sup>30</sup> Gaan S, Sun G, Hutches K, Engelhard M. Polym Degrad Stab. 2008;93:99.

<sup>31</sup> Liu YL, Chou CI. Polym Degrad Stab. 2005;90:515.

<sup>32</sup> Zhang S, Horrocks AR. Prog Polym Sci. 2003;28:1517.

## 1.4

### Tests de retardancia al fuego

El comportamiento al fuego de un material polímero no puede ser evaluado completamente por la simple determinación de algunos parámetros en el laboratorio. Fuego y combustión son procesos sumamente complejos y al menos deberían tenerse en cuenta cuatro aspectos, que están interrelacionados en el proceso total de combustión. Estos aspectos son la ignición, la velocidad de propagación de la llama, la velocidad de desprendimiento de calor y la formación de humos y gases, contribuyendo todos ellos a la combustión y a los peligros asociados con el fuego.

A consecuencia de la naturaleza compleja y la poca reproducibilidad de un incendio, existen muchas técnicas para estimar la inflamabilidad de los materiales poliméricos, concentrándose cada una de ellas en ciertas características del proceso de combustión. La valoración del retardo a la llama generalmente se realiza utilizando distintos procedimientos que han sido estandarizados previamente por organismos nacionales e internacionales. Así pues existen tres categorías diferentes de tests: a pequeña escala, en los que una pequeña cantidad de muestra se quema y se observa el comportamiento de la combustión; a media escala, que incluye tests en túneles y paneles radiantes y a gran escala, con experimentos que se llevan a cabo en habitaciones y que proporciona la mejor reproducción de una situación de fuego real. Aunque los tests a gran escala son los que dan resultados más representativos de un incendio, son los más caros, ya que precisan instalaciones y equipos muy específicos y además de difíciles de controlar requieren largos periodos de tiempo, por lo que los tests a pequeña y media escala son los más ampliamente utilizados.

El objetivo de los ensayos en los que se utilizan tests de laboratorio consiste en determinar si el producto o material retardante al fuego cumple ciertos requisitos para una determinada aplicación, o proporciona una medida cuantitativa de la eficacia del retardante para el desarrollo de nuevos materiales resistentes al fuego. Los distintos ensayos pueden clasificarse en cuatro grupos en función del tipo de material polímero en estudio: plásticos, textiles, materiales de construcción y materiales para aplicaciones específicas como recubrimientos en electrónica o cables eléctricos.

Entre las técnicas más ampliamente utilizadas en el laboratorio se pueden citar<sup>17</sup>.

- El Índice Limitante de Oxígeno (LOI) (ASTM-D-2863), que determina la mínima concentración de oxígeno, en una corriente de gas formada por una mezcla de oxígeno y nitrógeno, necesaria para mantener la combustión de la llama.
- El test UL-94 (ASTM-D-3801), método estándar que se aplica especialmente a materiales para la fabricación de componentes eléctricos y electrónicos y que se basa en el tiempo de quemado, la velocidad de propagación de la llama y el goteo en el quemado del material.
- El análisis termogravimétrico (TGA), que determina la estabilidad térmica y la cantidad de residuo carbonoso formado por el polímero cuando descompone térmicamente en presencia de nitrógeno o aire.



- El calorímetro de cono que representa un avance importante a escala de laboratorio en test del fuego de materiales poliméricos y composites, usando el principio de consumición de oxígeno. Este test proporciona una idea no solo del riesgo del fuego, sino de velocidad de la liberación de calor (HRR), del calor total liberado (THR), y del tiempo de ignición, liberación de humo y producción de CO y CO<sub>2</sub>.

## 1.5

### Objetivo general

Con todos estos antecedentes, se ha planteado como objetivo general de esta tesis doctoral el desarrollo de nuevos sistemas poliméricos termoestables resistentes al fuego, sin detrimento de las propiedades del material y no agresivos medioambientalmente. Se pretende mejorar las buenas propiedades de algunos materiales estándar actualmente empleados, tales como resinas epoxi y resinas fenólicas, pero introduciendo la condición de no inflamabilidad mediante nuevos sistemas de ignifugación alternativos a los sistemas halogenados clásicos. Para ello se propone la síntesis y caracterización de nuevos tipos de sistemas en los que se ha incorporado fósforo y/o silicio a resinas epoxi y benzoxazinas y se han evaluado sus propiedades.

La presente memoria consta de cuatro capítulos:

- En este primer capítulo, con una breve introducción se pretende enmarcar el trabajo y señalar el interés del estudio, así como de los objetivos marcados.

- En el segundo capítulo se describe la síntesis de nuevas resinas epoxi fosforadas y/o sililadas y se estudian sus propiedades térmicas, mecánicas y de retardancia a la llama, con objeto de establecer una relación entre la presencia y proporción de los heteroátomos y las propiedades físicas de los materiales. Además, se estudia el efecto sinérgico entre fósforo y silicio. El capítulo se inicia con una breve introducción en la que se exponen los antecedentes y características de las resinas objeto del estudio.
  
- En el tercer capítulo se estudia la síntesis de nuevos sistemas epoxi-benzoxazina fosforados o sililados obtenidos por copolimerización de los glicidilos fosforados o sililados descritos en el capítulo anterior y nuevas benzoxazinas fosforadas. Se discuten los resultados de su caracterización estructural y de su reacción de entrecruzamiento, así como sus propiedades térmicas, mecánicas, y de retardancia a la llama. De forma similar al capítulo anterior, éste también se inicia con la descripción de los antecedentes y peculiaridades de estos sistemas epoxi-benzoxazina-heteroátomo.
  
- En el cuarto capítulo se describe brevemente la técnica del calorímetro de cono y se aplica al estudio de algunos de los sistemas anteriores para estimar su inflamabilidad a través de parámetros que nos permiten correlacionar la influencia de la estructura química sobre el comportamiento de retardancia a la llama del material.

# CAPÍTULO 2

## Síntesis y caracterización de resinas epoxi fosforadas y/o sililadas

---

*Las resinas epoxi despiertan un gran interés entre los compuestos poliméricos por la gran versatilidad de sus aplicaciones debido a sus buenas propiedades. Sin embargo, la inflamabilidad de estos materiales es una seria limitación en aquellas aplicaciones en las que se requiere retardancia a la llama. Por esta razón, en este capítulo se estudia la síntesis de nuevos sistemas epoxi fosforados y/o sililados retardantes a la llama y se describe la evaluación de sus propiedades.*

---

2.1 Resinas epoxi retardantes a la llama

2.2 Objetivos

2.3 Parte experimental y resultados

2.3.1 Flame retardant epoxy resins based on diglycidyl ether of (2,5-dihydroxyphenyl)diphenyl phosphine oxide

2.3.2 Preparation, thermal properties and flame retardancy of phosphorus- and silicon-containing epoxy resins

UNIVERSITAT ROVIRA I VIRGILI  
RESINAS EPOXI Y BENZOXAZINAS FOSFORADAS Y SILILADAS RETARDANTES A LA LLAMA  
Marisa Elisabet Spontón  
ISBN:978-84-691-9480-5/DL:T-22-2009

## 2.1

### Resinas epoxi retardantes a la llama

Desde su aparición en el mercado, hacia 1950, las resinas epoxi han experimentado un continuo desarrollo. Su empleo en la actualidad no llega a los valores de consumo de otros materiales poliméricos, sin embargo en términos de versatilidad, es posible que no exista otro tipo de polímeros para los que se hayan encontrado mayor número de aplicaciones. A pesar de las numerosas resinas desarrolladas hasta ahora, todavía más del 90% de su producción se basa en bisfenol A y epiclorhidrina (figura 2.1), que son los materiales de partida para la síntesis de las resinas epoxi convencionales.

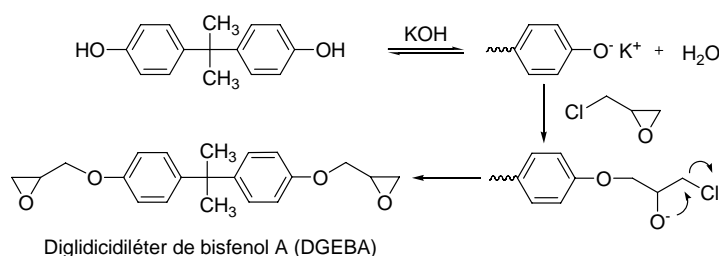


**Figura 2.1** Mecanismo de reacción del bisfenol A con epiclorhidrina en medio básico.

En general estos materiales se caracterizan por su buena dureza, buena resistencia química y eléctrica, buenas propiedades mecánicas tales como alta adhesión a los diferentes sustratos, bajo encogimiento y bajo estrés térmico después del curado. Por esta razón su utilización está orientada a diferentes sectores, entre los que se incluye, la industria química, eléctrica, aeronáutica y aeroespacial<sup>1</sup>.

<sup>1</sup> Epoxy Resins: Chemistry and Technology. Ed: May C.A. Marcel Dekker, Inc. NY 1998.



A pesar de las grandes ventajas que presentan las resinas epoxi, su inflamabilidad es una seria limitación en aplicaciones en las que se requiere resistencia a la llama. De hecho, son mucho más inflamables que otros termoestables comparables a estos materiales, ya que tienen una reducida tendencia a carbonizar. Por ello y como consecuencia de la legislación cada vez más estricta respecto a su inflamabilidad, se está haciendo un gran esfuerzo para mejorar la retardancia a la llama de estas resinas.

La utilización de retardantes reactivos, como ya se ha mencionado en la introducción, resulta mucho más efectiva que la de los aditivos, al estar permanentemente unidos a la cadena polimérica. Además, bajos niveles de modificación de los polímeros pueden tener efectos comparables a los conseguidos con cargas relativamente altas de aditivos, ejerciendo una pequeña influencia sobre las propiedades físicas y químicas del polímero.

Desde hace varias décadas los compuestos halogenados han demostrado ser eficientes agentes retardantes a la llama. Así, en el mercado todavía predominan las resinas epoxi bromadas, como por ejemplo el tetrabromobisfenol A (TBBA)<sup>2</sup> que es ampliamente utilizado en la industria electrónica. Las propiedades mecánicas y eléctricas de las resinas epoxi bromadas son excelentes, pero en caso de incendio pueden desprender humos densos y productos de descomposición altamente tóxicos. Para evitar estos problemas, la tendencia actual es la utilización de retardantes libres de halógenos<sup>3,4</sup>. Entre los heteroátomos utilizados, fósforo y silicio son los que muestran mayor efectividad.

---

<sup>2</sup> Luda MP, Balabanovich AI, Zanetti M, Guaratto D. *Polym Degrad Stab.* 2007;92:1088.

<sup>3</sup> Lu SY, Hamerton I. *Prog Polym Sci.* 2002;27:1661.

<sup>4</sup> Mauerer O. *Polym Degrad Stab.* 2005;88:70.

Los compuestos organofosforados pueden ser introducidos directamente en la resina epoxi utilizando la reactividad de los grupos P-OH de los fosfatos de dialquilo o diarilo con anillos oxiránicos. Las resinas de DGEBA modificadas con fosfatos de dialquilo muestran mejores propiedades de resistencia al fuego que las correspondientes formulaciones de resinas que contienen fosfatos como aditivos. Sin embargo, los mejores resultados de retardancia a la llama en resinas epoxi se han conseguido al utilizar monómeros oxiránicos o bien agentes de curado que contengan fósforo en su estructura<sup>5-8</sup>.

Existe un gran número de retardantes a la llama que contienen fósforo dado que este elemento puede encontrarse en distintos estados de oxidación y es de gran interés la obtención de compuestos oxiránicos que posean alto contenido de fósforo mediante síntesis sencillas. Entre los derivados fosforados que se encuentran descritos en la literatura destacan los basados en óxidos de fosfina<sup>9-14</sup>, fosfonatos<sup>15-17</sup> y fosfatos<sup>18-20</sup>, así como diaminas

---

<sup>5</sup> Jain P, Choudhary V, Varma KJ. *Macromol Sci Polym Rev.* 2002;42:139.

<sup>6</sup> Levchik SV, Piotrowski A, Weil ED, Yao Q. *Polym Degrad Stab.* 2005;88:57.

<sup>7</sup> Levchik SV, Weil ED. *Polym Int.* 2004;53:1901.

<sup>8</sup> Weil ED, Levchik SV. *J Fire Sci.* 2004;22:25.

<sup>9</sup> Shau MD, Lin CW, Yang WH, Lin HR. *J Appl Polym Sci.* 2002;84:950.

<sup>10</sup> Alcón MJ, Ribera G, Galià M, Cádiz V. *Polymer.* 2003;44:7291.

<sup>11</sup> Alcón MJ, Ribera G, Galià M, Cádiz V. *J Polym Sci Part A: Polym Chem.* 2005;43:3510.

<sup>12</sup> Mercado LA, Ribera G, Galià M, Cádiz V. *J Polym Sci Part A: Polym Chem.* 2006;44:1676.

<sup>13</sup> Ribera G, Mercado LA, Galià M, Cádiz V. *J Appl Polym Sci.* 2006;99:1367.

<sup>14</sup> Shau M, Tsai P, Teng W, Hsu W. *Eur Polym J.* 2006;42:1899.

<sup>15</sup> Liu YL, Hsiue GH, Chiu YS, Jeng RJ. *J Appl Polym Sci.* 1996;61:1789.

<sup>16</sup> Xia XN, Lu YB, Zhou X, Xiong ZY, Zhang XH, Xu WJ. *J Appl Polym Sci.* 2006;102:3842.

<sup>17</sup> Ren H, Sun J, Wu B, Zhou Q. *Polym Degrad Stab.* 2007;92:956.

<sup>18</sup> Hergenrother PM, Thompson CM, Smith JG, Connell JW, Hinkley JA, Lyon RE, Moulton R. *Polymer.* 2005;46:5012.

<sup>19</sup> Wang H, Wang Q, Huang Z, Shi W. *Polym Degrad Stab.* 2007;92:1788.

<sup>20</sup> Gao LP, Wang DY, Wang YZ, Wang JS, Yang B. *Polym Degrad Stab.* 2008;93:1308.



fosforadas como agentes de curado<sup>21-25</sup>. Algunos de estos compuestos se recogen en la figura 2.3.

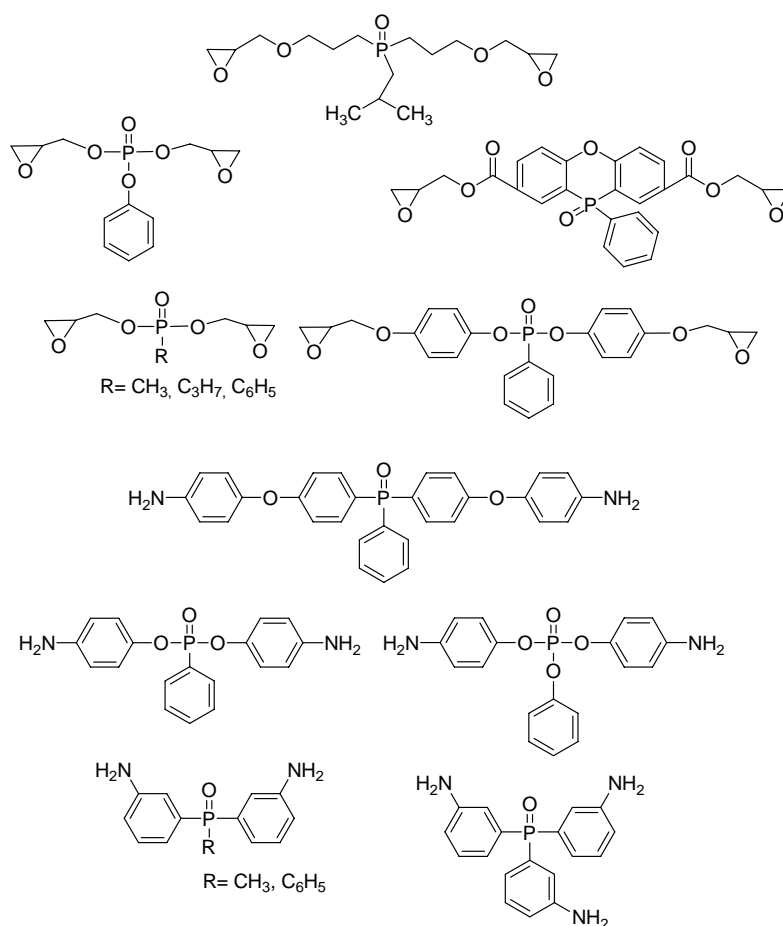


**Figura 2.3** Estructuras de monómeros epoxi y diaminas que contienen fósforo.

<sup>21</sup> Wang TS, Yeh JF, Shau MD. *J Appl Polym Sci.* 1996;59:215.

<sup>22</sup> Levchik SV, Camino G, Luda MP, Costa L, Muller G, Costes B, Henry Y. *Polim Adv Technologies.* 1996;7:823.

<sup>23</sup> Yeh CF, Wang TS, Cherng JY, Kuo JHS, Shau MD. *J Appl Polym Sci.* 2002;86:141.

<sup>24</sup> Varley RJ, Liu W, Simon GP. *J Appl Polym Sci.* 2006;99:3288.

<sup>25</sup> Toldy A, Anna P, Csontos I, Szabó A, Marosi G. *Polym Degrad Stab.* 2007;92:2223.

Muchos de éstos compuestos sintetizados a partir de ácidos fosfóricos, fosfónicos o fosfínicos contienen enlaces P-O-C poco estables<sup>26</sup>. Como consecuencia de ello es preferible que el fósforo se encuentre unido directamente al carbono, ya que el enlace P-C en un fosfonato es más estable a la hidrólisis que el enlace P-O-C de un fosfato. Aún así, el enlace P-C se rompe a temperaturas ligeramente inferiores que el enlace C-C a causa de su menor energía atómica<sup>27</sup>, lo que favorece la formación de una capa carbonacea que puede proteger al polímero de la degradación.

En los últimos años destaca la síntesis de glicidilos y aminas a partir del óxido de 10-[9,10-dihidro-9-oxa-10-fosfafenantreno] (DOPO), compuesto rígido y voluminoso, cuya incorporación supone una mejora importante de las propiedades retardantes a la llama de las resinas epoxi<sup>6,7,28,29</sup>. A pesar de contener enlaces P-O-C, esta estructura cíclica posee una inusual estabilidad térmica que se atribuye al grupo O=P-O de la estructura rígida tipo fenantreno, en la que queda protegido por los grupos fenílicos. El P-H activo del DOPO puede actuar frente a una gran variedad de electrófilos, tales como: compuestos carbonílicos<sup>30,31</sup>, benzoquinona<sup>32-38</sup>, iminas<sup>39</sup> y

<sup>26</sup> Weil ED. Phosphorus-containing polymers. Encyclopedia of Polymer Science and Engineering. Vol 11, p 96. Ed: Kroschwitz JI. Wiley NY 1988.

<sup>27</sup> Quittmann U, Lecamp L, El Khatib W, Youssef B, Brunel C. Macromol Chem Phys. 2001;202:628.

<sup>28</sup> Wang CS, Shieh JY. Polymer. 1998;39: 5819.

<sup>29</sup> Ciesielski M, Schäfer A, Döring M. Polym Adv Technol. 2008;19:507.

<sup>30</sup> Liu YL. J Polym Sci Part A: Polym Chem. 2002;40:359.

<sup>31</sup> Liu YL. J Appl Polym Sci. 2002;83:1697.

<sup>32</sup> Cho CS, Chen LW, Fu SC, Wu TR. Journal of Polymer Research. 1998;5:59.

<sup>33</sup> Wang CS, Lin CH. J Appl Polym Sci. 2000;75:429.

<sup>34</sup> Wang X, Zhang Q. Eur Polym J. 2004;40:385.

<sup>35</sup> Ho TH, Leu TS, Sun YM, Shieh JY. Polym Degrad Stab. 2006;91:2347.

<sup>36</sup> Lligadas G, Ronda JC, Galià M, Cádiz V. J Polym Sci Part A: Polym Chem. 2006;44:5630.

<sup>37</sup> Canadell J, Mantecón A, Cádiz V. Polym Degrad Stab. 2008;93:59.

<sup>38</sup> Guo W, Leu WT, Hsiao SH, Liou GS. Polym Degrad Stab. 2006;91:21.

epoxi<sup>40,41</sup> obteniéndose así una gran variedad de compuestos oxiránicos y aminas que contienen esta unidad de DOPO<sup>42-44</sup>. Algunos de estos compuestos se recogen en la figura 2.4.

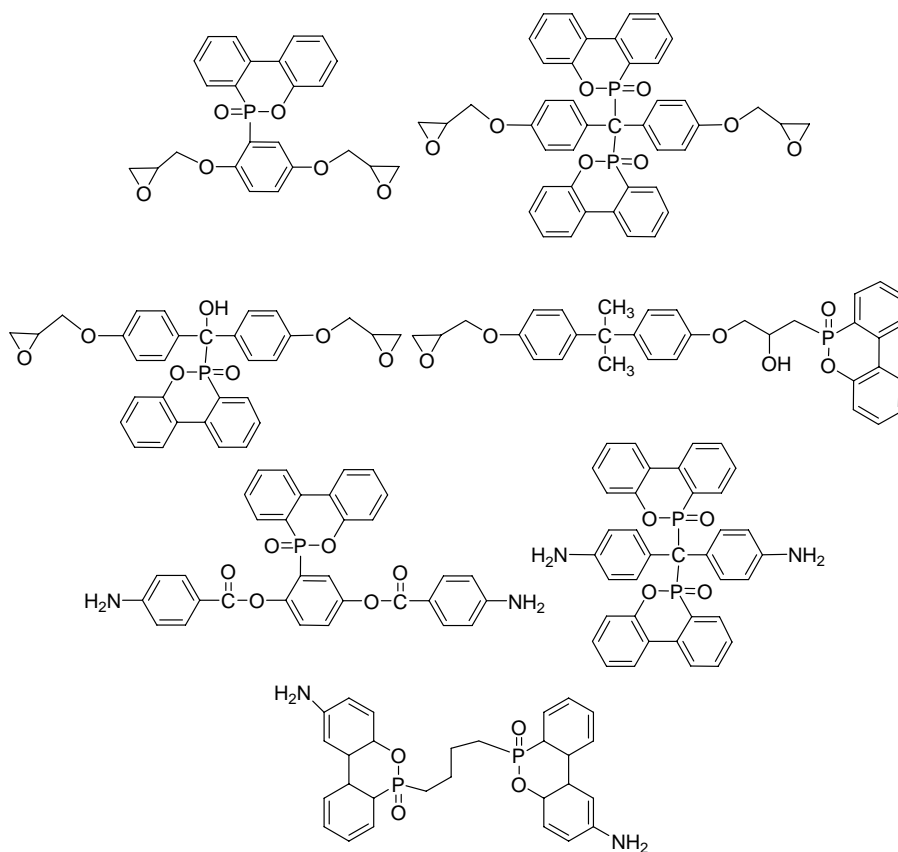


**Figura 2.4** Estructuras de monómeros epoxi y diaminas derivados de DOPO.

<sup>39</sup> Lin CH, Hwang TY, Taso YR, Lin TL. *Macromol Chem Phys.* 2007;208:2628.

<sup>40</sup> Alcón MJ, Espinosa MA, Galià M, Cádiz V. *Macromol Rapid Commun.* 2001;22:1265.

<sup>41</sup> Schäfer A, Seibold S, Walter O, Döring M. *Polym Degrad Stab.* 2008;93:557.

<sup>42</sup> Artner J, Cesielski M, Walter O, Döring M, Perez RM, Sandler JKW, Altstädt V, Schartel B. *Macromol Mater Eng.* 2008;293:503.

<sup>43</sup> Schartel B, Braun U, Balabanovich AI, Artner J, Ciesielski M, Döring M, Perez RM, Sandler JKW, Altstädt V. *Eur Polym J.* 2008;44:704.

<sup>44</sup> Gan J, Goodson A. *PST Patent Application WO 01/42359* 2001.

Los óxidos de fosfina orgánicos son compuestos muy atractivos por su alta estabilidad a la hidrólisis y a la oxidación debido a los enlaces P-C, así como también a la alta estabilidad del grupo fosforilo (P=O). La naturaleza de este grupo mejora las propiedades de resistencia a la llama del polímero termoestable y la polaridad del enlace aumenta la capacidad de formación de puentes de hidrógeno de la resina epoxi resultante mejorando su adhesividad a distintos tipos de sustratos<sup>45,46</sup>.

Los óxidos de fosfina secundarios se adicionan fácilmente a una variedad de electrófilos, entre ellos a los compuestos  $\alpha,\beta$ -insaturados a través de una reacción tipo Michael<sup>47,48</sup>. Estos óxidos muestran gran reactividad debido a la presencia de los enlaces P-H en equilibrio con su forma tautómera<sup>49</sup> que confiere un carácter nucleófilo al átomo de fósforo (figura 2.5).

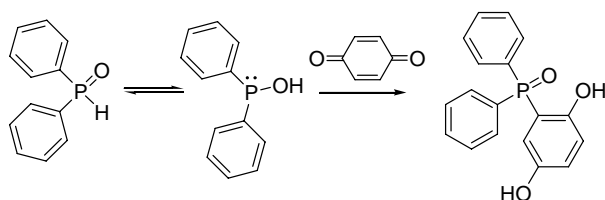


Figura 2.5

Por otra parte, en los últimos años se han descrito algunas aproximaciones sobre resinas epoxi con silicio unido covalentemente a la matriz polimérica que han demostrado ser eficientes retardantes a la llama.

<sup>45</sup> Wang S, Zhuang H, Shobha HK, Glass TE, Sakarapandian M, Ji Q, Shultz AR, McGrath JE. *Macromolecules*. 2001;34:8051.

<sup>46</sup> Shobha HK, Johnson H, Sakarapandian M, Kim YS, Rangarajan P, Baird DG, McGrath JE. *J Polym Sci Part A: Polym Chem*. 2001;39:2904.

<sup>47</sup> Brown JM, Woodward S. *J Org Chem*. 1991;56:6803.

<sup>48</sup> Rey P, Taillades J, Rossi JC, Gros G. *Tetrahedron Letters*. 2003;44:6169.

<sup>49</sup> Magiera D, Szmigielska A, Pietrusiewicz KM, Duddeck H. *Chirality*. 2004;16:57.

En la figura 2.6 se muestran las estructuras de algunos monómeros<sup>7,50-53</sup> y agentes de curado<sup>54</sup> que contienen silicio y que han resultado efectivos proporcionando una mejora en las propiedades de retardo a la llama, sin sacrificar las propiedades mecánicas, de las resinas epoxi curadas.

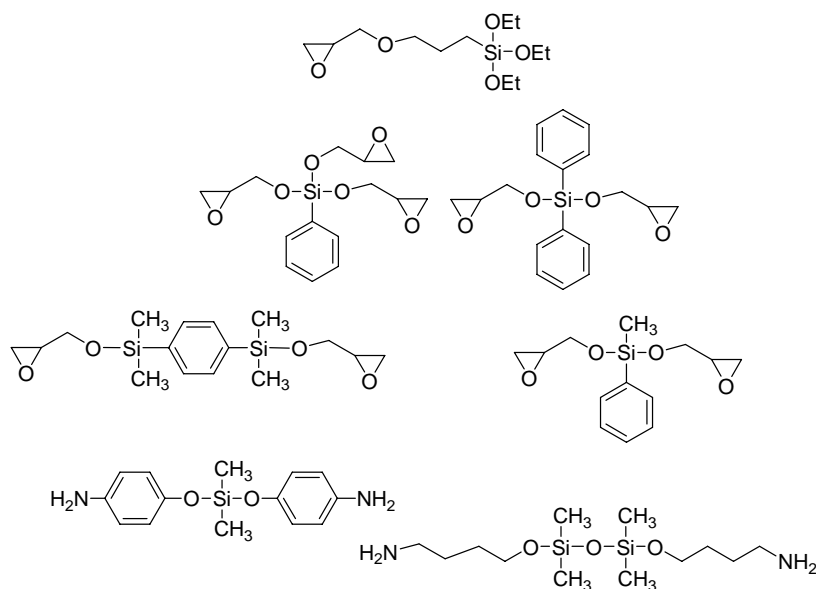


**Figura 2.6** Estructuras de monómeros epoxi y diaminas derivados de silicio.

También se ha estudiado el efecto sinérgico entre el fósforo y silicio frente a la llama. Como ya se ha comentado, el fósforo aumenta la tendencia a formar restos carbonados mientras que el silicio proporciona un aumento de la estabilidad térmica de este resto, por lo que la introducción de los dos elementos en la composición de la resina epoxi puede combinar ambos factores presentando un efecto sinérgico en el mecanismo de retardancia a

<sup>50</sup> Cardiano P, Ponterio RC, Sergi S, Schiavo SL, Piraino P. *Polymer*. 2005;46:1857.

<sup>51</sup> Wang WJ, Perng LH, Hsiue GH, Chang FC. *Polymer*. 2000;41:6113.

<sup>52</sup> Mercado LA, Reina JA, Galià M. *Polym Sci Part A: Polym Chem*. 2006;44:5580.

<sup>53</sup> Mercado LA, Reina JA, Galià M. *Polym Degrad Stab*. 2006;91:2588.

<sup>54</sup> Hsiue GH, Wei HF, Shiao SJ, Kuo WJ, Sha YA. *Polym Degrad Stab*. 2001;73:309.

la llama<sup>55-57</sup>. Además, este efecto fue estudiado en resinas híbridas epoxi-silicio<sup>58</sup> y en nanocomposites<sup>59</sup>.

## 2.2

### Objetivos

Con el fin de obtener nuevos sistemas epoxi retardantes a la llama libres de halógenos, el objetivo del trabajo descrito en este capítulo es la síntesis de resinas epoxi fosforadas y/o sililadas, la evaluación de sus propiedades y el estudio de su comportamiento de degradación y de retardancia a la llama, y la investigación del posible efecto sinérgico de fósforo y silicio.

## 2.3

### Parte experimental y resultados

En este capítulo se expondrán la parte experimental y los resultados de nuevos sistemas de resinas epoxi retardantes a la llama, que han sido publicadas en dos revistas científicas.

**2.3.1** El trabajo descrito en esta sección fue publicado en *Journal of Polymer Science: Part A: Polymer Chemistry*, 2007, 45, 2142-2151, e incluye la síntesis y caracterización de un nuevo compuesto diglicidílico fosforado, el diglicidiléter del óxido de (2,5-dihidroxifenil) difenil fosfina, y su

---

<sup>55</sup> Wu SC, Liu YL, Chiu YS. *Polymer*. 2002;43:4277.

<sup>56</sup> Liu YL, Chiu YC, Wu CS. *J Appl Polym Sci*. 2003;87:404.

<sup>57</sup> Liu YL, Chou CI. *Polym Degrad Stab*. 2005;90:515.

<sup>58</sup> Liu YL, Wu CS, Chiu YC, Ho WH. *J Polym Sci Part A: Polym Chem*. 2003;41:2354.

<sup>59</sup> Lin CH, Feng CC, Hwang TY. *Eur Polym J*. 2007;43:725.

entrecruzamiento con una diamina aromática. Además, con el fin de comparar el efecto que provoca la presencia y proporción de fósforo en el material, se prepararon mezclas de la nueva resina epoxi fosforada con una resina epoxi comercial. Se evaluaron las propiedades térmicas y dinamomecánicas de los materiales así obtenidos y se estudió su degradación térmica. Los resultados del índice limitante de oxígeno (LOI) pusieron de manifiesto las buenas propiedades retardantes a la llama de los materiales sintetizados.

**2.3.2** En esta sección se describe el trabajo que ha sido publicado en *Polymer Degradation and Stability* 2008, DOI 10.1016/j.polymdegradstab.2008.02.014. Utilizando distintas resinas epoxi y agentes de curado que contienen fósforo y/o silicio se han sintetizado nuevos sistemas con ambos heteroátomos y con distinto porcentaje de cada uno de ellos. Además de evaluar sus propiedades térmicas y dinamomecánicas se determinaron los valores de LOI. Aunque se obtuvieron buenos resultados de retardancia a la llama, no se observó un efecto sinérgico por la presencia de fósforo y silicio en la resina.

UNIVERSITAT ROVIRA I VIRGILI  
RESINAS EPOXI Y BENZOXAZINAS FOSFORADAS Y SILILADAS RETARDANTES A LA LLAMA  
Marisa Elisabet Spontón  
ISBN:978-84-691-9480-5/DL:T-22-2009



---

---

*2.3.1. FLAME RETARDANT EPOXY RESINS BASED ON DIGLYCIDYL  
ETHER OF (2,5-DIHYDROXYPHENYL)DIPHENYL PHOSPHINE OXIDE*

---

---

UNIVERSITAT ROVIRA I VIRGILI  
RESINAS EPOXI Y BENZOXAZINAS FOSFORADAS Y SILILADAS RETARDANTES A LA LLAMA  
Marisa Elisabet Spontón  
ISBN:978-84-691-9480-5/DL:T-22-2009

## FLAME RETARDANT EPOXY RESINS BASED ON DIGLYCIDYL ETHER OF (2,5-DIHYDROXYPHENYL)DIPHENYL PHOSPHINE OXIDE

M. Spontón, J.C. Ronda, M. Galià, V. Cádiz

Departament de Química Analítica i Química Orgànica. Universitat Rovira  
i Virgili. Campus Sescelades Marcel·lí Domingo s/n. 43007 Tarragona. Spain.  
virginia.cadiz@urv.cat

### ABSTRACT

Phosphine oxide-containing epoxy resins were prepared from diglycidyl ether of (2,5-dihydroxyphenyl)diphenyl phosphine oxide and diglycidyl ether of bisphenol A by crosslinking with 4,4'-diaminodiphenylmethane. Several (2,5-dihydroxyphenyl)diphenyl phosphine oxide / diglycidyl ether of bisphenol A molar ratios were used to obtain materials with different phosphorus content. The properties of the thermosetting materials were evaluated by differential scanning calorimetry, dynamic mechanical analysis, thermogravimetric analysis, and limiting oxygen index and related to the phosphorus content. Thermal and thermooxidative degradation was studied by GC/MS,  $^{31}\text{P}$  MAS NMR spectroscopy, and scanning electron microscopy. Limiting oxygen index values indicate good flame retardant properties that are related to the formation of a protective phosphorus-rich layer that slowed down the degradation and prevented it from being total.

**Keywords:** epoxy resin; flame retardant; phosphorus-containing.

## INTRODUCTION

Epoxy resins are high-performance thermosetting resins that have a unique combination of properties including good adhesion to many substrates, chemical and heat resistance, superior electrical and mechanical properties, and good dimensional stability.<sup>1-3</sup> In addition, almost any property of epoxy can be modified to meet specific need. However, some disadvantages such as poor flame resistance of epoxy resins limit their usage in some fields, such as special adhesives and coatings, advanced composites in aerospace, and electronic industries. It demands the development of flame retardant systems to reduce fire hazards. Various flame retardants, depending on their nature, can inhibit or suppress accidental fires or flames spread either chemically and/or physically in the solid, liquid, or gas phase. Classical flame retardants commercially used are inorganic compounds or halogen-based organic compounds, which can, however, give rise to corrosive gases and toxic smoke during combustion. The stringent conditions set by statutory governmental regulations for the use of flame retardants demand the development of halogen free flame retardant materials, and there is a strong trend toward the development of more environmentally friendly systems, in which phosphorus-based intumescent systems used as substitutes for halogenated flame retardant compounds seem to be most attractive.<sup>4</sup>

Epoxy polymers could be endowed with flame retardancy by covalent incorporation of phosphorus.<sup>5-8</sup> Series of diglycidyl phosphates, diglycidyl phosphonates, and glycidyl phosphinates have been prepared. A large number of publications discuss the use of 9,10-dihydro-9-oxa-10-phosphaphenanthrene 10-oxide in the formulation of epoxy resins.<sup>5</sup> Moreover, phosphine oxide structures are often used to impart flame

retardancy to epoxy resins, specially through curing agents because polymers with phosphine oxide moieties have the major advantages, such as good flame retardant properties, high thermal oxidative stability, enhanced solubility in organic solvents, improved miscibility, and good adhesion to other compounds.<sup>9-11</sup> Indeed, the P-C bond in a phosphonate is more stable to hydrolysis than the P-O-C bond in a phosphate and the P-C bond is broken just before the C-C bond because of its lower bond energy.<sup>12</sup> Moreover, the polarity of the phosphoryl group increases the hydrogen bonding ability of the resulting epoxy, thus improving network adhesion to various substrates<sup>13</sup>. However, these phosphine oxide structures are not frequent in epoxy monomers. In a previous paper we described how we obtained advanced phosphorous-containing epoxy resins by reacting isobutyl bis(hydroxypropyl) phosphine oxide (IHPO) with diglycidyl ether of bisphenol A (DGEBA) and how they were cured with primary amines to give V-0 materials.<sup>14</sup> We also synthesized isobutyl bis(glycidylpropylether) phosphine oxide (IHPOGly) from IHPO and epichlorohydrin and investigated its thermal behaviour. We studied the reactivity of this novel diglycidyl compound using initiators and hardeners<sup>15</sup> and we described how epoxy systems containing different amounts of this new diglycidylether were prepared from a phosphine oxide (IHPOGly) and DGEBA by curing with a primary amine.<sup>16</sup>

In an attempt to find new phosphine oxide-containing epoxy monomers, in this work, the diglycidyl ether of (2,5-dihydroxyphenyl)diphenyl phosphine oxide (Gly-HPO) was synthesized and crosslinked with diaminodiphenylmethane (DDM) as curing agent. We examined the incorporation of different amounts of phosphorus into the epoxy resin by curing the Gly-HPO/DGEBA system with DDM. The properties of the materials were evaluated by using differential scanning calorimetry (DSC),

dynamic mechanical analysis (DMTA), and the limiting oxygen index (LOI). It is of importance to understand the thermal decomposition of a polymer for practical applications, therefore thermal degradation mechanisms of these phosphine oxide-containing resins have been studied by thermogravimetric analysis (TGA), GC/MS,  $^{31}\text{P}$  MAS NMR spectroscopy and scanning electron microscopy (SEM).

## EXPERIMENTAL

### Materials

Epichlorhydrin (Fluka), benzoquinone (Fluka), (DGEBA) Eq. Epoxy (E.E= 192 g/eq) (Aldrich), and benzyltrimethylammonium chloride (Fluka) were used as received. All solvents were purified by standard procedures.

The curing agent (DDM) was purchased from Aldrich and used without any further purification. Diphenylphosphine oxide was synthesized as previously described.<sup>17</sup>

### Synthesis of (2,5-Dihydroxyphenyl)diphenylphosphine Oxide (HPO)<sup>18,19</sup>

Into a three-neck round-bottomed flask equipped with a magnetic stirrer, *p*-benzoquinone (4.36 g, 0.04 mol) and toluene (108 ml) were placed. The reaction was carried out under argon, pressure equalizing addition funnel, and drying tube. Diphenylphosphine oxide (8.15 g, 0.04 ml) in toluene (36 ml) was added dropwise over 0.5 h to the stirred solution at room temperature under nitrogen. The solution color changed from a dark brown to yellow with the formation of a gum that with stirring became a grey solid. This solid was isolated by filtration, washed with toluene and then diethyl ether, and dried at 110 °C. Recrystallization from ethanol with

active charcoal afforded a white solid (10 g, 80 % yield) mp 214-215 °C (lit. mp 214-215 °C<sup>19</sup>).

<sup>1</sup>H NMR (CD<sub>3</sub>OD/TMS, δ (ppm)): 7.70 (m, 4H, *J* = 13.60 Hz), 7.57 (m, 2H), 7.52 (m, 4H), 6.92 (ddd, 1H, *J* = 8.4 Hz, *J* = 2.8 Hz, *J* = 0.8 Hz), 6.87 (dd, 1H, *J* = 13.90 Hz, *J* = 2.8 Hz), 6.72 (dd, 1H, *J* = 8.8 Hz, *J* = 6 Hz), 5.3 (s, 2H).

<sup>13</sup>C NMR (CD<sub>3</sub>OD/TMS, δ (ppm)): 154.7 (*J* = 3.02 Hz), 151.5 (*J* = 14.1 Hz), 133.7 (*J* = 2.31 Hz), 133.1 (*J* = 107.5 Hz), 132.9 (*J* = 11.6 Hz), 129.7 (*J* = 12.9 Hz), 123.2 (*J* = 2.3 Hz), 119.8 (*J* = 8.6 Hz), 118.7 (*J* = 9.1 Hz), 117.1 (*J* = 106.5 Hz),

<sup>31</sup>P NMR (CD<sub>3</sub>OD/H<sub>3</sub>PO<sub>4</sub>, δ (ppm)): 34.09.

### Synthesis of Gly-HPO

HPO (10 g, 0.032 mol) was dissolved in 180 ml (1.9 mol) of epichlorohydrin in a three-necked round bottomed flask equipped with reflux condenser and magnetic stirrer. Then, 1g (6 mmol) of benzyltrimethylammonium chloride was added and the mixture was heated a reflux temperature for 60 min. Excess of epichlorohydrin was removed under reduced pressure and the solid residue was dissolved in CH<sub>2</sub>Cl<sub>2</sub>, washed with water, and dried over MgSO<sub>4</sub>. By solving the residue in ethyl acetate and adding diethyl ether the product was obtained as a white solid after cooling (yield 65%), mp 145-147 °C.

C<sub>24</sub>H<sub>23</sub>O<sub>5</sub>P (422): calcd C 68.27%; H 5.47%; P 7.33%; Found: C 68.28%; H 5.87%; P 7.20%.

<sup>1</sup>H NMR (CDCl<sub>3</sub>/TMS, δ (ppm)): 7.70 (m, 4H, *J*<sub>P-H2'</sub> = 13.60 Hz), 7.46 (m, 7H), 7.10 (dd, 1H, *J*<sub>orto</sub> = 9.2 Hz, *J*<sub>meta</sub> = 2.8 Hz), 6.85 (dd, 1H, *J*<sub>orto</sub> = 8.8 Hz, *J*<sub>P-H3</sub> = 5.6), 4.28 (dd, 1H, *J*<sub>gem</sub> = 11.2 Hz, *J*<sub>trans</sub> = 2.8 Hz), 3.97 (m, 1H, *J*<sub>gem</sub> = 11.2 Hz, *J*<sub>cis</sub> = 5.6 Hz), 3.84 (dd, 1H, *J*<sub>gem</sub> = 11.2 Hz, *J*<sub>trans</sub> = 2.4 Hz), 3.71 (dd, 1H, *J*<sub>gem</sub> = 11.2 Hz, *J*<sub>cis</sub> = 5.6 Hz), 3.33 (m), 2.88 (dd, 1H, *J*<sub>gem</sub> = 4.8 Hz, *J*<sub>cis</sub> = 4.4 Hz), 2.72 (dd, 1H, *J*<sub>gem</sub> = 4.8 Hz, *J*<sub>trans</sub> = 2.8 Hz), 2.67 (m), 2.61 (dd, 1H, *J*<sub>gem</sub> = 4.8 Hz, *J*<sub>cis</sub> = 4.4 Hz), 2.32 (dd, 1H, *J*<sub>gem</sub> = 4.8 Hz, *J*<sub>trans</sub> = 2.8 Hz).

$^{13}\text{C}$  NMR ( $\text{CDCl}_3/\text{TMS}$ ,  $\delta$  (ppm)): 153.7 ( $J_{\text{P-C5}} = 3.12$  Hz), 153.2 ( $J_{\text{P-C2}} = 13.78$  Hz), 132.9 ( $J_{\text{P-C1}} = 101.5$  Hz), 132.0 ( $J_{\text{P-C4}} = 2.3$  Hz), 131.8 ( $J_{\text{P-C2}} = 11.6$  Hz), 128.4 ( $J_{\text{P-C3}} = 12.9$  Hz), 122.3, 121.0, 119.0 ( $J_{\text{P-C6}} = 7.64$  Hz), 114.4 ( $J_{\text{P-C3}} = 7.62$  Hz), 69.8, 69.6, 50.2, 49.5, 44.6, 44.3

$^{31}\text{P}$  NMR ( $\text{CDCl}_3/\text{H}_3\text{PO}_4$ ,  $\delta$  (ppm)): 26.90

### Crosslinking Reaction

Diglycidyl compounds and amine hardener were mixed in stoichiometric amounts by dissolving the components in  $\text{CH}_2\text{Cl}_2$  and subsequently evaporating the solvent, at room temperature. Sample bars for dynamomechanical analysis, TGA and burn tests were obtained by placing in a mold and cured at  $140^\circ\text{C}$  for 2h and postcured at  $200^\circ\text{C}$  for 2h.

### Instrumentation

$^1\text{H}$  400 MHz,  $^{13}\text{C}$  100.5 MHz and  $^{31}\text{P}$  161,9 MHz NMR spectra were obtained using a Varian Gemini 400 spectrometer with Fourier transform,  $\text{CD}_3\text{OD}$  or  $\text{CDCl}_3$  as solvents, and TMS or phosphoric acid as internal standards.

Calorimetric studies were carried out on a Mettler DSC821e thermal analyzer using  $\text{N}_2$  as a purge gas (20 ml/min) at scan rates between 5 and  $20^\circ\text{C}/\text{min}$ . Samples were prepared by dissolving Gly-HPO in  $\text{CH}_2\text{Cl}_2$  and mixing the resulting solution with the required amount of DGEBA. This solution was evaporated at room temperature under vacuum. About 5 mg of a known weight of the mixture was put into the aluminium pan and polymerization was monitored in a DSC experiment.

Thermal stability studies were carried out on a Mettler TGA/SDTA851e/LF/1100 with  $\text{N}_2$  or air as a purge gas at scan rates of  $10^\circ\text{C}/\text{min}$ .



Mechanical properties were measured using a dynamic mechanical thermal analysis (DMTA) apparatus (TA DMA 2928). Specimens ( $0.5 \times 10 \times 40 \text{ mm}^3$ ) were tested in a single cantilever configuration. The thermal transitions were studied in the 30-250 °C range at a heating rate of 2 or 5 °C/min and at a fixed frequency of 1 Hz.

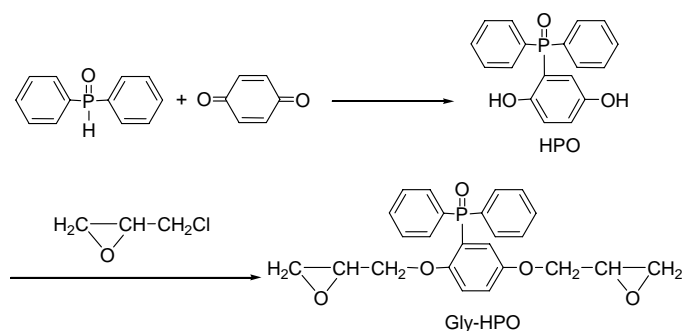
LOI values were measured on a Stanton Redcroft, provided with an Oxygen Analyzer, on polymer bars that measured  $100 \times 6 \times 4 \text{ mm}^3$  and which were prepared by molding. The char produced by the samples was characterized by  $^{31}\text{P}$  MAS NMR spectroscopy.

Degradation studies were carried out in a Carbolite TZF 12/38/400 oven connected to a condenser cooled by liquid nitrogen. GC-MS measurements were carried out using an HP 6890 gas chromatograph with an Ultra 2 capillary column (crosslinked 5% PH ME siloxane) and an HP 5973 mass detector.

SEM was performed on a JEOL JSM 6400 scanning electron microscope, at an activation voltage of 10 kV. For the atomic mapping, an Oxford INCA Energy Dispersive X-Ray Micro Analyzer was used.

## RESULTS AND DISCUSSION

In this work, flame retardant effect of diglycidyl ether of Gly-HPO monomer on amine cured epoxy resins was studied. Scheme 1 depicts the synthesis route of phosphorus-containing epoxy monomer. The starting point for our work was the easy preparation of HPO by Michael addition of diphenyl phosphine oxide to benzoquinone. The reaction was carried out in toluene at room temperature since higher reaction temperatures lead to the formation of Ph-P(O)-P(O)-Ph dimer.<sup>20</sup>



**Scheme 1.**

A very successful method for obtaining glycidyl derivatives utilizes a large excess of epichlorohydrin and benzyltrimethylammonium chloride as a catalyst. This method gave very good results in the synthesis of glycidyl ethers, glycidyl esters, and glycidyl imides,<sup>21</sup> and so we used it to obtain Gly-HPO. The reaction was carried out at 110 °C for 1h and the yield was found as 65%. Both FTIR and NMR spectra were consistent with the expected structures. Characteristic absorptions at 1437 and 1127  $\text{cm}^{-1}$  corresponding to P-Ar and P=O respectively can be observed, as well as the absorption at 914  $\text{cm}^{-1}$  attributed to the oxirane ring. Figure 1 shows the  $^1\text{H}$  NMR spectrum of Gly-HPO with all the assignments. Signals between 7.8 and 6.8 ppm (13H) could be assigned to aromatic protons. The expansion of the spectrum between 4.4 and 2.2 ppm (10H) shows the nonequivalent protons of both glycidylic groups which appear at the chemical shifts expected for glycidylethers. The different chemical shifts for both glycidylic groups are due to the anisotropic effect of aromatic rings on  $\text{H}_{a'}$ ,  $\text{H}_{b'}$ ,  $\text{H}_{c'}$ ,  $\text{H}_{d'}$ , and  $\text{H}_{e'}$  that causes a slight shielding.  $^{13}\text{C}$  NMR spectrum of Gly-HPO and all the assignments are shown in Figure 2. The expansion between 80 and 43 ppm also shows the non equivalence of glycidylic groups. The NMR signals could be assigned unequivocally by means of DEPT, HMBC and gHMQC experiments.

In this work, Gly-HPO has been crosslinked with DDM to obtain final thermosets containing about 6% of phosphorus (DP-6). Mixtures of Gly-HPO and DGEBA were prepared in suitable molar ratios to obtain final materials with a lower phosphorus content, of 1 and 3% (DP-1 and DP-3). Table 1 summarizes the sample compositions, crosslinking data, and  $T_g$ s of the final materials. To compare, the crosslinking data of DGEBA with DDM (DT-0) were also collected in the same table.

Figure 3 shows the DSC plots of these mixtures. As can be seen from the crosslinking exotherms, the reaction starts at about 120 °C and the temperature of the maximum rate of heat release decreases as the Gly-HPO content increases in the mixture. The epoxy monomer with the lowest peak exothermic temperature, under the same curing conditions, was more reactive towards the amine curing agent. Thus, Gly-HPO seems to be more reactive than commercial DGEBA. The  $T_g$  values could be observed in a second dynamic DSC run and are collected in Table 1. It should be pointed out that samples with higher amount of Gly-HPO have higher  $T_g$  values. The differences in  $T_g$  values can be related to the chemical structure of Gly-HPO with a strong polar P=O group and with a bulky pendant moiety that causes restriction in the segmental mobility. The reaction enthalpy values cannot be correlated with the mixture compositions but are slightly lower for the mixtures than for the pure diglycidyl compounds.

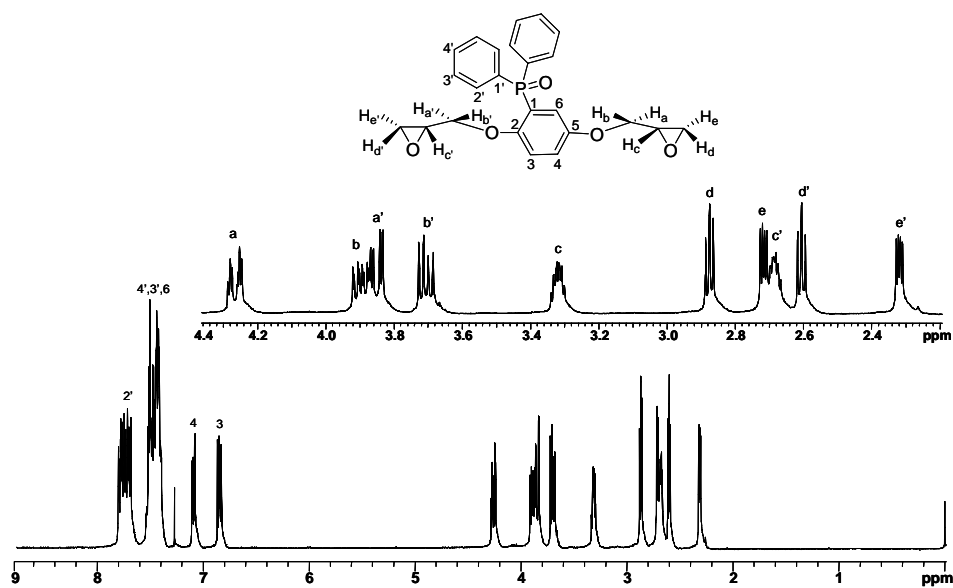


Figure 1.  $^1\text{H}$  NMR spectrum of Gly-HPO ( $\text{CDCl}_3$ , 400 MHz)

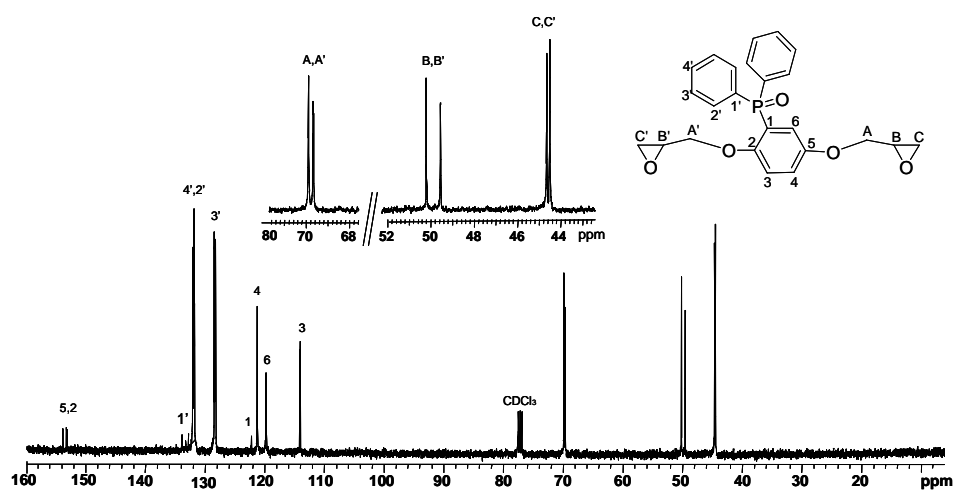


Figure 2.  $^{13}\text{C}$  NMR spectrum of Gly-HPO ( $\text{CDCl}_3$ , 100.5 MHz)

According to DSC data, the networks were prepared by heating at 140 °C for 2h and at 200 °C for 2h. FTIR spectroscopy showed the disappearance of the absorption at 914 cm<sup>-1</sup> due to oxirane ring, thus confirming that the curing reaction takes place to completion.

**Table 1.** Crosslinking of Gly-HPO / DGEBA using DDM as Hardener

| Sample | Gly-<br>HPO/DGEBA<br>Molar ratio, % | P, % | T <sub>onset</sub> <sup>a</sup><br>°C | T <sub>max</sub> <sup>b</sup><br>°C | ΔH <sub>0</sub> <sup>c</sup><br>Kj/ee | T <sub>g</sub> , °C |                    |                     |
|--------|-------------------------------------|------|---------------------------------------|-------------------------------------|---------------------------------------|---------------------|--------------------|---------------------|
|        |                                     |      |                                       |                                     |                                       | 1/2ΔCp              | E'' <sub>Max</sub> | Tanδ <sub>max</sub> |
| DP-0   | 0/100                               | 0    | 137                                   | 168                                 | 109                                   | 160                 | 148                | 158                 |
| DP-1   | 46/53                               | 1    | 128                                   | 163                                 | 88                                    | 179                 | 168                | 179                 |
| DP-3   | 57/ 42                              | 3    | 119                                   | 158                                 | 88                                    | 183                 | 181                | 186                 |
| DP-6   | 100/0                               | 6    | 117                                   | 149                                 | 110                                   | 193                 | 186                | 195                 |

<sup>a</sup> Initial temperature of the crosslinking exotherm.

<sup>b</sup> Temperature of the maximum heat release rate.

<sup>c</sup> Reaction enthalpy values extrapolated to zero heating rate.

The dynamic mechanical behavior of the cured epoxy resins was obtained as a function of the temperature, beginning in the glassy state of each composition to the rubbery plateau of each material (Fig.4). The crosslinking density of a polymer can be estimated from the plateau of the elastic modulus in the rubbery state.<sup>22</sup> However, this theory is strictly valid only for lightly crosslinked materials, and was therefore used only to make qualitative comparisons of the level of crosslinking among the various polymers. As can be seen, crosslinking density results similar for DGEBA/DDM and Gly-HPO/DGEBA/DDM systems and decreases for Gly-HPO/DDM system. It seems that the bulky pendant diphenyl phosphine oxide moieties lead to looser networks.

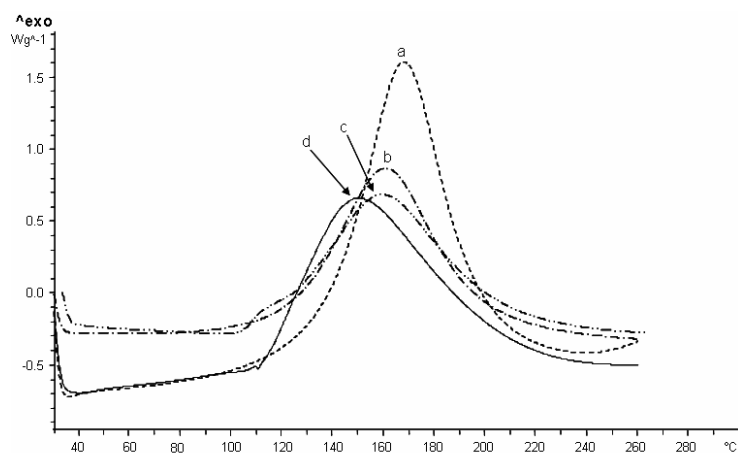


**Figure 3.** DSC plots (10 °C / min) of curing of Gly-HPO/DGEBA with DDM (a) DP-0, (b) DP-1, (c) DP-3 and (d) DP-6.

Figure 5 shows the plots of loss factor ( $\text{Tan } \delta$ ) versus temperature. The  $T_g$ s of the crosslinked materials can be detected as the maximum of the loss modulus ( $E''$ ) or as the  $\alpha$  relaxation peak of the loss factor. Table 1 shows the  $T_g$  values of both measurements. From a practical point of view, the maximum  $E''$  is the most appropriate value since it corresponds to the highest temperature of use. As can be seen,  $T_g$  values from DMTA follow the trend mentioned above:  $T_g$ s increase as the content of Gly-HPO increases. Moreover, the analysis of the height and width of the  $\alpha$  relaxation peak shows trends in the crosslinking densities and network homogeneities as the composition of the material changes. The height of the  $\text{Tan } \delta$  peak, which is associated with the crosslinking density, increases as the Gly-HPO content increases. Because  $\text{Tan } \delta$  is the ratio of viscous components to elastic components, it can be assumed that the decreasing height is associated with lower segmental mobility and fewer relaxing species and is therefore indicative that the networks for the DGEBA-rich samples are tighter.

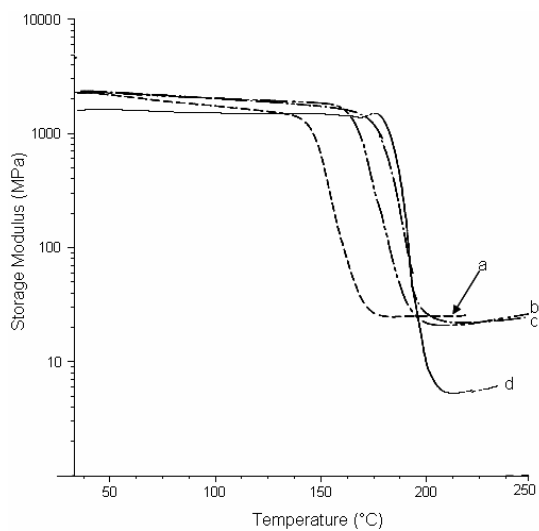


**Figure 4.** Storage moduli of crosslinked polymers (a) DP-0, (b) DP-1, (c) DP-3, and (d) DP-6.

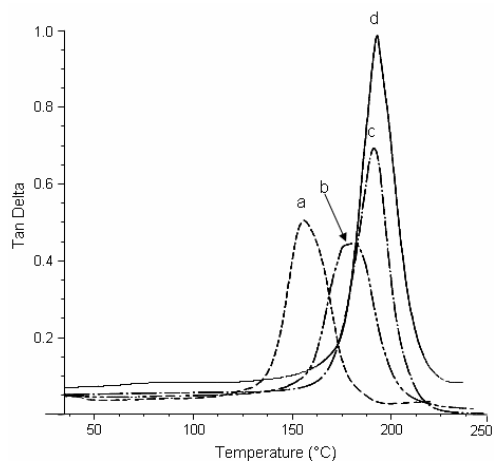


**Figure 5.** Loss factor of crosslinked polymers (a) DP-0, (b) DP-1, (c) DP-3, and (d) DP-6.

The peak width at half-height broadens as the number of branching modes increases, which produces a wider distribution of structures. The range of temperatures at which the different network segments gain mobility therefore increases. There were no significant differences among the samples, thus showing similar branching distribution for all of them.

To examine the effect of phosphorus content on thermal stability and the decomposition behavior, TGA data under nitrogen and air atmospheres were determined and analysed. Figure 6 shows the weight loss with the temperature for the epoxy compositions as well as the derivative curves. Table 2 summarizes the thermogravimetric data.

In nitrogen, when the phosphorus content increases two maximum weight loss rates appear. DP-0 and DP-1 have a single major break in their decomposition curve before their major weight losses level off. This behaviour indicates that there is a single decomposition mechanism which is similar for these resins. However, DP-3 and DP-6 resins, that have a higher phosphorus content, show a two-step break in the decomposition curves, suggesting two distinct and separate decomposition pathways. The decomposition temperatures of these resins are slightly lower than the ones for resins with lower phosphorus content. In air, a second stage of weight loss for the resins with lower phosphorus content and a third stage for the resins with higher phosphorus content are observed at temperatures above 500 °C. Under an air atmosphere, a polymeric material at these temperatures lost weight because the char formed oxidized. It can be seen that the weight loss rate of phosphorus-containing resins is significantly lower than that of the phosphorus-free resins for the thermoxidative degradation. This behavior is in accordance with the mechanism of improved fire performance via phosphorus modification. In this retarded-



degradation phenomenon, the phosphorus groups form an insulating protective layer, which prevents the combustible gases from transferring to the surface of the materials, increases the thermal stability at higher temperatures and improves the fire resistance.

**Table 2.** Thermogravimetric Data of Gly-HPO/DGEBA Mixtures Cured with DDM

| Sample | P % | Nitrogen                        |                                 |                                 |                       | Air                             |                                 |                                 |                                 | LOI<br>%O <sub>2</sub><br>(V/V) |                       |
|--------|-----|---------------------------------|---------------------------------|---------------------------------|-----------------------|---------------------------------|---------------------------------|---------------------------------|---------------------------------|---------------------------------|-----------------------|
|        |     | T <sub>5%</sub> <sup>a</sup> °C | T <sub>m1</sub> <sup>b</sup> °C | T <sub>m2</sub> <sup>b</sup> °C | Char <sup>c</sup> (%) | T <sub>5%</sub> <sup>a</sup> °C | T <sub>m1</sub> <sup>b</sup> °C | T <sub>m2</sub> <sup>b</sup> °C | T <sub>m3</sub> <sup>b</sup> °C |                                 | Char <sup>c</sup> (%) |
| DP-0   | 0   | 365                             | 376                             | -                               | 20                    | 365                             | 376                             | 567                             | -                               | 0                               | 24.4                  |
| DP-1   | 1   | 359                             | 376                             | -                               | 21                    | 353                             | 374                             | 618                             | -                               | 2                               | 31.2                  |
| DP-3   | 3   | 350                             | 376                             | 444                             | 22                    | 356                             | 374                             | 447                             | 570                             | 13                              | 31.1                  |
| DP-6   | 6   | 348                             | 369                             | 444                             | 23                    | 347                             | 383                             | 450                             | 550                             | 22                              | 31.2                  |

<sup>a</sup>Temperature of 5 % weight loss.

<sup>b</sup>Temperature of the maximum weight loss rate.

<sup>c</sup>Char yield at 800 °C.

Char yield under nitrogen is correlated to the polymer's flame retardancy<sup>23</sup> but it should be pointed out that, in our case, the experimental char yields of the phosphorus-containing resins and the phosphorus-free resins are not significantly different. Under air, the char yield is low and increases with the phosphorous content.

To further investigate the thermal degradation mechanism, samples were heated in an oven at 350 °C for 4h with nitrogen or air as purge gas. The degradation temperature was selected from dynamic TGA data and the time at which no weight loss was detected at 350 °C in an isothermal TGA experiment was selected as the degradation time. Volatile products were trapped at the liquid nitrogen temperature and subsequently analysed by GC/MS. At first, the thermal degradation of DGEBA/DDM was carried out to compare to the phosphorus-containing resins. The analysis of the evolved gases shows that the dehydration of secondary alcohol groups is the first step of degradation in epoxy resins, as has been previously described.<sup>24,25</sup> C-

C double bonds formed in this step induce the  $\beta$ -escision of weakened C-N or C-O bonds. Thus, GC/MS analysis identified benzene and nitrogen-containing aromatic compounds such as benzene, aniline, N-methylaniline, N,N-dimethylaniline, N-ethylaniline, N,4-dimethylaniline, substituted indols, and quinoleines. Samples containing Gly-HPO were studied in a similar way heating at 350 °C for 4h.

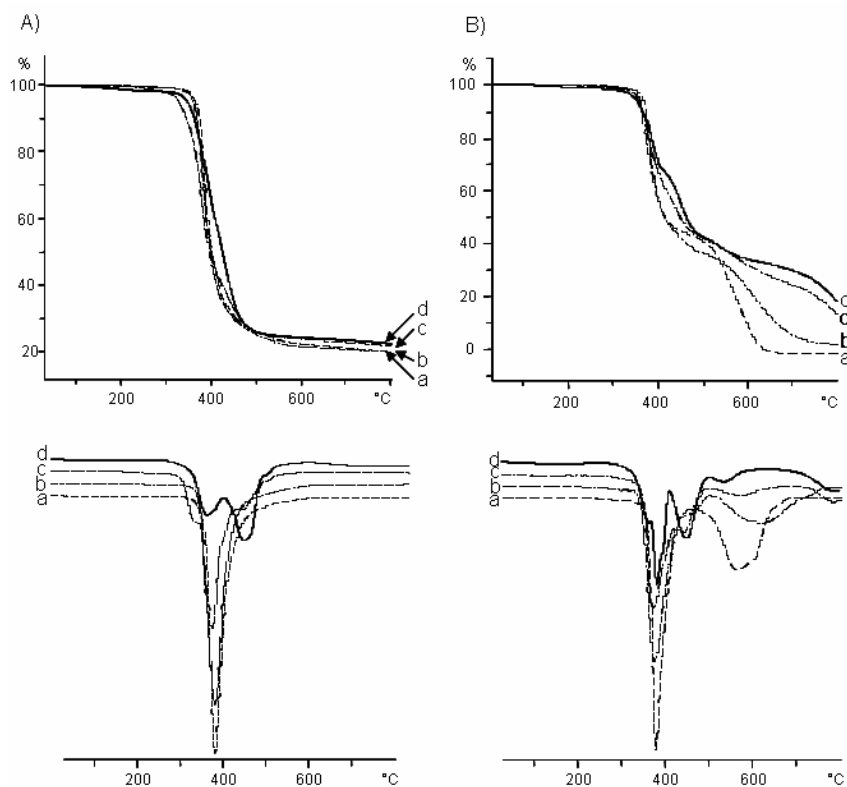
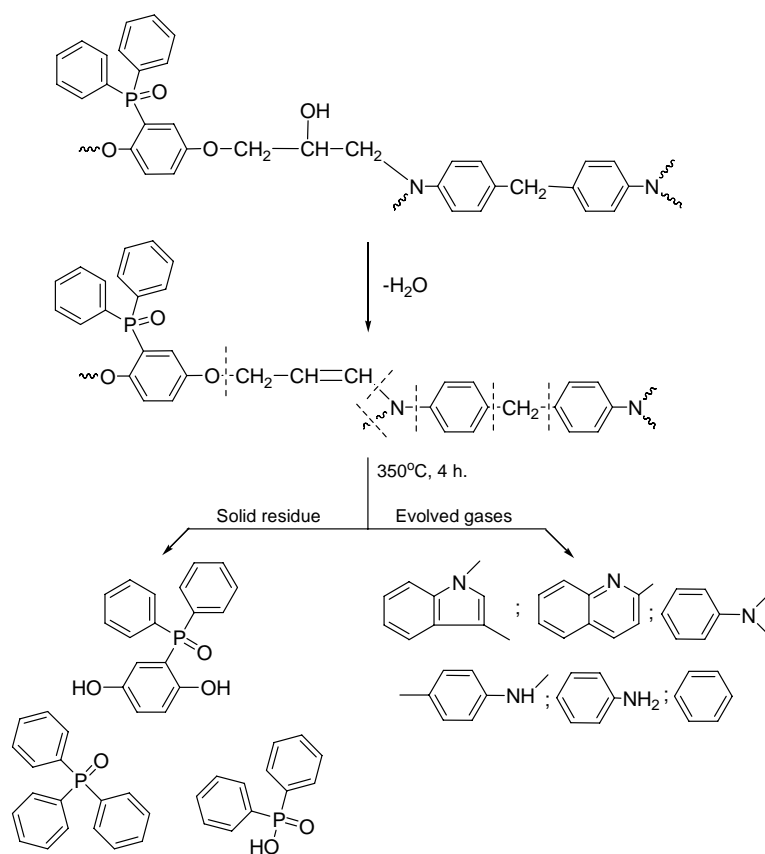


**Figure 6.** TGA plots (10 °C /min) and first derivative curves of crosslinked polymers (a) DP-0, (b) DP-1, (c) DP-3, and (d) DP-6, (A) in N<sub>2</sub> and (B) in air.

The analysis of evolved gases resulted completely similar to the one described earlier. Solid residues were extracted with methanol, and  $^{31}\text{P}$  NMR spectroscopy allowed to identify phosphorus-containing compounds as is shown in Scheme 2. When they were heated at 600 °C the characterization of the solid residues by  $^{31}\text{P}$  MAS NMR spectroscopy show a broad peak at 0 ppm typical of phosphoric acid.

The LOI values, which can be taken as an indicator to evaluate the polymer's flame retardancy of the phosphorus-containing resins, were also measured and shown in Table 2. As can be seen the presence of phosphorus increases the LOI values even when the phosphorus content is low, and no significant differences with the phosphorous content are observed.

To better understand the role of phosphorous in the flame retardant properties of the polymer, element mapping was performed with energy-dispersive X-ray spectroscopy on the surfaces of the initial samples and of the samples after the LOI test. P mapping of the DP-2 initial sample indicated a homogeneous distribution of this element, as can be observed in the micrograph (Fig. 7(a,b)). The white points in the Figure denote P rich zones. After burning, the presence of phosphorus in the char was confirmed by  $^{31}\text{P}$  MAS NMR spectroscopy, which shows a broad peak at 0 ppm typical of phosphoric acid. Figure 7(c) is the SEM micrograph of the top surface view of the DP-2 specimen after the LOI test.



Scheme 2.

The burned zone has the appearance of a black charred material with small cavities. The P distribution (Fig. 7(d)) shows that the phosphorus density increased towards the top burned surface and that a phosphorus-rich layer formed. When they are heated, phosphorus compounds can form glass like polyphosphoric acid, which protects the burning surface, or they can form inflammable phosphorus-carbon char by reacting with organic components. This protective layer is resistant to even higher temperatures and shields the underlying polymer from attack by oxygen and radiant heat as well as prevents the combustible gases from transferring to the surface of the materials and feed the flame, thus improving the fire resistance.

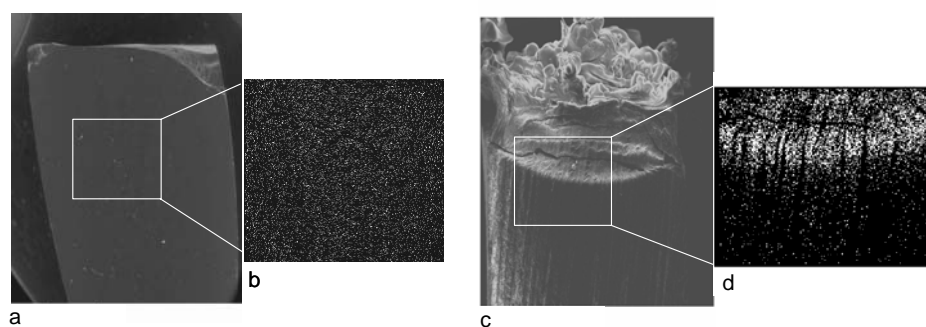


**Figure 7.** SEM and SEM-energy-dispersive X-ray spectroscopy P mapping micrographs of sample DP-2 before (a,b) and after (c,d) burning LOI test.

## CONCLUSIONS

Phosphorus-containing epoxy resins with different phosphorus content were obtained from Gly-HPO and DGEBA by crosslinking with DDM. The crosslinking behavior does not show significant differences among the different mixtures or between the mixtures and pure diglycidyl compounds.  $T_g$  values of thermosets increase with the DGEBA content, as well as crosslinking density. Char yields under nitrogen do not show significant differences among the phosphorus-containing resins and the phosphorus-free resin. The presence of phosphorus increases the LOI values even when the phosphorus content is low (1%), and no significant differences with the phosphorus content are observed.

## Acknowledgements

The authors express their thanks to CICYT (Comisión Interministerial de Ciencia y Tecnología) (MAT2005-01593) for financial support for this work.

## REFERENCES

- <sup>1</sup> May, C.A. Epoxy Resins: Chemistry and Technology, Marcel Dekker. New York 1998.
- <sup>2</sup> Petrie, E.M. Epoxy Adhesive Formulations; McGraw-Hill, New York 2006.
- <sup>3</sup> Dean, J. M.; Vergheese, N.E.; Pham, H. Q.; Bates, F. S. *Macromolecules* 2003, 36, 9267.
- <sup>4</sup> Lu, S.-Y.; Hamerton, I. *Prog Polym Sci* 2002, 27, 1661.
- <sup>5</sup> Levchik, S. V.; Weil, E. D. *Polym Int* 2004, 53, 1901 and references therein.
- <sup>6</sup> Jain, P. ; Choudhary, V.; Varma, I. K. *J Macromol Sci-Polymer Reviews* 2002, C42(2), 139 and references therein.
- <sup>7</sup> Weil, E.; Levchik, S. V. *J Fire Sci* 2004, 22, 25 and references therein.
- <sup>8</sup> Hergenrother, P.M.; Thompson, C. M.; Smith Jr, J.G.; Connell, J.W.; Hinkley, J. A.; Lyon, R. E.; Moulton, R. *Polymer* 2005, 46, 5012.
- <sup>9</sup> Wu, Q.; Lu, J.; Qu, B. *Polym Int* 2003, 52, 1326.
- <sup>10</sup> Gravalos, K. G. *J Polym Sci Part A: Polym Chem* 1992, 30, 2521.
- <sup>11</sup> Liu, Y. L.; Jeng, R. J.; Chiu, Y. S. *J Polym Sci Part A: Polym Chem* 2001, 39, 1716.
- <sup>12</sup> Quittmann, U.; Lecamp, L. ; Youssef, W.; Brunel, C. *Macromol Chem Phys* 2001, 202, 608.
- <sup>13</sup> Wang, S.; Zhuang, H.; Shobha, H.K.; Glass, T. E.; Shankarapandian, M.; Shultz, A. R.; McGrath, J. E. *Macromolecules* 2001, 34, 8051.
- <sup>14</sup> Alcón, M. J.; Ribera, G.; Galià, M.; Cádiz, V. *J Polym Sci Part A: Polym Chem* 2005, 43, 3510.
- <sup>15</sup> Alcón, M.; Ribera, G.; Galià, M.; Cádiz, V. *Polymer* 2003, 44, 7291.
- <sup>16</sup> Ribera, G.; Mercado, L.A.; Galià, M.; Cádiz, V. *J Appl Polym Sci* 2006, 99, 1367.
- <sup>17</sup> Rauhut, M.M.; Currier, H.A. *J Org Chem* 1961, 26, 4626.
- <sup>18</sup> Hergenrother, P.M.; Watson, K.A.; Smith Jr, J.G.; Connell, J.W.; R. Yokota. *Polymer* 2002, 43, 5077.
- <sup>19</sup> Brown, J.M.; Woodward, S. *J Org Chem* 1991, 56, 6803.
- <sup>20</sup> Rey, P.; Taillades, J.; Rossi, J.C.; Gros, G. *Tetrahedron Lett* 2003, 44, 6169.
- <sup>21</sup> Serra, A.; Cádiz, V.; Mantecón, A.; Martínez P.A. *Tetrahedron*, 1985, 41, 763.
- <sup>22</sup> Tobolsky, A. V.; Carlson, D.W.; Indictor, N. J. *J Polym Sci* 1961, 54, 175.
- <sup>23</sup> Van Krevelen D.W. *Polymer* 1975, 16, 615.
- <sup>24</sup> Levchik, S.V.; Camino, G; Luda, M.P.; Costa, L.; Muller, G.; Costes, B. *Polym Deg Stab* 1998, 60, 169
- <sup>25</sup> Grassie, N.; Guy, M.J. *Polym Deg Stab* 1985, 13, 11.

---

*2.4.2. PREPARATION, THERMAL PROPERTIES AND FLAME  
RETARDANCY OF PHOSPHORUS- AND SILICON-CONTAINING EPOXY  
RESINS*

---

UNIVERSITAT ROVIRA I VIRGILI  
RESINAS EPOXI Y BENZOXAZINAS FOSFORADAS Y SILILADAS RETARDANTES A LA LLAMA  
Marisa Elisabet Spontón  
ISBN:978-84-691-9480-5/DL:T-22-2009



## PREPARATION, THERMAL PROPERTIES AND FLAME RETARDANCY OF PHOSPHORUS- AND SILICON-CONTAINING EPOXY RESINS

M. Spontón, L. A. Mercado, J.C. Ronda, M. Galia, V. Cádiz

Departament de Química Analítica i Química Orgànica. Universitat Rovira i Virgili Campus Sescelades Marcel·lí Domingo s/n. 43007 Tarragona. Spain.  
e-mail: marina.galia@urv.cat

### ABSTRACT

Phosphorus and silicon-containing epoxy resins were prepared from (2,5-dihydroxyphenyl) diphenyl phosphine oxide (Gly-HPO), diglycidyl ether methylphenyl silane (DGMPS) and 1,4-bis(glycidyl dimethyl silyl)benzene (BGDMSB) as epoxy monomers and diaminodiphenylmethane (DDM), Bis(3-aminophenyl)methyl phosphine oxide (BAMPO) and bis(4-aminophenoxy)dimethyl silane (APDS) as curing agents. Epoxy resins with different phosphorus and silicon content were obtained. Their thermal, dynamic mechanical and flame retardant properties were evaluated. The high LOI values confirmed that epoxy resins containing hetero-atoms are effective flame retardants, but a synergistic efficiency of phosphorus and silicon on flame retardation was not observed.

**Keywords:** Flame retardance, Epoxy Phosphorus-containing resins, Silicon-containing resins.

## INTRODUCTION

Epoxy resins are used worldwide on a large scale for adhesive, lamination, coating applications, so forth. They have excellent moisture, solvent and chemical resistances, toughness, low shrinkage on cure, high adhesion to many substrates and superior electrical and mechanical resistance properties.<sup>1,2</sup> To extend the applications of epoxy resins as electronic materials and in the aerospace industry, it is crucial to improve their thermal and flame resistance. Several approaches have been reported in the literature for the improvement of flame resistance. Halogenated compounds have been widely used as flame retardant in the past. The major problem encountered with these systems is the fire hazards derived from the formation of highly toxic and corrosive products during combustion. With safety and environmental concerns in mind, epoxy resins that are flame resistant and halogen-free have been the focus of attention by researchers in recent years.<sup>3,4</sup>

A traditional technique of preparing flame retardant epoxy resins is to blend the flame retardant additive with the polymer. As there is no chemical bonding between the flame retardant additive and the polymer, some shortcomings, such as low efficiency of flame retardance, leaking out during processing and usage, and detrimental effects on polymer's thermal and mechanical properties accompany the introduction of flame retardant into the polymer. Therefore, the present trend is moving towards using reactive type flame retardants, which are permanently bonded to the polymer.<sup>5</sup> Preparing a reactive type flame retardant requires developing novel compounds with specific reactive functional groups, as flame retardant oxirane and diamine compounds for epoxy resins. Among non-halogenated flame retardants, phosphorus containing compounds are

attractive owing to their low generation of smoke and toxic gases and the high flame retardant efficiency.<sup>6</sup> Phosphorus-containing polymers confer fire resistance mainly by modifying the thermal decomposition of the polymers, in favor of reactions yielding carbonaceous char rather than CO and CO<sub>2</sub>. They form a surface layer of protective char during fire before the unburned material begins to decompose. The char acts as a barrier to inhibit gaseous products from diffusing to the pyrolysis zone and to shield the polymer surface from heat and air.<sup>7</sup> The efficiency of flame retardation of phosphorus basically depends on the amount of char formation, thus, by improving the thermal stability of phosphorus char at high temperatures the flame retardant efficiency could be improved. Silicon-containing polymers are described that can degrade forming thermally stable silica, which have the tendency to migrate to the char surface serving as a protection layer to prevent further degradation of char at high temperatures.<sup>8</sup>

Moreover, enhancement of flame retardancy of epoxy resins has been achieved by incorporation of phosphorus and silicon into epoxy resins with bringing a P-Si synergistic effect of flame retardation.<sup>9-13</sup> While under flame exposure, phosphorus provided a tendency for char formation, silicon provided an enhancement of the thermal stability of the char and introducing both elements may successfully combine these two factors in a strong flame retardation mechanism.

In our search for new flame retardant epoxy monomers and curing agents, we considered phosphine oxides. In a previous work, we synthesized the diglycidyl ether of (2,5-dihydroxyphenyl)diphenyl phosphine oxide (Gly-HPO) and investigated its thermal behaviour and reactivity. Systems containing different amounts of Gly-HPO and DGEBA

cured with primary amines were also described and their thermal, mechanical and flame retardant properties were discussed.<sup>14</sup> We also investigated silicon-containing compounds as flame retardants: silicon containing glycidyl monomers and pre-polymers have been cured with primary amines and the thermal stability and flame retardant properties have been reported.<sup>15</sup> We described a new silicon containing monomer, diglycidyloxymethylphenyl silane (DGMPS) and we examined the incorporation of different amounts of silicon into the epoxy resin by the curing of DGMPS/DGEBA system.<sup>16</sup> In the present work, phosphorus and silicon were introduced into the epoxy resins by curing phosphorus and silicon epoxy monomers with diaminodiphenylmethane (DDM) or a phosphorus- or silicon- containing diamines. In this way, the phosphorus and silicon contents of the resins were altered. The degradation behaviours and flame retardant properties were investigated to examine the possibility of phosphorus-silicon synergistic effect.

## EXPERIMENTAL

### Materials

Methylphenyl silane (Aldrich), 1,4-bis(hydroxydimethyl silyl) benzene (ABCR), bis(dimethylamino)dimethyl silane (ABCR), 4,4' diaminodiphenyl methane (DDM) (Aldrich), triphenylphosphine (Aldrich), copper (II) chloride (Probus), sodium sulfite (Baker), potassium *tert*-butoxide (Fluka) and Wilkinson catalyst (Aldrich) were used as received. Glycidol (Aldrich) was vacuum distilled over CaH<sub>2</sub> prior to use. *p*-Aminophenol (Fluka) was recrystallized from ethanol. Copper (I) chloride was prepared by the reduction of copper (II) chloride with sodium sulfite. All solvents were purified by standard procedures.

Diglycidyl ether of (2,5-dihydroxyphenyl)diphenyl phosphine oxide (Gly-HPO) was obtained from (2,5-dihydroxyphenyl)diphenyl phosphine oxide by reaction with epichlorohydrin and BTMA as catalyst as has been previously described.<sup>14</sup> Bis(3-aminophenyl)methyl phosphine oxide (BAMPO) was prepared by nitration of diphenylmethyl phosphine oxide and subsequent reduction with HCl and SnCl<sub>2</sub>.<sup>17</sup>

#### **Synthesis of [(Ph<sub>3</sub>P)CuH]<sub>6</sub>**

Triphenylphosphine (31.0 g, 0.12 mol), copper(I) chloride (4.6 g, 0.045 mol) and toluene (200 mL) were added to a dry, septum-capped 500 mL Schlenk flask and placed under argon. The resultant solution was stirred and potassium *tert*-butoxide (5.1 g, 0.45 mol) was added. The yellow mixture was placed under positive pressure of hydrogen and stirred overnight. During this period the solution turned red, then dark red, and some brown material precipitated. The reaction mixture was transferred under argon pressure to a 500 mL flask and 250 mL of pentane was added. The solution was cooled promoting crystallization of the product, which was filtered and washed several times with pentane and toluene and dried under vacuum to give 10.5 g (75% yield) of dark red crystals.

#### **Synthesis of diglycidyloxy methylphenyl silane (DGMPS)**

Into a three-necked round bottom flask equipped with a magnetic stirrer, a dropping funnel and a reflux condenser, 30 mL of anhydrous toluene, 12.0 g (0.162 mol) of freshly distilled glycidol and 6.7×10<sup>-2</sup> g (7.2×10<sup>-2</sup> mol, 0.05 mol% per Si-H) of Wilkinson catalyst were placed. The red solution was degassed with argon and heated at 60 °C for 30 min., after which 8.8 g (0.072 mol) of methylphenyl silane was added dropwise over 1h. Vigorous H<sub>2</sub> evolution was observed immediately and the reaction mixture was kept under positive argon pressure during the entire course of the reaction in

order to flush the H<sub>2</sub> gas from the reaction mixture. The solution was stirred at 60 °C for 1h to ensure complete conversion and was allowed to cool down to ambient temperature overnight. The reaction mixture was washed with water and phosphate buffer and the organic layer was dried over MgSO<sub>4</sub>, filtered and then the solvent was evaporated at reduced pressure. The product obtained was dissolved in hexane/ethylacetate (8:2) mixture and filtered through a short column of silicagel to remove traces of catalyst and other polar impurities. The obtained colorless solution was concentrated under vacuum to give a clear oil (74% yield) essentially pure by <sup>1</sup>H NMR.

<sup>1</sup>H NMR (CDCl<sub>3</sub>/TMS, δ (ppm)): 7.65 (2H, m); 7.42 (3H, m); 4.03 (2H, dd, 12.0, 3.2 Hz); 3.75 (2H, dd, 12.0, 5.2 Hz); 3.15 (2H, m); 2.78 (2H, dd, 4.4, 2.8 Hz); 2.65 (2H, dd, 4.4, 2.8 Hz); 0.42 (3H, s).

<sup>13</sup>C NMR (CDCl<sub>3</sub>/TMS, δ (ppm)): 134.0 (d) ; 132.2 (s) ; 130.4 (d); 127.9 (d); 63.6 (t); 52.0 (d); 44.5 (t) ; -4.4 (q).

#### **Synthesis of 1,4-bis(glycidylodimethyl silyl)-benzene (BGDMSB)**

20 mL (22.4 g, 0.3 mol) of glycidol dissolved in 40 ml of anhydrous toluene and 0.3 g (0.5 mol % per Si-H) of copper hydride hexamer catalyst were introduced into a 250 ml Schlenk flask containing a magnetic stirrer and sealed with a rubber septum. The mixture was degassed and infused with argon. 19.5 g (22.4 mL, 0.1 mol) of 1,4-bis(dimethylsilyl benzene) was introduced dropwise into the reaction flask via dropping funnel for 10 min. At this time the reaction solution became red in colour and gas evolution was observed. The reaction mixture was kept at room temperature and after 5 h the reaction was complete. After washing with 5% of NH<sub>3</sub> and water three times and drying with MgSO<sub>4</sub>. The resulting clear oil was dissolved in hexane/ethyl acetate (9:1) mixture and filtered through a short column of

silicagel to remove polar impurities. By concentration under vacuum a colorless oil (78% yield), pure by  $^1\text{H}$  NMR, was obtained.

$^1\text{H}$  NMR ( $\text{CDCl}_3/\text{TMS}$ ,  $\delta$  (ppm)): 7.58 (4H, s); 3.82 (2H, dd, 12.0, 3.3 Hz); 3.60 (2H, dd, 12.0, 5.4 Hz); 3.09 (2H, m); 2.76 (2H, dd, 5.2, 4.1 Hz); 2.59 (2H, dd, 5.2, 2.9 Hz); 0.42 (12H, s).

$^{13}\text{C}$  NMR ( $\text{CDCl}_3/\text{TMS}$ ,  $\delta$  (ppm)): 139.7 (s) ; 132.8 (d); 63.8 (t); 52.1 (d); 44.6 (t); -1.9 (q).

### Synthesis of bis(4-aminophenoxy)dimethyl silane (APDS)

Into a three-necked round bottom flask equipped with a magnetic stirrer, a dropping funnel and a reflux condenser, 37.3 g (0.34 mol) of p-aminophenol and 100 mL of anhydrous toluene were placed. The mixture reaction was vigorously stirred under argon and heated to 110 °C. Bis(dimethylamino)dimethyl silane (25 g, 0.17 mol) was added dropwise for 60 min. The reaction was kept at this temperature for 36 h until no dimethylamine evolution was observed. The dark yellow suspension was filtered to obtain a yellow solution that was concentrated under vacuum to obtain 40 g of a yellow oil that solidifies on standing overnight. The product was purified by recrystallization from hexane/ethyl acetate (9:1), and obtained as a yellow solid with a 62% yield.

$^1\text{H}$  NMR ( $\text{CDCl}_3/\text{TMS}$ ,  $\delta$  (ppm)): 6.75 (4H, d); 6.55 (4H, d); 3.43 (4H, s); 0.30 (6H, s).

$^{13}\text{C}$  NMR ( $\text{CDCl}_3/\text{TMS}$ ,  $\delta$  (ppm)): 146.7 (s) ; 140.0 (s); 120.3 (d); 116.2 (d); -2.5 (q).

### Curing reactions

The curing conditions were established by Differential Scanning Calorimetry. Samples (Table 1) were prepared by the dissolution of epoxy monomers and curing agent in  $\text{CH}_3\text{OH}$  or  $\text{CH}_2\text{Cl}_2$ . Then this solution was

evaporated at room temperature in vacuum. About 5 mg of a known weight of the mixture was put into the aluminum pan, and the polymerization was monitored in a dynamic DSC experiment using a heating rate of 10 °C/min. The curing conditions are shown in Table 2. Molded epoxy resins for DMTA and LOI measurements were obtained by molding about 1.5 g of a known weight of the mixture obtained as above described.

### Instrumentation

<sup>1</sup>H (400 MHz) and <sup>13</sup>C (100.5 MHz) NMR spectra were obtained with a Varian Gemini 400 spectrometer with Fourier Transform, with CDCl<sub>3</sub> as a solvent, and with TMS as an internal standard. The IR spectra were obtained with a ATR-FTIR JASCO 680.

Calorimetric studies were carried out on a Mettler DSC821e thermal analyser using N<sub>2</sub> as a purge gas (20 ml/min). Thermal stability studies were carried out on a Mettler TGA/SDTA851e/LF/1100 with N<sub>2</sub> and air as a purge gas at scan rates of 10 °C/min. Mechanical properties were measured using a dynamic mechanical thermal analysis (DMTA) apparatus (TA DMA 2928). Specimens (3 x 6 x 10 mm<sup>3</sup>) were tested in a three point bending configuration. The thermal transitions were studied in the -100 -250 °C range at a heating rate of 5 °C/min and at a fixed frequency of 1 Hz. LOI values were measured on a Stanton Redcroft, provided with an oxygen analyser, on bars of the polymers 100 x 6 x 3 mm<sup>3</sup>).

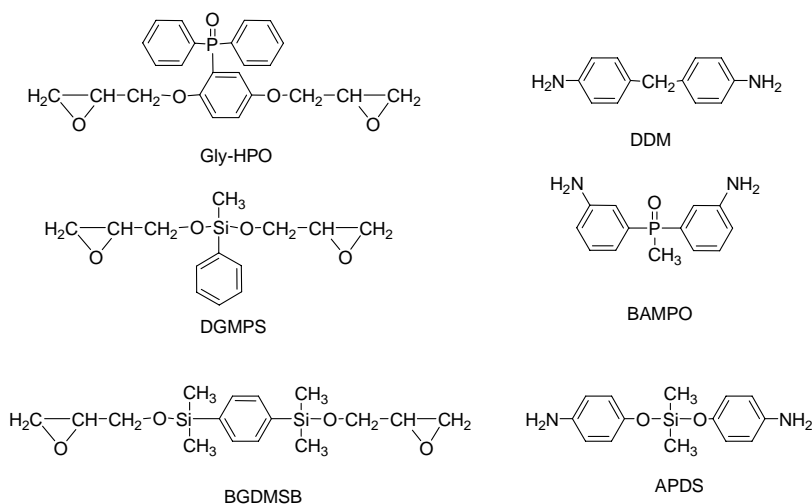
## RESULTS AND DISCUSSION

By using phosphorus- or silicon-containing epoxy compounds or phosphorus- or silicon-containing diamine compounds as curing agents, epoxy resins with different phosphorus or silicon contents are obtained.



Based on the above, phosphorus-containing epoxy, Gly-HPO<sup>14</sup>, and phosphorus-containing amine, BAMPO, previously described<sup>17</sup> are used (Scheme 1). Silicon-containing diepoxides, DGMPS<sup>16</sup> and BGDMSB<sup>15</sup> (Scheme 1) were previously synthesized by catalysed transesterification of the dimethoxymethylphenyl silane with allylic alcohol and by condensation of 1,4-bis(hydroxydimethyl silyl)benzene with allylic alcohol respectively, followed by the epoxidation of the intermediate compounds in both cases. These synthetic approaches in two steps, led to a products with moderate yields.

Alkoxysilanes are usually prepared by reaction of chlorosilanes with either alcohols or alkoxides. Since these reactions either involve acidic (evolution of HCl) or basic conditions (alkoxide, or base as HCl acceptor), alternative methods are advantageous. A particularly mild method is the alcoholysis of hydrogen-substituted silanes, because only H<sub>2</sub> is formed as a byproduct. However, alcohols normally do not attack silanes in the absence of a catalyst and most silanes undergo alcoholysis only in the presence of either strongly nucleophilic or electrophilic catalysts. A limited number of transition metal complexes have been reported as homogeneous catalyst for the alcoholysis of hydrosilanes. The Wilkinson catalyst, one of the more active catalyst has been used in the present work in the synthesis of DGMPS. The reaction took place at 60 °C for 1h. The Wilkinson catalyst, as most of the transition metal complexes is not active to catalyze the alcoholysis of trialkylsilanes. On the other hand, the copper hydride complex [(Ph<sub>3</sub>P)CuH]<sub>6</sub> is a very reactive catalyst for the alcoholysis of hydrosilanes under mild reaction conditions.<sup>18</sup> It provides silyl ethers in generally high yields. In this case the tertiary silane, 1,4-bis(dimethyl silyl)benzene, reacts with glycidol at room temperature for 5h to give the corresponding silylglycidylether.



Scheme 1

Epoxy resins have been prepared by curing with stoichiometric amounts of diamine with the compositions, phosphorus and silicon contents that are shown in Table 1. The reactions were monitored by DSC and showed exotherms with crosslinking enthalpy values and onset and maximum heat release rate temperatures collected in Table 1. Fig. 1 depicts the crosslinking exotherms for Gly-HPO with different amines (a), for the APDS amine with different epoxy compounds (b) and for the system Gly-HPO/DGMPMS with different amines (c). The diamine curing agent with the lowest peak exotherm temperature under the same curing conditions was more reactive toward the epoxy resin. The APDS amine showed the highest reactivity and the BAMPO the lowest, either when reacts with pure epoxy monomer, Gly-HPO, or with a mixture of epoxy monomers, Gly-HPO/DGMPMS. The reactivity may vary because of the electronic effects. An electron-donating group by resonance in the amine compound, e.g. the oxygen atom in APDS, increased the electron density of the amine groups toward oxirane ring. This effect is lower for DDM because methylene group is an electron-

donating group by inductive effect. Incorporating electron-withdrawing groups such as  $-P=O$  groups in BAMPO, reduced the activity in curing epoxides.

In addition, the epoxy resins with the lowest peak exothermic temperature under the same curing conditions were more reactive towards the curing agent. As can be seen in Fig. 1 b) Gly-HPO and DGMPs showed the highest reactivity. We previously reported<sup>16,19</sup> that silicon-containing oxiranes have higher reactivity due to electronic effects. The silicon atom acts as a  $\pi$  acceptor, withdrawing the electron density of the oxygen atom and increasing its electron-withdrawing character. Therefore, the electrophilic character of the oxirane carbons increases. The high reactivity of Gly-HPO may be also explained due to an increase in the electron-withdrawing character of the oxygen, because the resonance effect of  $P=O$  group in the ortho position to the glycidyl moiety. BGDMSB showed the lowest reactivity because the  $\pi$  acceptor character of the silicon atom towards oxygen atom diminishes due to the adjacent aromatic ring. Even for the systems Gly-HPO/BGDMSB which show the higher reactivity difference between epoxy monomers only an exotherm appears, thus indicating that crosslinking takes place homogeneously.

**Table 1.** Compositions, phosphorus and silicon content and curing data of the epoxy resins.

| Sample | Epoxy monomer <sup>a</sup> | Curing agent <sup>b</sup> | P % | Si%  | T <sub>onset</sub> <sup>c</sup><br>(°C) | T <sub>max</sub> <sup>d</sup><br>(°C) | ΔH <sub>0</sub> <sup>e</sup><br>(Kj/ee) |
|--------|----------------------------|---------------------------|-----|------|---|---------------------------------------|---|
| 1      | Gly-HPO                    | DDM                       | 6.0 | -    | 120                                     | 150                                   | 82                                      |
| 2      | Gly-HPO                    | BAMPO                     | 8.5 | -    | 137                                     | 168                                   | 95                                      |
| 3      | Gly-HPO                    | APDS                      | 5.5 | 2.5  | 112                                     | 143                                   | 82                                      |
| 4      | DGMPS                      | DDM                       | -   | 7.7  | 120                                     | 157                                   | 83                                      |
| 5      | DGMPS                      | BAMPO                     | 4.0 | 7.2  | 132                                     | 172                                   | -                                       |
| 6      | DGMPS                      | APDS                      | -   | 10.4 | 117                                     | 145                                   | 84                                      |
| 7      | BGDMSB                     | DDM                       | -   | 12.8 | 111                                     | 168                                   | 83                                      |
| 8      | BGDMSB                     | BAMPO                     | 3.4 | 12.2 | 148                                     | 196                                   | -                                       |
| 9      | BGDMSB                     | APDS                      | -   | 14.7 | 129                                     | 162                                   | 83                                      |
| 10     | Gly-HPO/DGPMS              | DDM                       | 3.5 | 3.2  | 119                                     | 159                                   | 88                                      |
| 11     | Gly-HPO/DGPMS              | BAMPO                     | 6.6 | 3.0  | 136                                     | 170                                   | -                                       |
| 12     | Gly-HPO/DGPMS              | APDS                      | 3.2 | 5.8  | 111                                     | 142                                   | 82                                      |
| 13     | Gly-HPO/BGDMSB             | DDM                       | 3.2 | 5.8  | 117                                     | 163                                   | 91                                      |
| 14     | Gly-HPO/BGDMSB             | BAMPO                     | 6.2 | 5.5  | 123                                     | 170                                   | 97                                      |
| 15     | Gly-HPO/BGDMSB             | APDS                      | 3.0 | 8.1  | 114                                     | 156                                   | 81                                      |

<sup>a</sup> For the mixtures of epoxy monomers, a 1:1 mol ratio was used.

<sup>b</sup> Stoichiometric amounts were used in all cases.

<sup>c</sup> Initial temperature of the crosslinking exotherm (10 °C/min).

<sup>d</sup> Temperature of the maximum heat release rate (10 °C/min).

<sup>e</sup> Reaction enthalpy values per epoxy equivalent.

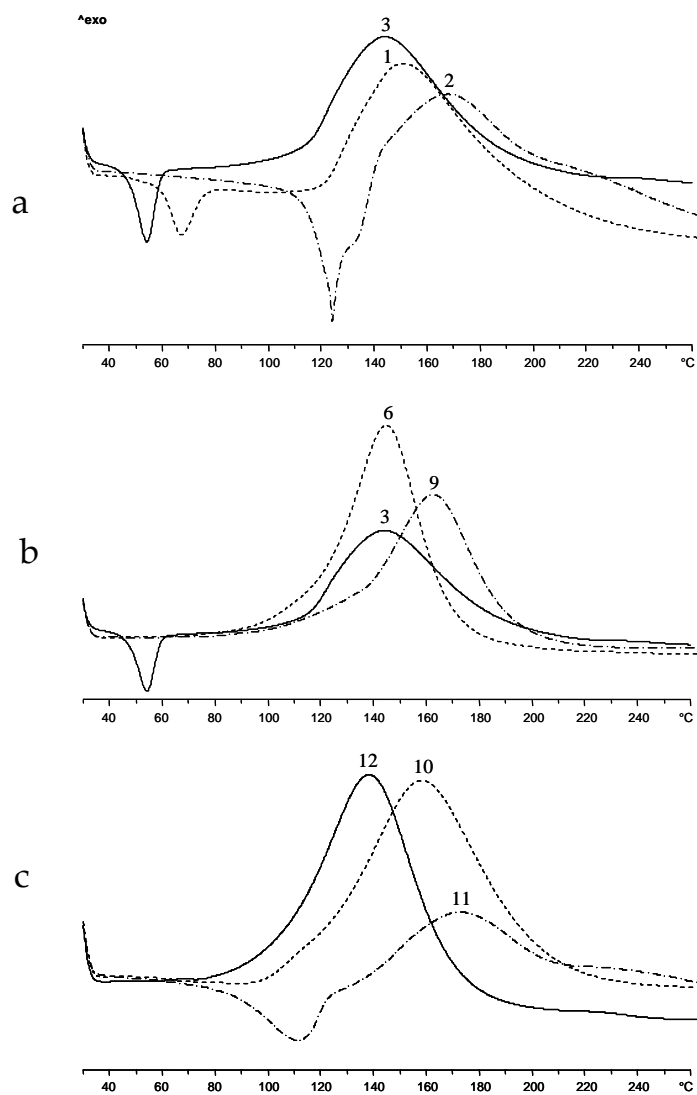


**Figure 1.** DSC plots of systems a. 1 (Gly-HPO/DDM), 2 (Gly-HPO/BAMPO) and 3 (Gly-HPO/APDS); b. 3 (Gly-HPO/APDS), 6 (DGMPs/APDS) and 9 (BGDMSB/APDS); c. 10 (Gly-HPO/DGMPs/DDM), 11 (Gly-HPO/DGMPs/BAMPO) and 12 (Gly-HPO/DGMPs/APDS)

According to DSC data epoxy networks were prepared at the curing and post-curing conditions showed in Table 2. FTIR spectroscopy showed the disappearance of the absorption at  $910\text{ cm}^{-1}$  of the oxirane ring, thus confirming that the curing reaction takes place to completion.

Table 2 also summarizes the  $T_g$ s of the crosslinked materials that can be detected as an endothermic step in the heat flow by DSC, as the maximum of the loss modulus ( $E''$ ) and as the  $\alpha$  relaxation peak of the loss factor by DMTA. As can be seen the most decisive parameter that affect the  $T_g$  value is the epoxy monomer. Higher  $T_g$  values were obtained for Gly-HPO, which contains a strong polar P=O group and a bulky pendant moiety that causes restriction in the segmental mobility. The  $T_g$  values decrease for the DGMPS epoxy thermosets, what can be explained by the presence of Si-O and Si-C units and the lower proportion of aromatic moieties in the backbone.

The  $T_g$  of thermosets from BGDMSB have the lowest  $T_g$  values that must be related to a larger volume fraction of Si-O and Si-C units in the backbone. The mixed epoxy systems exhibit a single  $T_g$  between the  $T_g$ s of pure epoxy monomers, indicating a homogeneous morphology for these systems, in accordance with the observations of other authors.<sup>20</sup>

The dynamic mechanical behaviour of the phosphorus- and silicon-containing epoxy resins was studied as a function of the temperature beginning in the glassy state of each composition to the rubbery plateau of each material. Fig. 2 shows the obtained plots for Gly-HPO (a), for the APDS amine (b) and for the system Gly-HPO/DGMPS (c).

**Table 2.** Curing and post-curing conditions and  $T_g$  data of the epoxy resins.

| Sample | Epoxy monomer <sup>a</sup> | Curing agent <sup>b</sup> | Curing    | Post-curing | $T_g$ (°C)                 |               |                     |
|--------|----------------------------|---------------------------|-----------|-------------|----------------------------|---------------|---------------------|
|        |                            |                           |           |             | $\frac{1}{2} \Delta C_p^c$ | $E''_{max}^d$ | $Tan\delta_{max}^e$ |
| 1      | Gly-HPO                    | DDM                       | 140°C, 2h | 200°C, 2h   | 193                        | 186           | 193                 |
| 2      | Gly-HPO                    | BAMPO                     | 140°C, 2h | 200°C, 2h   | 198                        | 154           | 194                 |
| 3      | Gly-HPO                    | APDS                      | 120°C, 2h | 180°C, 2h   | 167                        | 158           | 167                 |
| 4      | DGMPs                      | DDM                       | 105°C, 2h | 165°C, 2h   | 77                         | 72            | 87                  |
| 5      | DGMPs                      | BAMPO                     | 150°C, 2h | 180°C, 1h   | 75                         | 76            | 84                  |
| 6      | DGMPs                      | APDS                      | 120°C, 3h | 160°C, 3h   | 70                         | 63            | 70                  |
| 7      | BGDMSB                     | DDM                       | 120°C, 2h | 180°C, 2h   | 60                         | 62            | 64                  |
| 8      | BGDMSB                     | BAMPO                     | 145°C, 2h | 195°C, 2h   | 80                         | 90            | 105                 |
| 9      | BGDMSB                     | APDS                      | 120°C, 3h | 180°C, 2h   | 59                         | 53            | 68                  |
| 10     | Gly-HPO/DGMPs              | DDM                       | 120°C, 2h | 180°C, 2h   | 125                        | 123           | 139                 |
| 11     | Gly-HPO/DGMPs              | BAMPO                     | 145°C, 3h | 195°C, 2h   | 146                        | 136           | 148                 |
| 12     | Gly-HPO/DGMPs              | APDS                      | 120°C, 3h | 160°C, 3h   | 120                        | 100           | 118                 |
| 13     | Gly-HPO/BGDMSB             | DDM                       | 120°C, 2h | 180°C, 2h   | 123                        | 119           | 138                 |
| 14     | Gly-HPO/BGDMSB             | BAMPO                     | 145°C, 3h | 195°C, 3h   | 145                        | 130           | 148                 |
| 15     | Gly-HPO/BGDMSB             | APDS                      | 120°C, 3h | 160°C, 3h   | 100                        | 84            | 99                  |

<sup>a</sup> For the mixtures of epoxy monomers, a 1:1 mol ratio was used.

<sup>b</sup> Stoichiometric amounts were used in all cases.

<sup>c</sup> From DSC measurements (10 °C /min).

<sup>d</sup> Maximum of the loss modulus from DMTA measurements.

<sup>e</sup>  $\alpha$  relaxation peak of the loss factor.

The crosslinking density of a polymer can be estimated from the plateau of the elastic modulus in the rubbery state. <sup>21</sup> This theory is strictly valid for

lightly crosslinked materials, and was therefore used to make qualitative comparisons of the crosslinking density among the various polymers. As can be seen in Fig. 2 for the crosslinking of Gly-HPO, the lower crosslinking density is obtained when APDS is used as a curing agent. As far as the chemical structures of these networks are concerned, this behaviour is to be expected since longer Si-O and Si-C bonds should provide flexibility to the backbone. A similar trend can be observed for the systems Gly-HPO/DGMPS. When comparing the crosslinking density of the epoxy monomers cured with APDS (Fig. 2b), it can be seen that the lower crosslinking density is achieved for DGMPS, which contains additional Si-O and Si-C units that confer flexibility to the network.

The plots of loss factor versus temperature show the  $\alpha$  relaxation peak, which is associated with the  $T_g$  of the materials and follow the trend mentioned earlier. Moreover, the analysis of the height and width of the  $\alpha$  relaxation peak shows trends in the crosslinking densities and network homogeneities. The height of  $\text{Tan } \delta$  peak decreases for the APDS crosslinked systems. Because  $\text{Tan } \delta$  peak is the ratio of viscous component to elastic component, it can be assumed that the decreasing height is associated with lower segmental mobility and fewer relaxing species, and is therefore indicative that networks for the APDS containing systems show higher flexibility.



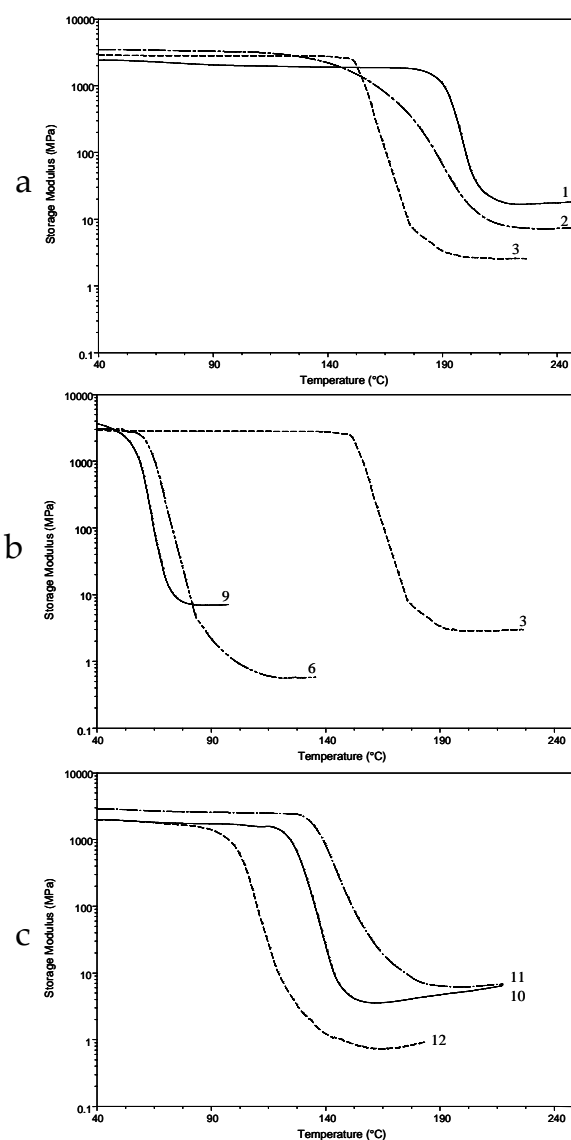


**Figure 2.** Storage modulus for a. 1 (Gly-HPO/DDM), 2 (Gly-HPO/BAMPO) and 3 (Gly-HPO/APDS); b. 3 (Gly-HPO/APDS), 6 (DGMPs/APDS) and 9 (BGDMSB/APDS); c. 10 (Gly-HPO/DGMPs/DDM), 11 (Gly-HPO/DGMPs/BAMPO) and 12 (Gly-HPO/DGMPs/APDS)

The peak width at half height broadens as the number of branching modes increases, which produces a wider distribution of structures. The

range of temperatures at which the different network segments gain mobility therefore increases. There were no significant differences among the different samples, thus showing similar branching distribution for all samples.

To examine the effect of phosphorus and silicon content on thermal stability and the decomposition behaviour, TGA data under nitrogen and air atmospheres were determined and analyzed. Fig. 3 shows the weight loss with the temperature for some of the epoxy compositions. Table 3 summarizes the thermogravimetric data. Decomposition temperatures ( $T_{5\%}$ ) for the phosphorus-containing resins are lower than for the conventional epoxy resins due to the decomposition of P-C bonds which have lower thermal stability than C-C bonds<sup>22</sup>. Moreover, decomposition temperatures for the silicon-containing resins are also expected to be lower than conventional epoxy resins. The Si-O unit can decompose at lower temperatures leading to the formation of the silicone-containing group.<sup>16</sup> In our case, independent of the atmosphere, all the thermosets start the degradation at similar temperatures, being slightly lower in air. No relationships between decomposition temperatures and phosphorus or/and silicon contents can be established.

In nitrogen, two different behaviours can be observed. Some samples exhibit a single major break in their decomposition curve before their major weight losses level off. This behaviour is indicative of a single mechanism of decomposition which is similar for these resins. The others show a two step break in the decomposition curves, suggesting a more complex decomposition pathway. Again, no relationships can be established. In air a third stage in the decomposition process is observed at temperatures above

500 °C. Under an air atmosphere, the weight loss of a polymeric material at these temperatures came from the oxidation of the formed char.

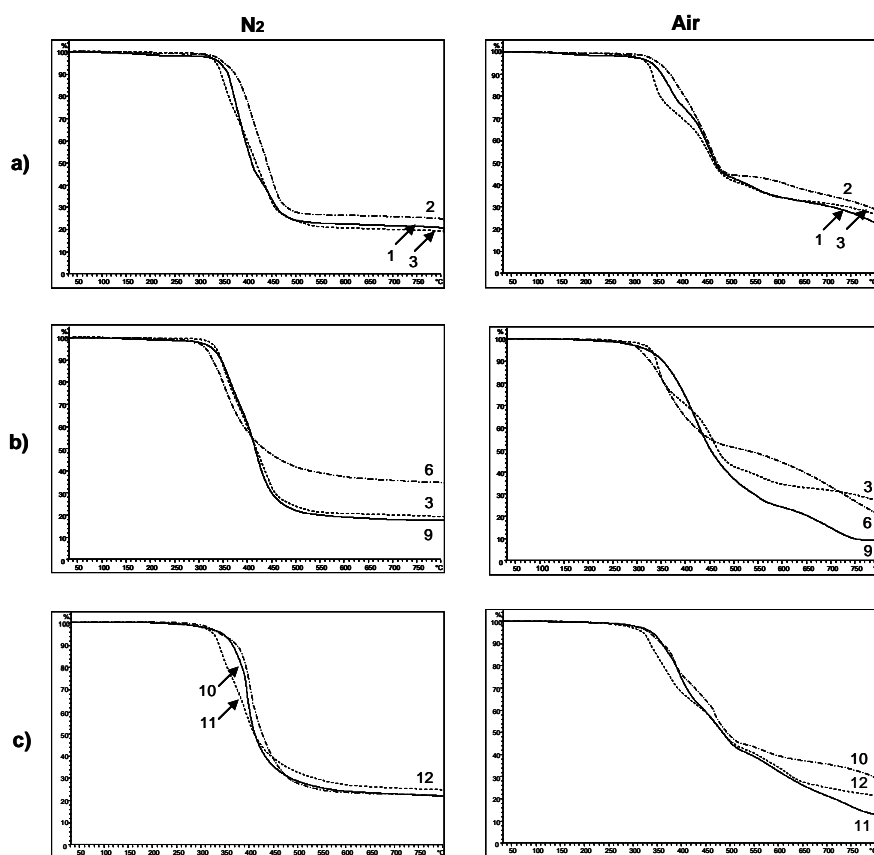


**Figure 3.** TGA plots in nitrogen and air for a. 1 (Gly-HPO/DDM), 2 (Gly-HPO/BAMPO) and 3 (Gly-HPO/APDS); b. 3 (Gly-HPO/APDS), 6 (DGMPs/APDS) and 9 (BGDMSB/APDS); c. 10 (Gly-HPO/DGMPs/DDM), 11 (Gly-HPO/DGMPs/BAMPO) and 12 (Gly-HPO/DGMPs/APDS).

**Table 3** Thermogravimetric data of epoxy resins.

| Sample | P(%) | SI(%) | Nitrogen                          |                                    |                                    |                       | Air                               |                                    |                                    |                       | LOI<br>%O <sub>2</sub><br>(V/V) |      |
|--------|------|-------|-----------------------------------|------------------------------------|------------------------------------|-----------------------|-----------------------------------|------------------------------------|------------------------------------|-----------------------|---------------------------------|------|
|        |      |       | T <sub>5%</sub> <sup>a</sup> (°C) | T <sub>10%</sub> <sup>b</sup> (°C) | T <sub>15%</sub> <sup>b</sup> (°C) | Char <sup>c</sup> (%) | T <sub>5%</sub> <sup>a</sup> (°C) | T <sub>10%</sub> <sup>b</sup> (°C) | T <sub>15%</sub> <sup>b</sup> (°C) | Char <sup>c</sup> (%) |                                 |      |
|        |      |       |                                   |                                    |                                    |                       |                                   |                                    |                                    |                       |                                 |      |
| 1      | 5.9  | -     | 348                               | 369                                | 444                                | 23                    | 347                               | 383                                | 450                                | 550                   | 22                              | 31.2 |
| 2      | 8.5  | -     | 352                               | 410                                | 450                                | 25                    | 352                               | 393                                | 458                                | 560                   | 29                              | 32.0 |
| 3      | 5.5  | 2.5   | 335                               | 350                                | 435                                | 20                    | 328                               | 342                                | 460                                | 630                   | 27                              | 31.0 |
| 4      | -    | 7.7   | 318                               | -                                  | 415                                | 34                    | 302                               | 325                                | 412                                | 580                   | 16                              | 36.0 |
| 5      | 4.0  | 7.2   | 308                               | -                                  | 430                                | 33                    | 312                               | 380                                | 470                                | 750                   | 31                              | 38.0 |
| 6      | -    | 10.4  | 320                               | 350                                | -                                  | 35                    | 306                               | 356                                | -                                  | 745                   | 22                              | 37.0 |
| 7      | -    | 12.8  | 362                               | -                                  | 439                                | 21                    | 348                               | 419                                | -                                  | 690                   | 12                              | 33.5 |
| 8      | 3.4  | 12.2  | 358                               | -                                  | 420                                | 15                    | 307                               | 416                                | -                                  | 680                   | 11                              | 33.9 |
| 9      | -    | 14.7  | 329                               | 362                                | 420                                | 18                    | 320                               | 430                                | -                                  | 700                   | 9                               | 33.0 |
| 10     | 3.5  | 3.2   | 336                               | -                                  | 400                                | 23                    | 338                               | 380                                | 470                                | 595                   | 13                              | 36.5 |
| 11     | 6.6  | 3.0   | 341                               | -                                  | 406                                | 24                    | 332                               | 385                                | 460                                | 560                   | 31                              | 34.0 |
| 12     | 3.2  | 5.8   | 327                               | 340                                | 390                                | 25                    | 319                               | 350                                | 478                                | 575                   | 22                              | 34.6 |
| 13     | 3.2  | 5.8   | 330                               | -                                  | 400                                | 19                    | 302                               | 390                                | 470                                | 600                   | 9                               | 34.0 |
| 14     | 6.2  | 5.5   | 331                               | 395                                | 447                                | 16                    | 323                               | 380                                | 475                                | 564                   | 24                              | 33.5 |
| 15     | 3.0  | 8.1   | 317                               | 355                                | -                                  | 17                    | 304                               | 420                                | 480                                | 605                   | 16                              | 33.6 |

<sup>a</sup>Temperature of 5% weight loss.

<sup>b</sup>Temperature of the maximum weight loss rate.

<sup>c</sup>Char yield at 800 (°C).

According to the mechanism of improved fire performance via phosphorus incorporation, the phosphorus groups form an insulating protective layer which prevents the volatiles from transferring to the surface of the materials and increases the thermal stability of the char at higher temperatures. Silicon-containing polymers are described that can degrade forming thermally stable silica, which have the tendency to migrate to the char surface serving as a protection layer to prevent further degradation of char at high temperatures.<sup>8</sup> For the P-Si synergistic effect of flame retardation, it has been described that phosphorus provides a tendency for char formation and silicon favorably provides an enhancement of the thermal stability of the char, resulting in a high efficiency of char formation which exhibit extremely thermal stability and antioxidant properties. In our case, no increase in the amount of char yield in air at 800 °C with the P+Si content was observed.

The LOI values of the phosphorus-silicon containing epoxy resins are shown in Table 2. Materials with outstanding LOI values are obtained, with the corresponding excellent flame retardant properties. Fig. 4 depicts LOI values for phosphorus-<sup>14,23</sup>, silicon-<sup>15,16</sup> and phosphorus-silicon-containing epoxy resins.

As we described previously, it can be observed that the presence of phosphorus in phosphorus-containing epoxy resins increases the LOI values even when the phosphorus content is low, and no significant differences with the phosphorus content are observed. For the silicon-containing epoxy resins, the LOI values increase with increasing silicon content up to contents of 10%. However, a synergistic effect cannot be observed for phosphorus-silicon-containing epoxy resins and significant improvements in LOI values are not reached.

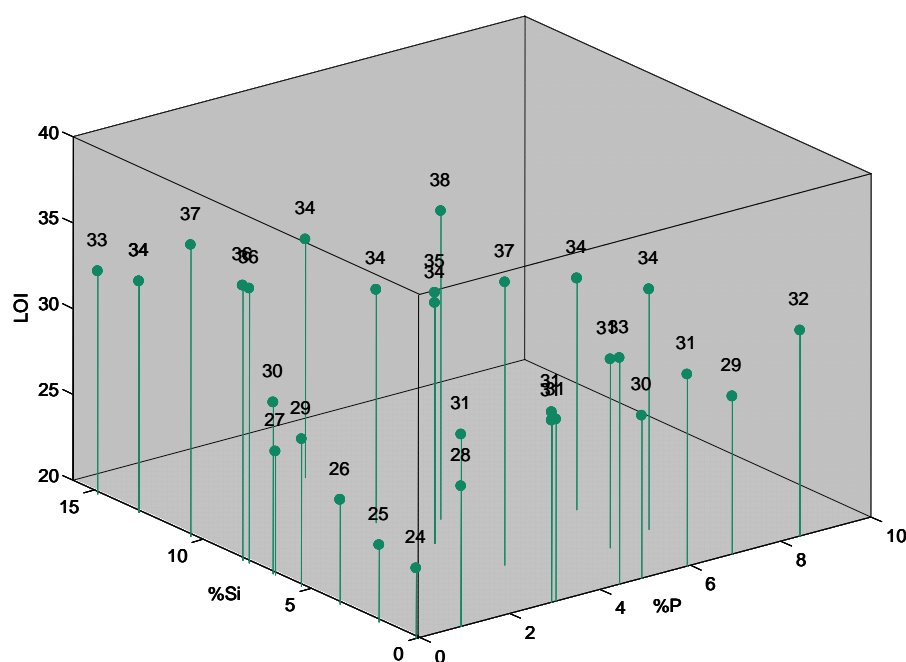


**Figure 4.** Plot of LOI values for phosphorus-, silicon- and phosphorus-silicon- containing epoxy resins.

## CONCLUSIONS

The curing of phosphorus- and silicon-containing epoxy monomers with conventional DDM and phosphorus- and silicon-containing amines was studied by DSC. The most reactive monomer was DGMPs and the most reactive curing agent was APDS because of the electronic effects. The thermal and flame retardant properties were evaluated. Materials with outstanding LOI values are obtained, with the corresponding excellent flame retardant properties that could bring some benefits to the epoxy resins in applications. A synergistic effect cannot be observed for phosphorus-silicon-containing resins.

## Acknowledgements

The authors express their thanks to CICYT (Comisión Interministerial de Ciencia y Tecnología) (MAT2005-01593) for providing financial support for this work.

## REFERENCES

- <sup>1</sup> May CA, editor. *Epoxy Resins Chemistry and Technology*. New York: Marcel Dekker, 1988.
- <sup>2</sup> Kinjo N, Ogata M, Nishi K, Kaneda A. *Adv Polym Sci* 1989;88:1.
- <sup>3</sup> Lu SY, Hamerton I. *Prog Polym Sci* 2002;27:1661.
- <sup>4</sup> Levchik SV, Weil ED. *Polym Int* 2004;53:1901.
- <sup>5</sup> Weil E, Levchik SJ. *Fire Sci* 2004;22:25.
- <sup>6</sup> Green J. *Fire Retardancy of Polymeric Materials*. Grand AF, Wilkie CA. Eds. Marcel Dekker, New York, 2000.
- <sup>7</sup> Ebdon JR, Jones MS. In: Salomone JC, editor *Polymeric Materials Encyclopedia*. Boca Raton: CRC Press, 1992.
- <sup>8</sup> Kashiwagi T, Gilman JW. *Fire retardancy of polymeric materials*. Grand AF, Wilkie CA. Eds. New York, Marcel Dekker, 2000.
- <sup>9</sup> Liu YL, Chiu CI. *Polym Degrad Stab* 2005;90:515.
- <sup>10</sup> Khurana P, Narula AK, Choudhary V. *J Appl Polym Sci* 2003;90:1739.
- <sup>11</sup> Wu CS, Liu YL, Chiu YS. *Polymer* 2002;43:4277.
- <sup>12</sup> Hsiue GH, Liu YL, Tsiao J. *J Appl Polym Sci* 2000;78:1.
- <sup>13</sup> Hsiue GH, Liu YL, Liao HH. *J Polym Sci Part A Polym Chem* 2001;39:986.
- <sup>14</sup> Spontón M, Ronda JC, Galià M, Cádiz V. *J Polym Sci Part A Polym Chem* 2007;45:2142.
- <sup>15</sup> Mercado LA, Galià M, Reina JA. *Polym Degrad Stab* 2006;91:2588.
- <sup>16</sup> Mercado LA, Reina JA, Galià M. *J Polym Sci Part A Polym Chem* 2006;44:5580.
- <sup>17</sup> Mercado LA, Ribera G, Galià M, Cádiz V. *J Polym Sci Part A Polym Chem* 2006;44:1676.
- <sup>18</sup> Brestensky DM, Huseland DE, McGettigan C, Stryker JM. *Tetrahedron Lett* 1988;29:3749.
- <sup>19</sup> Mercado LA, Galià M, Reina JA, Garrido M, Larrechi MS, Rius FX. *J Polym Sci Part A Polym Chem* 2006;44:1447.
- <sup>20</sup> Wang WJ, Perng LH; Hsiue, GH; Chang, FC. *Polymer*, 2000;41:6113
- <sup>21</sup> Tobolsky AV, Carlson DW, Indivictor NJ. *J Polym Sci* 1961;54:175.
- <sup>22</sup> Quittmann U, Lecamp L, El Khatib W, Youssef B, Bunel C. *Macromol Chem Phys* 2001;202:628.
- <sup>23</sup> Ribera G, Mercado LA, Galià M, Cádiz V. *J Appl Polym Sci* 2006;99:1367.

UNIVERSITAT ROVIRA I VIRGILI  
RESINAS EPOXI Y BENZOXAZINAS FOSFORADAS Y SILILADAS RETARDANTES A LA LLAMA  
Marisa Elisabet Spontón  
ISBN:978-84-691-9480-5/DL:T-22-2009



# CAPÍTULO 3

## Síntesis y caracterización de sistemas benzoxazina y benzoxazina-epoxi fosforados o sililados

---

*Las polibenzoxazinas son una nueva clase de resinas termoestables cuya síntesis es de gran simplicidad y presentan propiedades interesantes de potencial aplicación en diversos campos, entre otros en la industria electrónica. Debido a la demanda de materiales retardantes a la llama en esta industria es por lo que se ha utilizado la estrategia de introducir fósforo o silicio en la estructura de la benzoxazina. En este capítulo se estudia la síntesis y la evaluación de propiedades de benzoxazinas y sistemas benzoxazina-epoxi fosforados y sililados.*

---

- 3.1 Polibenzoxazinas
- 3.2 Benzoxazinas polifuncionales
- 3.3 Copolimerización de benzoxazinas
- 3.4 Polibenzoxazinas retardantes a la llama
- 3.5 Degradación térmica de polibenzoxazinas
- 3.6 Objetivos
- 3.7 Parte experimental y resultados
  - 3.7.1 Synthesis and study of the thermal crosslinking of bis(m-vaminophenyl) methylphosphine oxide based benzoxazine
  - 3.7.2 Studies on thermal and flame retardant behaviour of mixtures of bis(m-aminophenyl)methylphosphine oxide based benzoxazine and glycidylether or benzoxazine of bisphenol A
  - 3.7.3 Development of flame retardant phosphorus- and silicon- containing polybenzoxazines

UNIVERSITAT ROVIRA I VIRGILI  
RESINAS EPOXI Y BENZOXAZINAS FOSFORADAS Y SILILADAS RETARDANTES A LA LLAMA  
Marisa Elisabet Spontón  
ISBN:978-84-691-9480-5/DL:T-22-2009

### 3.1

#### Polibenzoxazinas

Las resinas fenólicas son conocidas desde hace muchos años, siendo el primer polímero sintético producido en masa<sup>1</sup>. Desde entonces, han desempeñado un papel importante en la industria en un amplio campo de aplicaciones desde aeroespaciales a electrónicas.

La síntesis de las resinas fenólicas tiene lugar por condensación de un fenol o una mezcla de fenoles y aldehídos. Entre los fenoles, los más utilizados son el fenol y los cresoles y entre los aldehídos, el formaldehído y en menor extensión, el furfural<sup>2,3</sup>. La estructura química de estas resinas es muy compleja, depende de las condiciones de reacción y de la relación fenol-formaldehído. En función de esta última se distinguen dos tipos de resinas fenólicas: las novolacas y los resoles<sup>4</sup>. Las novolacas se preparan por reacción del fenol con defecto de formaldehído en condiciones ácidas, mientras que los resoles son el producto de reacción del fenol y formaldehído en exceso en condiciones básicas.

Las resinas fenol-formaldehído tienen buena resistencia térmica, son excelentes aislantes eléctricos, presentan estabilidad dimensional, baja inflamabilidad y generan pocos humos tóxicos en su combustión. Sin embargo, son materiales quebradizos, que pueden corroer los equipos utilizados en su síntesis debido a la presencia de ácidos o bases fuertes y que liberan durante su entrecruzamiento subproductos tales como agua,

---

<sup>1</sup> Baekeland LH. U. S. Pat. 1907:942:699.

<sup>2</sup> Kopf PW. Phenol-formaldehyde Resin en Encyclopedia of Polymer Science and Engineering. Vol 11, p 45. John Wiley & Sons Inc. New York 1988.

<sup>3</sup> Fukuda A. Phenolic Resin en Polymeric Materials Science Enciclopedia. Vol 7, p 5035. Ed: Salomone JC. CRC Press. Boca Raton 1996.

<sup>4</sup> Reghunadhan Nair CP. Prog Polym Sci 2004:29:401.

formaldehído, amoniaco y aminas producidas en las reacciones de policondensación. Estos volátiles son un inconveniente ya que producen microporos en su estructura reduciendo las propiedades finales de las resinas fenólicas curadas<sup>5</sup>.

Como una alternativa atractiva a los materiales fenólicos convencionales se ha desarrollado un nuevo tipo de resinas fenólicas, las polibenzoxazinas, que se obtienen por apertura del anillo de 3,4-dihidro-2H-1,3-benzoxazinas. Estas benzoxazinas se suelen obtener a partir de un fenol, formaldehído y una amina primaria, en relación molar 1:2:1 en una reacción que puede ser considerada como una variante de la reacción de Mannich (figura 3.1). Las benzoxazinas fueron descritas por primera vez por Holly y Cope<sup>6</sup> en 1944, y a partir de entonces se han sintetizado un gran número de nuevas estructuras mono, di y polifuncionales<sup>7,8</sup>. Por otra parte, se ha descrito que las benzoxazinas son uno de los intermedios más importantes en las primeras etapas del entrecruzamiento de resinas novolaca con hexametilentetramina<sup>9,10</sup>.

---

<sup>5</sup> Gardziella A, Pilato LA, Knop A. *Phenolic Resins, Chemistry, Applications, Standardization, Safety and Ecology*. Springer-Verlag, Berlin 2000.

<sup>6</sup> Holly FW, Cope AC. *J Am Chem Soc.* 1944;66:1875.

<sup>7</sup> Burke WJ, Murdock KC, Grace EC. *J Am Chem Soc.* 1954;76:1677.

<sup>8</sup> Ghosh NN, Kiskan B, Yagci Y. *Prog Polym Sci.* 2007;32:1344.

<sup>9</sup> Zhang X, Potter AC., Solomon DH. *Polymer.* 1998;39:399.

<sup>10</sup> Zhang X, Solomon DH. *Polymer.* 1998;39:405.

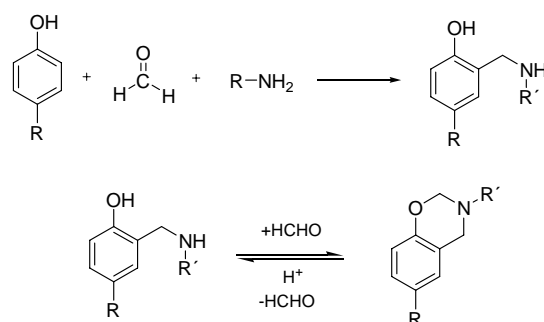


Figura 3.1 Síntesis de benzoxazinas.

Aunque la síntesis de las benzoxazinas a partir de fenol, formaldehído y aminas es la más habitual, se ha descrito la formación de dímeros y otras especies oligoméricas como productos secundarios debido a la reactividad de las diaminas aromáticas a las elevadas temperaturas utilizadas<sup>11,12</sup>. Para minimizar estas reacciones se viene utilizando otra estrategia sintética que evita la reacción directa entre la diamina y paraformaldehído. En esta síntesis, en tres etapas (figura 3.2), se utiliza la reacción de 2-hidroxibenzaldehído con la diamina y la imina resultante se reduce “*in situ*” dando lugar a la 2-hidroxibenzilamina derivada. En la última etapa se añade paraformaldehído para obtener la benzoxazina<sup>13-15</sup>.

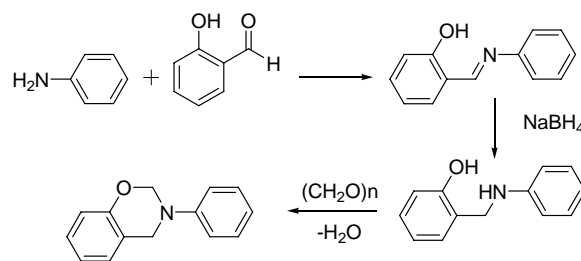


Figura 3.2

<sup>11</sup> Ishida H, Rodríguez Y. *Polymer*. 1995;36:3151.

<sup>12</sup> Ning X, Ishida H. *J Polym Sci Part A: Polym Chem*. 1994;32:921.

<sup>13</sup> Rivera A, Gallo GI, Gayon Ma. *Synth Commun*. 1994;24:2081.

<sup>14</sup> Reddy M, Madan MR, Rajeswar V. *Heterocyc Commun*. 2004;10:429.

<sup>15</sup> Andreu R, Ronda JC. *Synth Commun*. 2008;38:2316.

La polimerización térmica por apertura de anillo de las benzoxazinas que da lugar a polibenzoxazinas (Figura 3.3) fue llevada a cabo por Schreiber en 1973<sup>16</sup>. Posteriormente Riess et al. investigaron la polimerización de benzoxazinas monofuncionales con y sin iniciador, obteniendo polímeros lineales de bajo peso molecular<sup>17</sup>. Ishida et al.<sup>18</sup> han sintetizado y polimerizado numerosas benzoxazinas mono y polifuncionales a partir de diferentes sustratos fenólicos, formaldehído y aminas primarias alifáticas o aromáticas, utilizando diferentes condiciones de reacción.

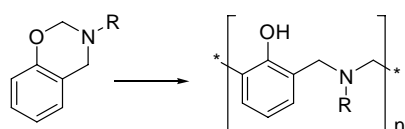


Figura 3.3 Síntesis de polibenzoxazinas.

Así pues las benzoxazinas eliminan el problema de la liberación de subproductos de condensación, que presentan las resinas fenólicas convencionales, y no necesitan catalizador para su entrecruzamiento. Además, ofrecen una mayor flexibilidad en el diseño estructural al poder utilizar fenoles y aminas de diferente estructura.

Por otra parte, dada su baja viscosidad permiten una mayor facilidad de procesado<sup>11</sup>, y entre otras ventajas se pueden citar la baja absorción de agua y constante dieléctrica<sup>19</sup>, buenas propiedades mecánicas<sup>20-22</sup>, elevada

<sup>16</sup> Schreiber H, Ger Offen 2:255:504:1973.

<sup>17</sup> Riess G, Schwob JM, Guth G, Roche M, Lande B. *Advances in Polymer Synthesis*. Ed: Culbertson BM, McGrath JE. Plenum New York 1985.

<sup>18</sup> Ning X, Ishida H. *J Polym Sci Part A: Polym Chem*. 1994;32:1121.

<sup>19</sup> Wirasate S, Allen J, Ishida H. *J Appl Polym Sci*. 1998;70:1299.

<sup>20</sup> Ishida H, Allen DJ. *J Polym Sci Phys*. 1996;34:1019.

<sup>21</sup> Shen S, Ishida H. *Polym Composites*. 1996;17:711.

estabilidad térmica<sup>23</sup> y encogimiento/expansión cercano a cero en el proceso de polimerización<sup>24</sup>.

Las polibenzoxazinas se obtienen generalmente por polimerización térmica de los correspondientes monómeros a elevadas temperaturas sin catalizador. En la literatura también se pueden encontrar diferentes ejemplos de catálisis de la reacción de apertura del anillo de oxazina. La reactividad de las benzoxazinas derivadas del Bisfenol A ha sido ampliamente estudiada usando diferentes tipos de ácidos como catalizadores<sup>25,26</sup> pudiéndose demostrar que la polimerización por apertura de anillo de la benzoxazina sigue un mecanismo catiónico<sup>27</sup>.

Para entender el mecanismo de la reacción de polimerización de las benzoxazinas, es muy importante una comprensión de la estructura química del anillo oxazina. Mediante espectroscopia de rayos X, se ha comprobado que la conformación preferida de una benzoxazina es una forma de silla distorsionada en la que el átomo de nitrógeno y el átomo de carbono enlazado a oxígeno y nitrógeno están por encima y por debajo, respectivamente, del plano del anillo de benceno<sup>26</sup>. La tensión resultante de este tipo de conformación molecular hace posible que este anillo de seis miembros experimente la apertura bajo condiciones específicas. Además, tanto el átomo de nitrógeno como el de oxígeno son potenciales puntos de iniciación de polimerización catiónica, dado su carácter de base de Lewis. Las distribuciones de carga calculadas sugieren que el oxígeno es el punto preferido de reacción, debido a su mayor carga negativa (O -0.311, N -

---

<sup>22</sup> Ning X, Ishida H. *J Polym Sci Part B: Polym Physics*. 1994;32:921.

<sup>23</sup> Kim HD, Ishida H. *J Appl Polym Sci*. 2001;79:1207.

<sup>24</sup> Ishida H, Low HY. *Macromolecules*. 1997;30:1099.

<sup>25</sup> Dunkers J, Ishida H. *J Polym Sci Part A: Polym Chem*. 1999;37:1913.

<sup>26</sup> Wang YX, Ishida H. *Macromolecules*. 2000;33:2839.

<sup>27</sup> Andreu R, Reina A, Ronda JC. *J Polym Sci Part A: Polym Chem*. 2008;46:3353.

0.270). En este sentido puede proponerse un mecanismo en el que este átomo actúa como punto de iniciación tras el ataque de un iniciador catiónico, formando un ión oxonio cíclico. La polimerización procederá entonces por inserción de los monómeros dando lugar a una polibenzoxazina con una estructura tipo fenóxido (figura 3.4).

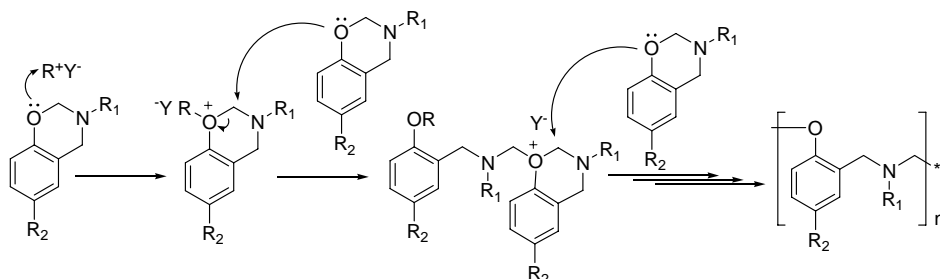


**Figura 3.4** Mecanismo de apertura del anillo tipo fenóxido iniciado en el oxígeno.

Se puede proponer otro mecanismo de polimerización alternativo, similar al mecanismo anteriormente descrito, en que los puntos de iniciación y propagación sean los átomos de nitrógeno, mecanismo que daría lugar al mismo tipo de estructura polibenzoxazínica tipo fenóxido (figura 3.5).

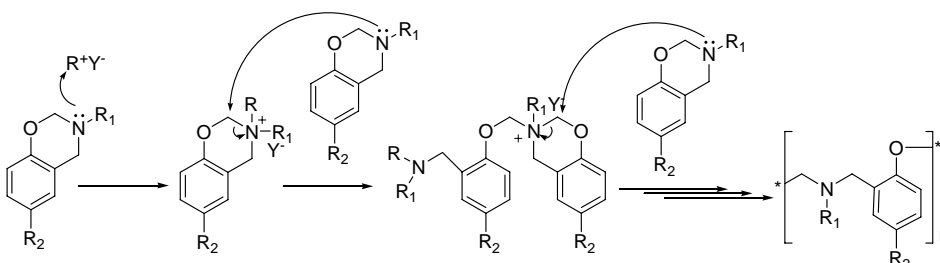


**Figura 3.5** Mecanismo de apertura del anillo tipo fenóxido iniciado en el nitrógeno.



En una molécula de benzoxazina, además de nitrógeno y oxígeno ricos en densidad electrónica, la posición *orto* del anillo de benceno respecto al grupo fenóxido posee también una alta reactividad en la polimerización térmica con o sin catalizador. Así, se puede asumir que tras la iniciación catiónica, la propagación tiene lugar por inserción de los monómeros a través de la reacción en la posición *orto*, dando una polibenzoxazina de tipo fenólico. En este último caso las especies responsables de la propagación son también iones oxonio pero especialmente estabilizados por la posible existencia de puentes de hidrógeno (figura 3.6).

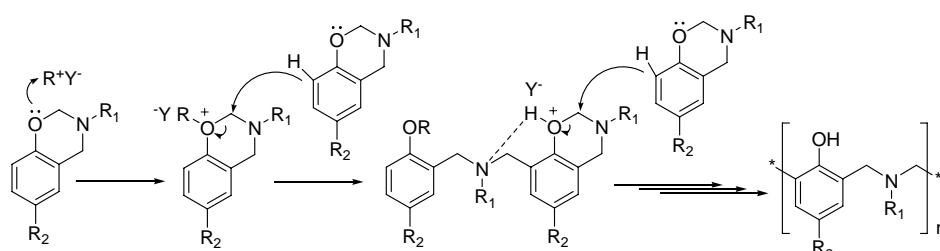


**Figura 3.6** Mecanismo de apertura del anillo tipo fenólico iniciado en el oxígeno.

Estos diferentes mecanismos dan lugar a estructuras de tipo fenóxido o fenólico. Se ha comprobado que la reacción de eterificación sólo se da en una extensión importante cuando las posiciones *orto* y *para* del anillo bencénico de la oxazina están sustituidas. En los demás casos, la reacción predominante es la formación de estructuras tipo fenólico.

Algunos estudios indican que la reacción de aminoalquilación puede tener lugar sobre las posiciones activadas del anillo de arilamina a las temperaturas de curado ordinarias. Además, se ha detectado, como reacción secundaria, la formación de cantidades importantes de uniones metileno

fenólicas y entre anillos de arilamina<sup>28</sup>. Estos estudios se refieren al comportamiento de benzoxazinas monofuncionales que dan lugar a oligómeros de bajo peso molecular, resultando de interés la investigación de las estructuras formadas en el curado de un sistema difuncional capaz de entrecruzar para formar redes termoestables<sup>29</sup>.

Si una benzoxazina difuncional polimeriza según el mecanismo convencional se forma una red con puentes de Mannich fenólicos, como se muestra en la figura 3.7a. Por otra parte si los anillos aromáticos de la amina reaccionan se forma una estructura con puentes de Mannich arilamina, como se puede ver en la figura 3.7b.

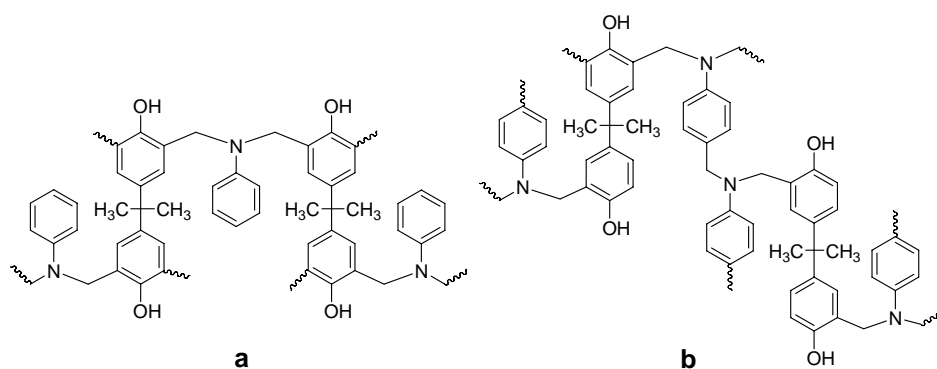


Figura 3.7

Dada la evidencia de la formación de puentes metileno en las benzoxazinas monofuncionales, cabe esperar también la formación de una estructura fenólica convencional, con puentes metileno, en la reacción de entrecruzamiento de una dibenzoxazina. Alternativamente, si el anillo de arilamina actúa como punto de formación de la unión metileno se forman

<sup>28</sup> Ishida H, Sanders DP. Polymer. 2001;42:3115.

<sup>29</sup> Ishida H, Sanders DP. Macromolecules. 2000;33:8149.

puentes metileno arilamina. Ambas estructuras se pueden observar en la figura 3.8 a y 3.8.b respectivamente.

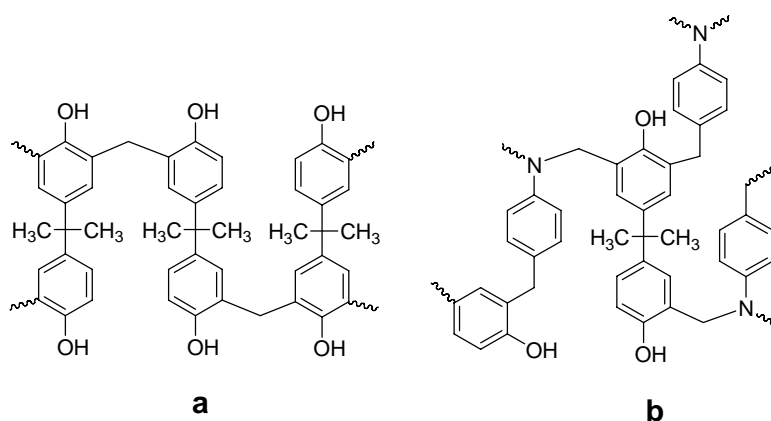


Figura 3.8

### 3.2

#### Benzoxazinas polifuncionales

Desde el punto de vista industrial los monómeros que presentan un mayor interés en la obtención de polibenzoxazinas son los difuncionales, ya que estos mediante la polimerización por apertura de anillo dan a lugar a materiales entrecruzados<sup>30-35</sup>. Entre las numerosas resinas desarrolladas hasta ahora, destacan las benzoxazinas derivadas del bisfenol A<sup>36-40</sup>.

<sup>30</sup> Xiang H, Ling H, Wang J, Gu Y. *Polym Composites*. 2005;26:563.

<sup>31</sup> Men W, Lu Z. *J Appl Polym Sci*. 2007;106:2769.

<sup>32</sup> Allen D, Ishida H. *Polymer*. 2007;48:6763.

<sup>33</sup> Lin CH, Chang SL, Hsieh CW, Lee HH. *Polymer*. 2008;49:1220.

<sup>34</sup> Men W, Lu Z, Zhan Z. *J Appl Polym Sci*. 2008;109:2219.

<sup>35</sup> Lin CH, Chang SL, Lee HH, Tu AP, Su C. *J Polym Sci Part A: Polym Chem*. 2008;46:4970.

<sup>36</sup> Kimura H, Taguchi, Matsumoto A. *J Appl Polym Sci*. 2001;79:2331.

<sup>37</sup> Takeichi T, Kano T, Agag T. *Polymer*. 2005;46:12172.

<sup>38</sup> Cherninykh A, Liu J, Ishida H. *Polymer*. 2006;47:7664.

<sup>39</sup> Hamerton I, Howlin BJ, Mitchell AL. *React & Func Polym*. 2006;66:21.

<sup>40</sup> Kiskan B, Yagci Y, Ishida H. *J Polym Sci Part A: Polym Chem*. 2008;46:414.

Sin embargo, a pesar de su altas prestaciones, su densidad de entrecruzamiento es más baja que la de otras resinas termoestables y una de sus limitaciones es la fragilidad de los materiales obtenidos. Además, en general son necesarias temperaturas elevadas para llevar a cabo la polimerización por apertura del anillo. Para mejorar el comportamiento de las benzoxazinas se utilizan estrategias que pueden agruparse en dos tipos: uno es la modificación de la estructura mediante el diseño de nuevos monómeros o la copolimerización con resinas epoxi. El segundo tipo corresponde a la formación de composites o mezclas con otros polímeros de elevada resistencia térmica como poliimidás<sup>41</sup>, composites reforzados con fibras<sup>42</sup>, y nanocomposites<sup>43,44</sup>.

La incorporación a la benzoxazina de otros grupos funcionales capaces de dar lugar a su vez a una polimerización se ha descrito como una de las estrategias más eficaces para aumentar la densidad de entrecruzamiento. Entre estos grupos cabe destacar: propargiléter<sup>45</sup>, alilo<sup>46,47</sup>, etinilo y feniletinilo<sup>48-50</sup>, nitrilo<sup>51,52</sup> y maleimida<sup>53</sup> (figura 3.9).

<sup>41</sup> Takeichi T, Agag T. *J Polym Sci Part A: Polym Chem*. 2001;39:2633.

<sup>42</sup> Jang J, Yang H. *J Mater Sci*. 2000;35:2297.

<sup>43</sup> Zhang J, Xu R, Yu D. *Eur Polym J*. 2007;43:743.

<sup>44</sup> Agag T, Takeichi T. *Polymer*. 2000;41:7083.

<sup>45</sup> Agag T, Takeichi T. *Macromolecules*. 2001;34:7257.

<sup>46</sup> Agag T, Takeichi T. *Macromolecules*. 2003;36:6010.

<sup>47</sup> Kumar Santhosh KS, Nair Reghunadhan CP, Sadhana R, Ninan KN. *Eur Polym J*. 2007;43:5084.

<sup>48</sup> Kim H, Brunovska Z, Ishida H. *Polymer*. 1999;40:6565.

<sup>49</sup> Huang J, Zhang Z, Wang F, Huang F, Du L. *React & Func Polym*. 2006;66:1395.

<sup>50</sup> Nagai A, Kamei Y, Wang XS, Omura M, Sudo A, Nishida H, Kawamoto E, Endo T. *J Polym Sci, Polym Chem Ed*. 2008;46:2316.

<sup>51</sup> Brunovska Z, Lyon R, Ishida H. *Thermochimica Acta*. 2000;357:195.

<sup>52</sup> Brunovska Z, Ishida H. *J Appl Polym Sci*. 1999;73:2937.

<sup>53</sup> Ishida H, Ohba S. *Polymer*. 2005;46:5588.

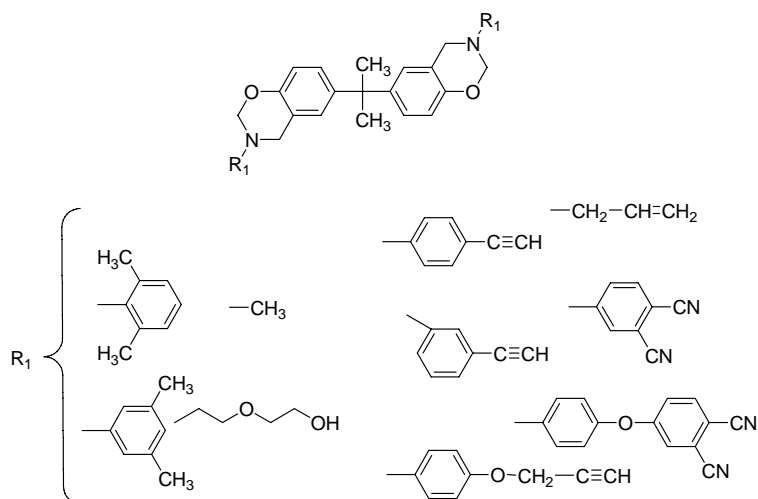


Figura 3.9 Benzoxazinas con diversos grupos funcionales.

Otro camino utilizado para modificar la estructura de las polibenzoxazinas es la copolimerización de la benzoxazina con resinas epoxi<sup>54-58</sup>.

### 3.3

#### Copolimerización de benzoxazinas

Como se ha mencionado anteriormente, los anillos de benzoxazina homopolimerizan térmicamente generando estructuras fenólicas capaces de reaccionar con los grupos epóxidos (figura 3.10).

<sup>54</sup> Ishida H, Allen DJ. *Polymer*. 1996;37:4487.

<sup>55</sup> Agag T, Takeichi T. *High Perform Polym*. 2002;14:115.

<sup>56</sup> Kimura H, Matsumoto A, Hasegawa K, Ohtsuka K. *J Appl Polym Sci*. 2008;107:710.

<sup>57</sup> Kimura H, Matsumoto A, Hasegawa K, Ohtsuka K, Fukuda A. *J Appl Polym Sci*. 1998;68:1903.

<sup>58</sup> Jain R, Narula AK, Choudhary V. *J Appl Polym Sci*. 2007;106:3327.

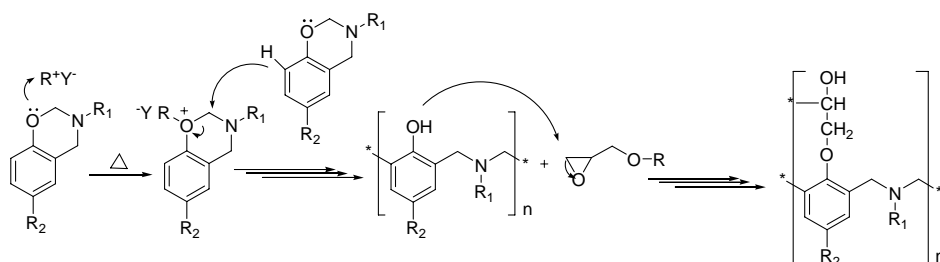


**Figura 3.10** Copolimerización de benzoxazina con resina epoxi.

Se obtienen así materiales que presentan elevadas densidades de entrecruzamiento y elevadas temperaturas de transición vítrea, además de mejoras tanto en la resistencia térmica como en las propiedades mecánicas y en la procesabilidad<sup>54,55</sup>.

Esta estrategia de copolimerización de las benzoxazinas con resinas epoxi requiere cantidades elevadas de resina epoxi si se pretenden mejoras significativas de las propiedades térmicas y mecánicas. Sin embargo, la inflamabilidad de estas resinas constituye una de sus principales limitaciones, especialmente para aplicaciones en la industria electrónica, y es necesaria la utilización de retardantes a la llama para compensar la disminución de la retardancia a la llama de las polibenzoxazinas resultantes, derivada de la presencia de resinas epoxi.

### 3.4

#### Polibenzoxazinas retardantes a la llama

Como ya se ha mencionado, dentro del interés que existe en la modificación de la estructura química de las resinas epoxi para aumentar su resistencia a la llama, los sistemas organofosforados y organosililados se han revelado como unos de los más eficientes. Así pues una primera

estrategia a seguir es la copolimerización de una benzoxazina comercial con resinas epoxi que contengan fósforo o silicio. En nuestro grupo de investigación se estudiaron nuevos materiales derivados de la copolimerización de sistemas novolaca–benzoxazina y resinas epoxi fosforadas, obteniéndose buenos resultados de retardancia a la llama<sup>59</sup>. Alternativamente los heteroelementos se pueden introducir en la estructura de la benzoxazina. Recientemente, se ha descrito la incorporación de fósforo<sup>60,61</sup> y de silicio<sup>62,63</sup> en la estructura de las benzoxazinas, algunas de las cuales se representan a continuación en la figura 3.11.

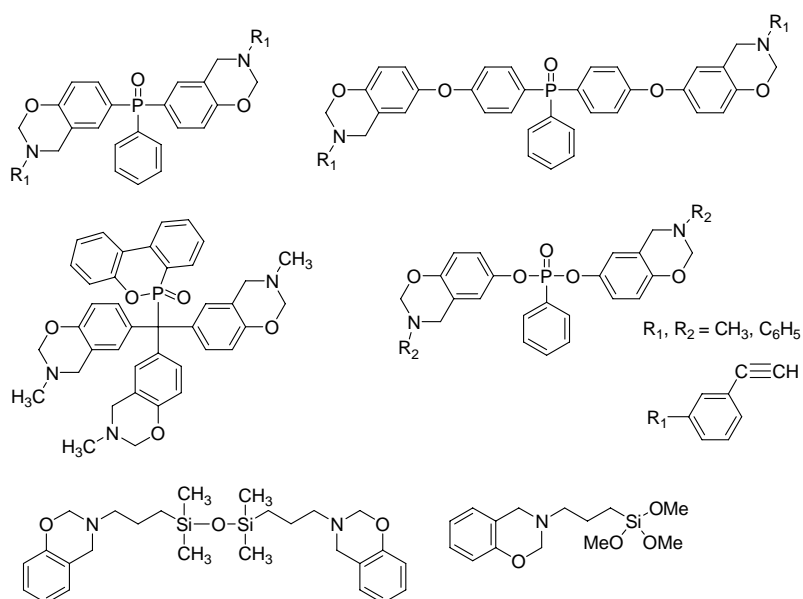


**Figura 3.11** Estructuras de benzoxazinas derivadas de fósforo y silicio.

<sup>59</sup> Espinosa MA, Galià M, Cádiz V. *Polymer*. 2004;45:6103.

<sup>60</sup> Choi SW, Ohba S, Brunovska Z, Hemvichian K, Ishida H. *Polym Degrad Stab*. 2006;91:1166.

<sup>61</sup> Lin CH, Gai SX, Leu TS, Lee HH. *J Polym Sci Part A: Polym Chem*. 2006;44:3454.

<sup>62</sup> Liu Y, Zhang W, Chen Y, Zheng S. *J Appl Polym Sci*. 2006;99:927.

<sup>63</sup> Liu YL, Hsu CW, Chou CI. *J Polym Sci Part A: Polym Chem*. 2007;45:1007.

### 3.5

#### Degradación térmica de polibenzoxazinas

El proceso de la descomposición térmica de las polibenzoxazinas ha sido ampliamente estudiado por Ishida y colaboradores<sup>64-68</sup> utilizando diferentes compuestos modelo debido a la complejidad de los sistemas polibenzoxazina. A bajas temperaturas las principales etapas de degradación que se producen son la escisión del enlace C-C y C-N, dando lugar a: dímeros (que pueden continuar la degradación en pequeños fragmentos), aminas, compuestos fenólicos, bases de Mannich y derivados bencénicos (figura 3.12). Estos compuestos se obtienen como resultado directo de la degradación del polímero. Como resultado de la recombinación o de la degradación de los compuestos formados durante la descomposición térmica se forman otra serie de compuestos. Los compuestos bifenílicos se obtienen por recombinación de dos radicales fenilo formados por pérdida de los sustituyentes de derivados de benceno, aminas y compuestos fenólicos (figura 3.13). Los anillos de benzofurano derivan de la degradación de los compuestos fenólicos y los derivados de isoquinolina y de fenantridina se forman cuando las bases de Mannich pierden su grupo hidroxilo y se deshidrogenan. La presencia de los derivados de 2,3-benzofurano, isoquinolina, fenantridina y compuestos bifenílicos es crítica y responsable de la formación del resto carbonado característica de las polibenzoxazinas.

<sup>64</sup> Low YH, Ishida H. *Polymer*. 1999;40:4365.

<sup>65</sup> Macko JA, Ishida H. *Polymer*. 2001;42:227.

<sup>66</sup> Hemvichian K, Ishida H. *Polymer*. 2002;43:4391.

<sup>67</sup> Hemvichian K, Laobuthee A, Chirachanchai S, Ishida H. *Polym Degrad Stab*. 2002;76:1.

<sup>68</sup> Hemvichian K, Kim HD, Ishida H. *Polym Degrad Stab*. 2005;87:213.



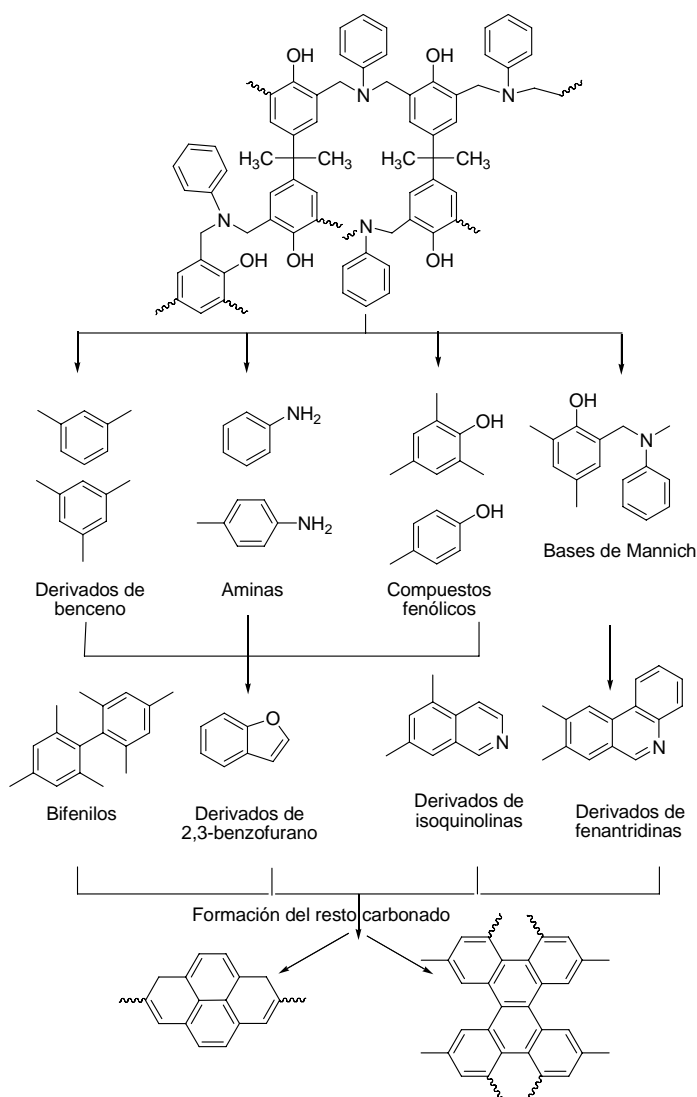
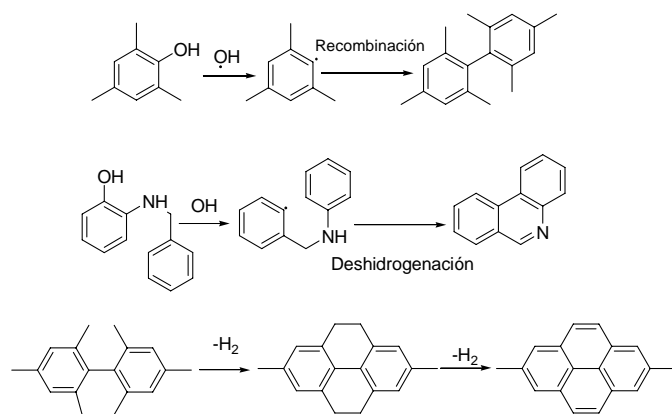


Figura 3.12 Compuestos de descomposición térmica de polibenzoxazinas.



**Figura 3.13** Mecanismo de degradación térmica de algunos compuestos.

### 3.6

#### Objetivos

El objetivo general del trabajo que se describe en este capítulo es la síntesis de nuevos sistemas retardantes a la llama derivados de benzoxazina, la evaluación de sus propiedades y el estudio de su comportamiento de degradación y de retardancia a la llama.

### 3.7

#### Parte experimental y resultados

En este capítulo se expondrán la parte experimental y los resultados de nuevas polibenzoxazinas retardantes a la llama, que han sido publicados en tres revistas científicas.

**3.7.1.** El trabajo descrito en esta sección ha sido publicado en *Journal of Polymer Science: Part A: Polymer Chemistry*, 2008, 46, 7162-7172, e incluye

la síntesis y caracterización de una nueva benzoxazina que contiene fósforo en su estructura, la benzoxazina derivada del óxido de bis(m-aminofenil)metilfosfina (Bz-BAMPO). Se investigó su cinética de curado por espectroscopia de FTIR, y se aplicó el método de análisis evolutivo del factor para describir el proceso. También, se estudió el entrecruzamiento por calorimetría diferencial de barrido y se aplicaron métodos de análisis isoconversional para evaluar la dependencia de la energía de activación con el grado de conversión. Se observó la coexistencia de distintas reacciones en el proceso de curado.

**3.7.2.** El segundo trabajo ha sido publicado en *Polymer Degradation and Stability* 2008, DOI: 10.1016/j.polymdegradstab.2008.08.004. En él se describe la copolimerización de Bz-BAMPO con la benzoxazina derivada del bisfenol A (Bz-BA) o con diglicidiléter del bisfenol A (DGEBA) y la preparación de sistemas fosforados con diferentes proporciones de fósforo. Se evaluaron sus propiedades térmicas y dinamomecánicas y se determinaron los valores del índice limitante de oxígeno que indicaron unas buenas propiedades de retardancia a la llama.

**3.7.3.** En esta sección se describe el trabajo enviado para su publicación a *European Polymer Journal*. A partir de la benzoxazina comercial derivada del bisfenol A y por copolimerización con diglicidiléter del óxido de (2,5-dihidroxifenil)difenil fosfina o con diglicidiloximetilfenil silano se han preparado sistemas benzoxazina-epoxi con distinto contenido de fósforo o silicio respectivamente. Se evaluaron sus propiedades térmicas y dinamomecánicas y se determinaron los valores del índice limitante de oxígeno poniendo de manifiesto el notable efecto del fósforo y la baja eficacia del silicio en la retardancia a la llama para los contenidos de heteroátomos ensayados.

UNIVERSITAT ROVIRA I VIRGILI  
RESINAS EPOXI Y BENZOXAZINAS FOSFORADAS Y SILILADAS RETARDANTES A LA LLAMA  
Marisa Elisabet Spontón  
ISBN:978-84-691-9480-5/DL:T-22-2009

---

**3.7.1. SYNTHESIS AND STUDY OF THE THERMAL CROSSLINKING OF  
BIS(*m*-AMINOPHENYL) METHYLPHOSPHINE OXIDE BASED  
BENZOXAZINE**

---

UNIVERSITAT ROVIRA I VIRGILI  
RESINAS EPOXI Y BENZOXAZINAS FOSFORADAS Y SILILADAS RETARDANTES A LA LLAMA  
Marisa Elisabet Spontón  
ISBN:978-84-691-9480-5/DL:T-22-2009

**SYNTHESIS AND STUDY OF THE THERMAL CROSSLINKING OF  
BIS(m-AMINOPHENYL) METHYLPHOSPHINE OXIDE BASED  
BENZOXAZINE.**

**M. Spontón, M. S. Larrechi, J.C. Ronda, M. Galià, V. Cádiz**

Departament de Química Analítica i Química Orgànica. Universitat Rovira i Virgili. Campus Sescelades Marcel·lí Domingo s/n. 43007 Tarragona. Spain.  
virginia.cadiz@urv.cat

**ABSTRACT**

Bis(m-aminophenyl)methylphosphine oxide based benzoxazine (Bz-BAMPO) was obtained using a three-step synthetic method from the aromatic diamine and 2-hydroxybenzaldehyde as starting materials. The structure and purity of the monomer was confirmed by elemental analysis, FTIR,  $^1\text{H}$ ,  $^{13}\text{C}$  and  $^{31}\text{P}$  NMR spectra. The curing kinetics of Bz-BAMPO was investigated by non-isothermal differential scanning calorimetry (DSC) at different heating rates and by FTIR spectroscopy. The isoconversional method was used to evaluate the dependence of the effective activation energy on the extent of conversion. The evolving factor analysis (EFA) method was applied to the spectroscopic FTIR data obtained in monitoring benzoxazine homopolymerizations.

**Keywords:** benzoxazine, crosslinking, flame retardance, infrared spectroscopy.

## INTRODUCTION

Among various high performance materials, polybenzoxazine is a newly developed addition polymerized phenolic system, having a wide range of interesting features and the capability to overcome several shortcomings of conventional phenolic resins. These thermosetting resins are obtained by a thermally activated polymerisation of the corresponding monomers without the need of strong acid catalyst and without releasing toxic by-products during the cure process.<sup>1-3</sup> These materials exhibit near-zero volumetric change upon curing,<sup>4</sup> low water absorption, high char yield, superior electrical properties and low surface energy.<sup>5</sup> In general, the approaches for improving the performance of polybenzoxazines can be classified into two ways. One is the structure modification by designing new benzoxazine monomers,<sup>6</sup> copolymerizing two or more than two benzoxazine monomers or copolymerizing with epoxy resins.<sup>7,8</sup> The other is the formation of composites or blends with other high temperature polymers like polyimide<sup>9</sup> as well as with inorganic fillers such as clay.<sup>10</sup>

According to the literature, most difunctional benzoxazines were synthesized from aromatic biphenols, monoamines, and formaldehyde. The large varieties of aromatic biphenols and monoamines allow considerable molecule-design flexibility for benzoxazines. This flexibility allows tailoring the properties of the cured materials for a wide range of applications and some special functional groups can be introduced via biphenols or monoamines to provide some desired properties. For example, Agag and Takeichi prepared phenyl propargyl ether-based<sup>11</sup> and allylamine-based<sup>12</sup> benzoxazines to increase  $T_g$  and thermal stability. Also Ishida et al. synthesized acetylene-<sup>13</sup>, maleimide-<sup>14</sup>, nitrile-<sup>15</sup> containing benzoxazines to



achieve highly thermal stable resins and phenylphosphine oxide-containing benzoxazines<sup>16</sup> to increase  $T_g$ , char yield and flame retardancy.

The common feature of these benzoxazines is that they are derived from aromatic biphenols, monoamines and formaldehyde. None of them is derived from aromatic diamines, phenol and formaldehyde. Benzoxazines based on difunctional,<sup>17-20</sup> multifunctional aromatic diamines or their derivatives<sup>21</sup> have been discussed in the literature. Recently, aromatic diamine-based benzoxazines, which could not easily be synthesized by traditional approaches, were prepared by a three step procedure.<sup>22,23</sup>

Polybenzoxazines with high flame retardant properties have attracted much attention owing to development demands for electronic materials. It is well known that phosphorus compounds are excellent candidates for thermal stable materials and organophosphorus compounds have been used as flame retardants for decades.<sup>24</sup> The presence of phosphorus compounds plays an important role in the high performance of thermally stable materials due to its ability to inhibit ignition and promote char formation. Therefore, incorporating a phosphorus-containing group into the benzoxazine monomer was thought to increase the char yield of benzoxazine.

In this study, a phosphorus-compound was incorporated into the structure of the benzoxazine in the form of phenylphosphine oxide functional group in a diamine-based benzoxazine. To make an optimum use of this benzoxazine resin, it is important to understand the nature of its curing process, the structure of the curing material and the kinetics of the curing reaction. The curing of this benzoxazine was investigated by FTIR and differential scanning calorimetry (DSC). Bisphenol A-based

benzoxazine was also investigated for the purpose of comparison. Chemometric methods have been applied to the spectroscopic FTIR data obtained in monitoring benzoxazine homopolymerizations. One of these methods for analyzing evolving data sets is evolving factor analysis (EFA).<sup>25,26</sup> This method allows estimate sequentially the rank of the matrix data by singular value decomposition (SVD).<sup>27</sup> This rank is related to the number of the independent reactions that take place in the process.<sup>28</sup>

## EXPERIMENTAL

### Materials

The following chemicals were obtained from the sources indicated: aniline, bisphenol A, methyldiphenylphosphine oxide, hydrazine monohydrate, 2-hydroxybenzaldehyde and sodium borohydride (NaBH<sub>4</sub>) from Aldrich. Paraformaldehyde from Probus. Bisphenol A based benzoxazine (Bz-BA)<sup>29</sup> and bis(m-aminophenyl)methylphosphine oxide (BAMPO)<sup>30</sup> were synthesized as previously described. All the solvents were purified with standard procedures.

### Synthesis of BAMPO Based Benzoxazine (Bz-BAMPO). (Scheme 1)

In a three-neck round-bottom flask equipped with a magnetic stirrer, BAMPO (20 g 81 mmol), 2-hydroxybenzaldehyde in excess (25 g 205 mmol) and ethanol (200 ml) were placed. The resultant mixture was stirred for 2 days at 60 °C under an argon atmosphere. The reaction was cooled at room temperature and NaBH<sub>4</sub> (4 g 105 mmol) was added in portions maintaining stirred the solution. After the solvent was removed under reduced pressure, the solid residue was dissolved in CH<sub>2</sub>Cl<sub>2</sub> and extracted with water. After the solvent was removed under reduced pressure, paraformaldehyde (6 g

0.2 mol) dissolved in dioxane was added. The mixture was stirred for 48 h at 100 °C. The reaction was followed by thin layer chromatography using ethyl acetate as eluent. After evaporating the solvent, the resulting product was dissolved in CH<sub>2</sub>Cl<sub>2</sub> and extracted with NaOH 2M solution three times and the organic phase was collected, dried over MgSO<sub>4</sub> and concentrated under reduced pressure. Thus, 35 g (95% yield) of yellowish power was afforded.

C<sub>29</sub>H<sub>27</sub> N<sub>2</sub>O<sub>3</sub>P (482.5): Calcd. C 72.19%; H 5.64%; N 5.82%, O 9.95%, P 6.42%; Found: C 71.19%; H 5.64%; N 5.81%, P 6.38%.

<sup>1</sup>H NMR (CDCl<sub>3</sub>/TMS, δ (ppm)): 7.50 (2 H, d, 13.2 Hz), 7.29 (2H, d, 3.2 Hz); 7.12 (2H), 7.09 (2H), 6.97 (2H) 6.82 (2H, dd, 1.6 Hz, 12 Hz); 6.77 (2H, m); 5.25 (4H, s); 4.52 (4H, s), 1.91 (3H, d, 13.2 Hz).

<sup>13</sup>C NMR (CDCl<sub>3</sub>, δ (ppm)): 154.26 (s), 148.67 (d), 135.47 (d); 129.77 (d); 128.05 (s), 126.87 (s), 122.75 (s), 121.11 (s), 120.71 (d), 120.63 (s), 120.00 (d) 117.07 (s), 78.78 (s), 50.36 (s), 17.01 (d).

<sup>31</sup>P NMR (CDCl<sub>3</sub>/H<sub>3</sub>PO<sub>4</sub>, δ (ppm)): 30.99

FTIR : 944 cm<sup>-1</sup> (N-C-O st), 1035 cm<sup>-1</sup> (Ar-O-C st), 1189 cm<sup>-1</sup> (P=O) 1223 cm<sup>-1</sup> (Ar-O st) 1425 cm<sup>-1</sup> ( P-Ar st).

### Instrumentation

The quantitative analyses of C, N and H were carried out on a Perkin-Elmer 2400 CHN microanalyzer. The FTIR spectra were recorded on a JASCO 680 FTIR spectrophotometer with a resolution of 4 cm<sup>-1</sup> in the absorbance mode. An attenuated total reflection (ATR) accessory with thermal control and a diamond crystal (Golden Gate heated single – reflection diamond ATR, Specac. Teknokroma) was used to determine FTIR spectra. <sup>1</sup>H (400 MHz), <sup>13</sup>C (100.5 MHz) and <sup>31</sup>P (161.9 MHz), NMR spectra were obtained using a Varian Gemini 400 spectrometer with Fourier transform, CDCl<sub>3</sub> as solvent and TMS or phosphoric acid as internal

standards. Calorimetric studies were carried out on a Mettler DSC821e thermal analyzer using N<sub>2</sub> as a purge gas (20 ml/min).

#### **Data acquisition of FTIR spectra**

The data obtained correspond to the FTIR/ATR between 600 and 4000 cm<sup>-1</sup> for Bz-BAMPO and Bz-BA homopolymerizations. The bands at 1485, 1222 and 943 cm<sup>-1</sup> associated to the benzoxazine ring, were used to follow the disappearance of oxazine ring. Thus, the reactions were considered to be completed when absorbance changes at these bands were not observed. In this way, we consider that the reactions ended after 10 h in both cases. The spectra were obtained each 15 min and therefore 40 spectra were obtained at the final reaction time.

The recorded spectra were arranged in two matrices **M** (40 × 1401) and **N** (40 × 1401) whose rows were the number of recorded spectra and whose columns were the wavelengths of Bz-BAMPO and Bz-BA reactions, respectively. The spectra recorded in the FTIR/ATR were exported and converted into MATLAB binary files.<sup>31</sup>

#### **Singular value decomposition (SVD)**

Singular value decomposition (SVD)<sup>27</sup> is used to estimate the rank of the FTIR data sets. To determine this number we are taking into account that the number of large singular values, significantly different in magnitude from the noise related singular values, indicates the rank of the matrix analyzed.

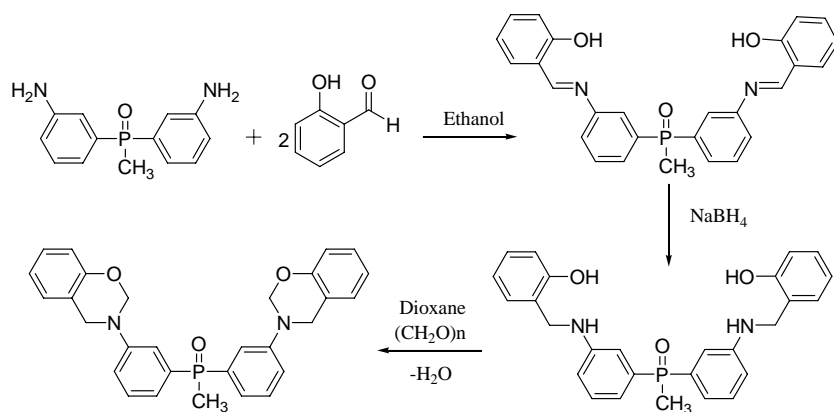
#### **Evolving Factor Analysis (EFA)**

The rank estimation has been confirmed using EFA.<sup>25,26</sup> This tool analyses the data set on gradually increasing submatrices in the process

direction, adding a row at a time and performing SVD for each submatrix. In our study we started with the first two spectra and then calculated the rank by adding one spectrum at a time until we reached the total matrix, **M** or **N**. This procedure is performed from top to bottom of the data set (forward EFA) and from bottom to top (backward EFA).

## RESULTS AND DISCUSSION

As it is well known, benzoxazines are synthesized by the Mannich reaction via condensation of phenol, formaldehyde, and diamines. Thus, we tried to synthesize the Bz-BAMPO from phenol, paraformaldehyde and BAMPO. This method gave a mixture of benzoxazine monomer, dimers, and high concentration of oligomeric species. The difunctional benzoxazine monomer separated by column chromatography was found to be only a 10%. It has been reported,<sup>29,32,33</sup> that the high concentration of oligomers can be attributed to the reactivity of aromatic diamines and high temperatures used. In an effort to minimize the generation of oligomers, the synthesis was conducted by a different pathway, preventing the direct reaction between diamine and paraformaldehyde. Thus, we used a three-step synthesis,<sup>34</sup> according to the procedure presented in Scheme 1. In the first step, 2-hydroxybenzaldehyde was reacted with BAMPO. The resulting imine compound was reduced *in situ* with NaBH<sub>4</sub> at room temperature yielding the *o*-hydroxybenzylamine derivatives. In the last step, paraformaldehyde in dioxane was added and the benzoxazine derivative was obtained with 95% of yield.



**Scheme 1.** Synthesis of Bz-BAMPO

The structure of Bz-BAMPO and the purity of the obtained product were verified by elemental analysis data, FTIR and NMR spectra. By IR spectroscopy, characteristic absorptions at 1425 and 1189  $\text{cm}^{-1}$  corresponding to absorptions of P-Ar and P=O respectively, were observed, as well as the absorptions at 1485, 1222 and 943  $\text{cm}^{-1}$  attributed to the benzoxazine ring. It was also observed the absence of bands from free or hydrogen-bonded hydroxyl group in the higher frequency region. The  $^1\text{H}$  and  $^{13}\text{C}$  NMR spectra of Bz-BAMPO and the assignment of each peak are shown in Figure 1. As shown in  $^1\text{H}$  NMR spectrum, signals at 4.52 (4H) and 5.25 (4H) were assigned to the O- $\text{CH}_2$ -N and Ph- $\text{CH}_2$ -N of oxazine ring, respectively, what verifies the formation of benzoxazines. No signal corresponding to N- $\text{CH}_2$ -Ph at around 3.80 ppm resulting from the ring opening of benzoxazine was observed,<sup>33</sup> revealing the purity of synthesized benzoxazines. The aromatic signals appear between 6.6 and 7.6 ppm (16H). The expansion of the spectrum shows the nonequivalent protons of both aromatic rings.  $^{13}\text{C}$ -NMR spectrum in Figure 1 shows signals at 50.3 and 78.7 ppm characteristic peaks of the methylene carbons in the oxazine ring.

The NMR signals could be assigned unequivocally by means of DEPT, HMBC, and gHMQC experiments.

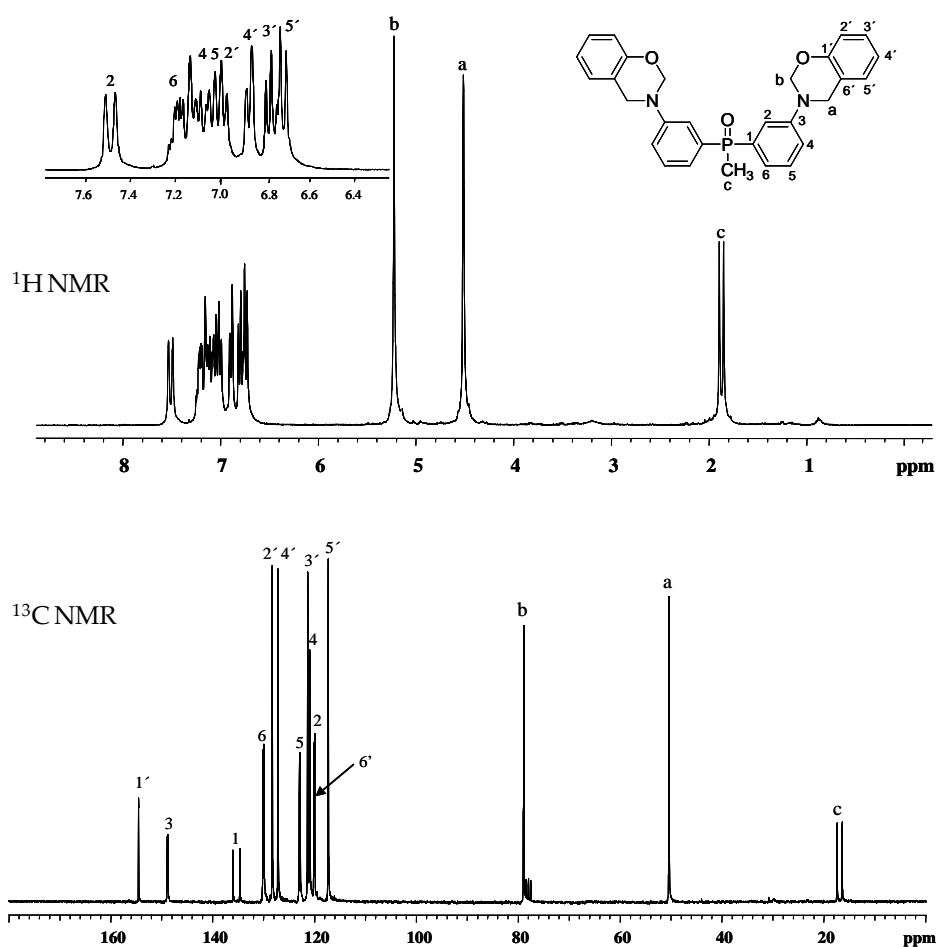


Figure 1.  $^1\text{H}$  and  $^{13}\text{C}$  NMR spectra of Bz-BAMPO

Figure 2 shows the DSC plot of Bz-BAMPO. The DSC of benzoxazine from Bisphenol A, aniline and formaldehyde (Bz-BA) is also shown for purpose of comparison. As can be seen from the crosslinking exotherms, the ring opening reaction starts, in all cases, about 210 °C. Bz-BA shows a

typical polymerisation exotherm for difunctional benzoxazines centered at 245 °C. In contrast, Bz-BAMPO exhibit different curing behaviour. A shifting of the main polymerisation exotherm to lower temperatures and a dual exotherm can be seen. Different polymerisation kinetics must be taking place in these two compounds. Benzoxazines with crosslinking mechanisms that also show this dual exotherm have been previously described.<sup>35</sup> It is postulated that the high temperature shoulder corresponds to the side reactions which generate bisphenolic methylene linkages and possibly reaction to the *para*-position of the arylamine ring. This was described for difunctional alkyl-substituted aniline-based benzoxazines from Bisphenol A.

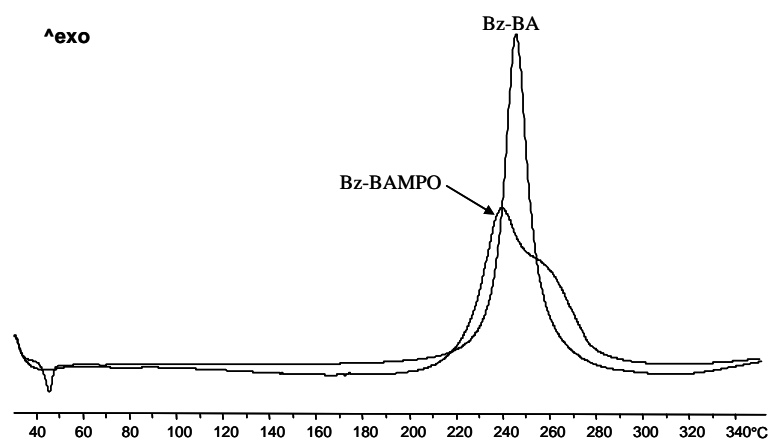
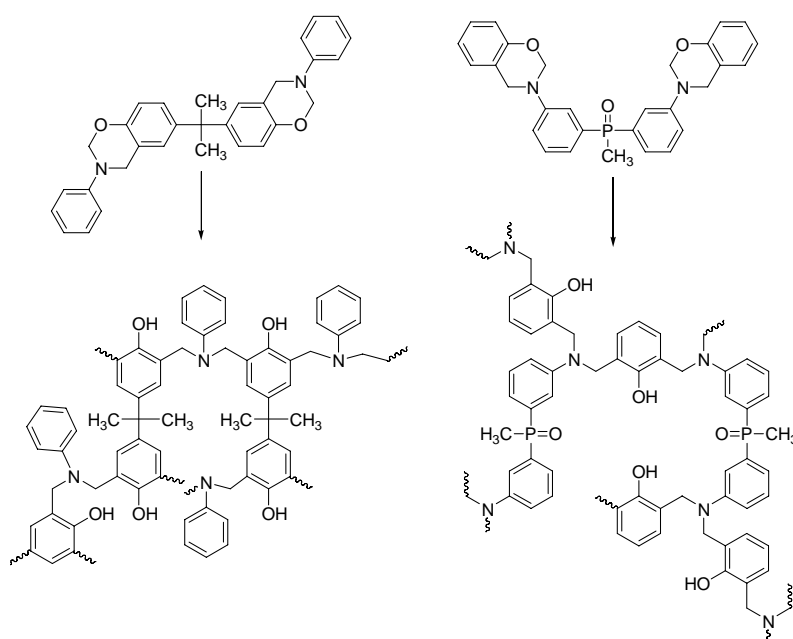


Figure.2. DSC plots of Bz-BAMPO and Bz-BA.

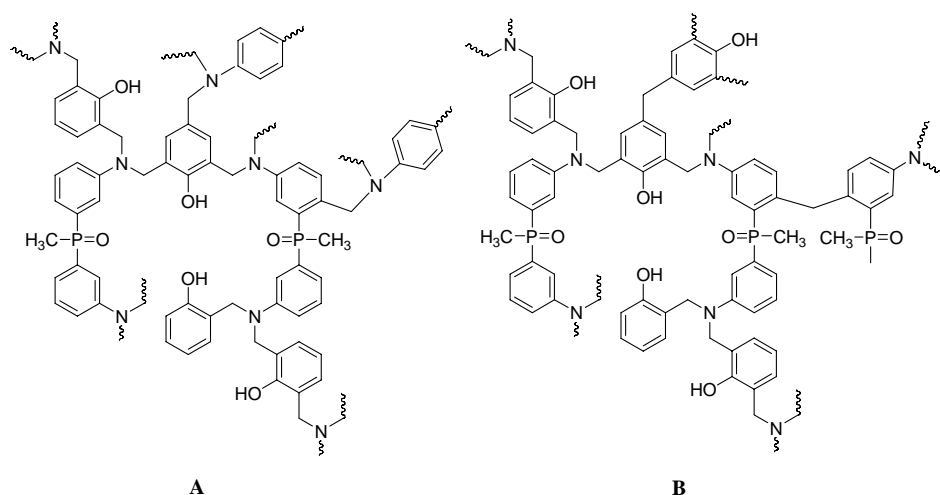
The curing kinetics of these polyfunctional benzoxazine resins were investigated by DSC.<sup>36</sup> Bz-BA resin shows only one dominant autocatalytic curing process whereas substituted arylamine based benzoxazine resins exhibits two dominant curing processes, the first one is found to be autocatalytic while the second exhibits nth-order curing kinetics.



In our case, Bz-BAMPO has *ortho*- and *para*- free phenolic positions, in addition to the *ortho*- and *para*-arylamine sites. Thus, a Mannich bridge network structure can develop as shown in Scheme 2. Moreover, evidence for various methylene linkages in thermally cured benzoxazines was given.<sup>35</sup> A network in which some oxazine rings cleave during cure could produce a phenolic network or alternatively a network with arylamine methylene bridges (Scheme 3). Such reactions would not require the same amount of mobility to occur and therefore could continue even after the main polymerization reactions becomes diffusion controlled.



**Scheme 2.** Formation of phenolic Mannich bridge network.



**Scheme 3.** (A) Phenolic and arylamine Mannich bridge network. (B) Phenolic and arylamine methylene bridge network.

The curing of benzoxazine resins is a chemical process that is complicated by the physical processes of gelation and vitrification. At the gel point, the growing chains connect into a single network, and the system cannot flow, but the chain segments are still capable of long-range motion. Further crosslinking within the network leads to vitrification, which is associated with the loss of long-range mobility. As the molecular motion becomes more restricted, the rate controlling step of curing shifts from the chemical reaction to diffusion. These two processes usually have different activation energy and the change from a kinetic regime to a diffusion regime can be seen as a change in the effective activation energy. The variations in the effective activation energy ( $E_a$ ) are determined with an isoconversional method.<sup>37</sup> This isoconversional kinetic analysis is based on the idea that the reaction rate at a constant conversion depends only on the temperature and its application gives the dependence of the effective activation energy on the degree of conversion. The obtained DSC data were used to evaluate this dependence (Fig. 3). As can be seen for Bz-BA system

the  $E_a$  value does not change in a significant way for conversion degrees lower than 0.8. This seems to indicate that multistep chemical processes or physical processes of gelation and vitrification do not contribute significantly to the curing process. For Bz-BAMPO, as conversion degree increases, the  $E_a$  increases and a significant change can be seen for  $\alpha = 0.4$ , thus indicating that the rate-determining step of curing changes to a process with a higher  $E_a$  and that chemical and physical process seems to become important.

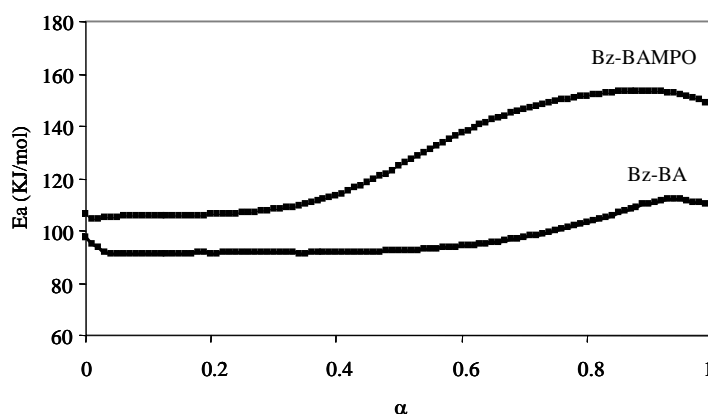


**Figure 3.** Activation energy versus curing degree for Bz-BAMPO and Bz-BA.

The most common method to monitor the benzoxazine curing reaction, DSC, do not provide direct information about the mechanism of the reaction. The number of species involved in the curing reaction can be obtained by separation techniques such as high performance liquid chromatography.<sup>38</sup> This is essentially an offline technique, it is often used for the kinetic investigation of reactions that do not evolve towards solid products. Spectroscopic techniques such as FTIR/ATR and chemometrics analysis of the recorded data through the reaction, make it possible to

monitor the process on line and provided useful information about the number of the chemical compounds evolved in the curing reaction.

We study the more complex behaviour of Bz-BAMPO polymerisation by monitoring by FTIR/ATR spectroscopy in isothermal experiments at 185 °C. The Bz-BA polymerization was also studied to compare. This technique allowed us to follow the evolution of the functional groups involved in the process by means of the variations in the corresponding absorptions.

Figure 4 shows FTIR spectra of the Bz-BAMPO and Bz-BA polymerizations at different times. As can be seen at 1485 cm<sup>-1</sup>, 1222 cm<sup>-1</sup> and 943 cm<sup>-1</sup>, characteristic benzoxazine bands, follow a progressive diminution with time, although a quicker evolution is observed for Bz-BA homopolymerization. Plots of absorbance intensity versus the number of spectra for these wavenumbers are shown in Figure 5. In addition, some other changes can be observed in several bands. Thus, in Fig. 6 the evolution of bands at 873, 1157 and 1580 cm<sup>-1</sup> is shown. As can be observed, in both reactions, for the first 150 min (10 spectra recorded) there is a quick increase of the absorbance for the three wavenumbers. At this time, the Bz-BA absorbances start to increase slowly whereas the Bz-BAMPO absorbances start to slightly decrease.

Moreover, in the Bz-BAMPO homopolymerization, a strong band at 1189 cm<sup>-1</sup> attributable to O=P groups is observed (Fig. 4) which decreases from the beginning of the reaction, what may be related to the formation of intensive intermolecular hydrogen bonds as OH...O=P.

At the beginning of the Bz-BA homopolymerization (Fig. 4) a strong band at 821 cm<sup>-1</sup> is observed which decreases quickly to keep constant. In

the Bz-BAMPO homopolymerization (Fig. 4) this band is weaker but it undergoes a similar evolution. However, for the band at  $690\text{ cm}^{-1}$ , different behaviour is observed. The intensity of this band, which is assigned to the trisubstituted benzene ring in the benzoxazine structure, decreases in the Bz-BA reaction as a tetrasubstituted benzene ring appears. In the Bz-BAMPO reaction a significant increase is observed just at the beginning due to the formation of trisubstituted benzene ring. (Scheme 2).

A global analysis of the earlier results indicates that the evolution of the benzoxazine bands is different in both processes. The data for Bz-BA reaction can fit to a kinetic of pseudofirst order whereas the data for Bz-BAMPO reaction does not fit. For Bz-BAMPO at 150 min reaction time (spectrum 10) a change of the slope in the evolution curve appears thus indicating that the reaction goes through two pathways with different kinetics. It must be pointed out that also at this time is when the behaviour of the bands at  $873$ ,  $1157$  y  $1580\text{ cm}^{-1}$  begins to be different for both processes.

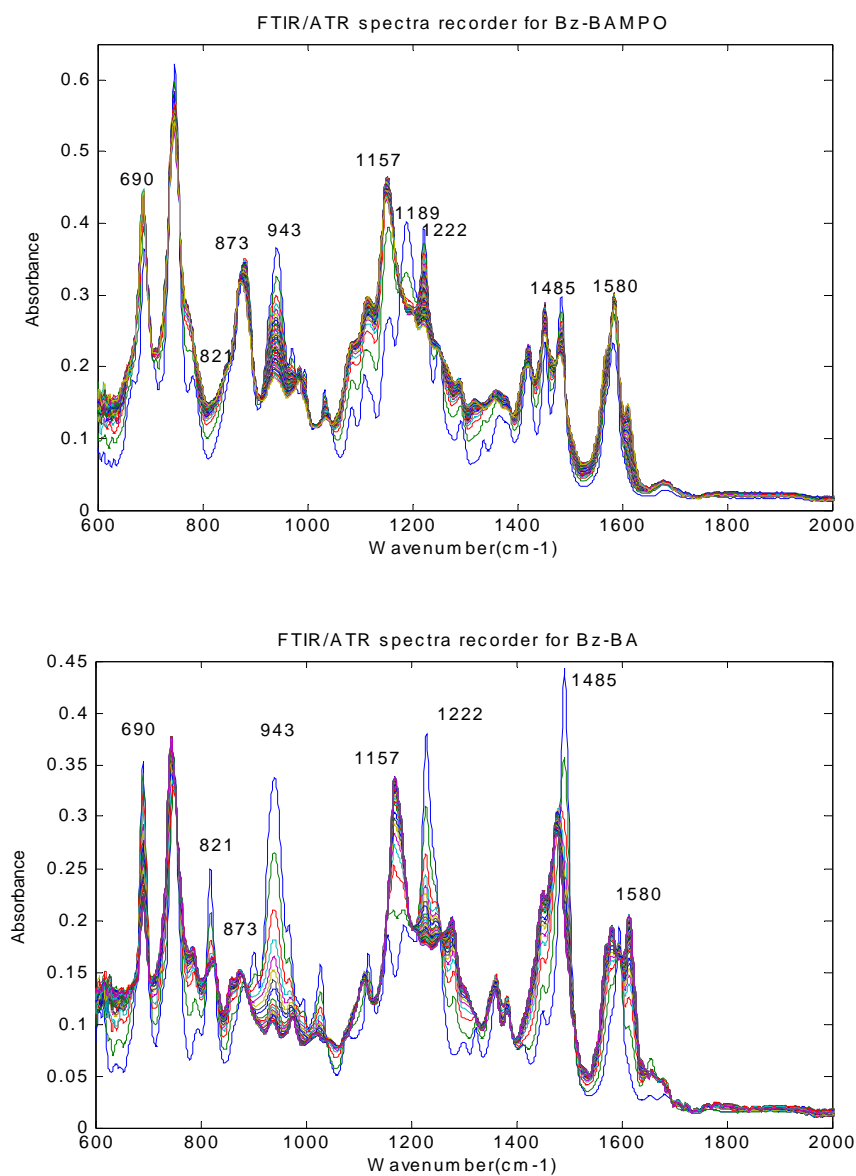


**Figure 4.** FTIR-ATR spectra of Bz-BAMPO and Bz-BA polymerizations at 185°C.

The singular values of the data sets are presented in Table 1. Considering as threshold singular values associated with noise the value ( $\lambda = 0.93$ ) achieved using the 100 channels of the spectrum between 1800 and 1900  $\text{cm}^{-1}$  where no signal contribution is observed, in the **M** matrix (Bz-BAMPO) three factors are significantly different from noise, while in **N** matrix (Bz-BA) is 2. According to Amrhein's<sup>28</sup> formulation, the rank of a process data set, as considered, is defined as the minimum of the number corresponding to number of independent reaction + 1. Thus, we can conclude that for the reaction in the case of Bz-BA an only reaction is involved whereas for Bz-BAMPO there are two.

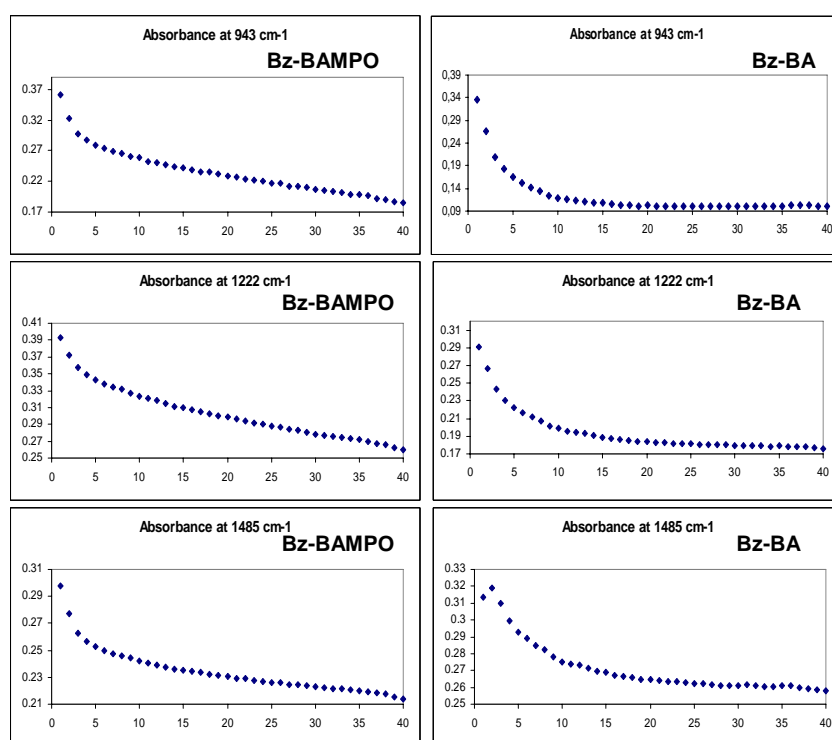


**Figure 5.** Absorbance values versus number of spectra at 943, 1222 and 1485 $\text{cm}^{-1}$  for Bz-BAMPO and Bz-BA.

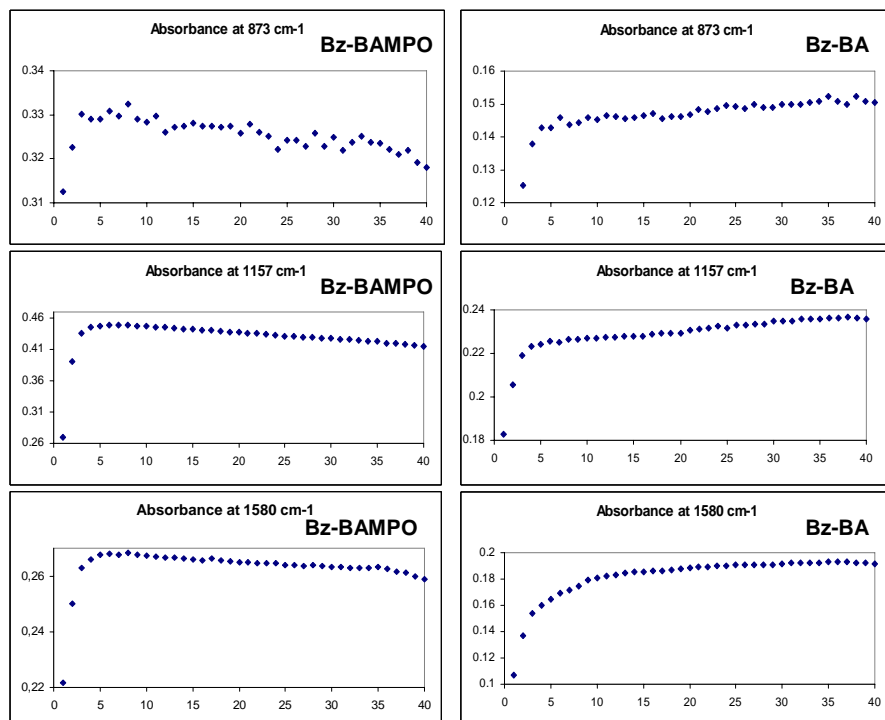


**Figure 6.** Absorbance values versus number of spectra at 873, 1157 and 1580cm<sup>-1</sup> for Bz-BAMPO and Bz-BA.

**Table 1** Rank Analysis of Matrices M and N

| Nº of factor | Singular value ( $\lambda$ ) of the M matrix (Bz-BAMPO) | Singular values ( $\lambda$ ) of the N matrix (Bz-BA) |
|--------------|---|---|
| 1            | 36.598  | 33.900  |
| 2            | 2.046   | 3.336   |
| 3            | 1.150   | 0.629   |
| 4            | 0.338   | 0.371   |
| 5            | 0.118   | 0.179   |

The singular values are tabulated the first five factors.



Additional information of the rank is given using EFA. Figure 7 shows the EFA results for Bz-BAMPO (matrix **M**) and Bz-BA (matrix **N**). Note that, in both cases, there are two significant factors at the beginning of the reaction, and for the Bz-BAMPO (matrix **M**) an additional factor in the forward direction becomes significant after the spectrum number 20. This is in accordance with the earlier described when an individual analysis of the spectroscopy changes at characteristics absorption bands was performed. From Figures 5 and 6, for both cases (Bz-BAMPO and Bz-BA), the evolution is similar until the spectrum number 10. At this time two factor appear in the EFA plots. The new chemical situation associated to a slope change in the evolution of the data recorded for the Bz-BAMPO is reflected in the fact that the third factor in the EFA plots become significant at the threshold considered.

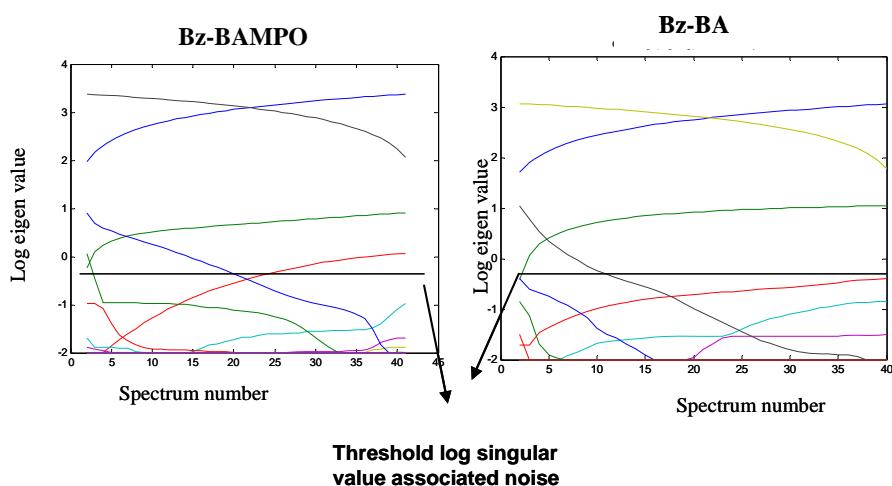
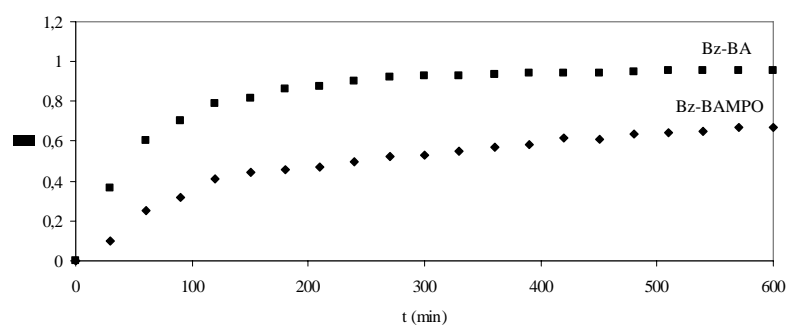


Figure 7. EFA plots of Bz-BAMPO and Bz-BA.

To relate the earlier observed changes with the conversion degree and isoconversional data, we calculated the conversion of benzoxazine groups

in both homopolymerization reactions by calculating the decrease of the band at  $943\text{ cm}^{-1}$ .

The absorbances were calculated in terms of peak areas. The conversions of the benzoxazine groups were determined by the Lambert-Beer Law from the normalized changes in absorbance respect to the band at  $747\text{ cm}^{-1}$  for the Bz-BA reaction and  $740\text{ cm}^{-1}$  for the Bz-BAMPO reaction. Figure 8 shows the conversions against time.



**Figure.8.** Conversion degree versus curing time for Bz-BAMPO and Bz-BA.

As we can see, the benzoxazine group reacts very fast at the beginning of the process for Bz-BA up to a conversion of about 0.8 and reaching its maximum conversion below 250 min. On the other hand, the evolution of benzoxazine group for Bz-BAMPO steadily progress up to a conversion of 0.6-0.7. From data in Figure 8, at 150 min of reaction a conversion degree of 0.8 is reached for Bz-BA. For Bz-BAMPO at 150 min of reaction a conversion degree of 0.4 is obtained. This reveals that the significant change in the  $E_a$  observed in the isoconversional analysis is related to the different chemical situations and the fact that a new factor becomes significant at the threshold considered, as can be seen in Table 1 and EFA plots. Both results could be

related to secondary reactions leading to the formation of methylene or Mannich bridges.

## CONCLUSIONS

In this article, we have shown that Bz-BAMPO which could not be synthesized by traditional approaches, was successfully synthesized by a three-step synthetic method. By non-isothermal differential scanning calorimetry, this monomer exhibits a clear split of the curing exotherm, according to the existence of several curing processes. The isoconversional method allowed to evaluate the dependence of the effective activation energy on the extent of conversion. The evolving factor analysis (EFA) method was applied to the spectroscopic FTIR data obtained in monitoring benzoxazine homopolymerizations. The significant change in the  $E_a$  observed is related to the different chemical situations observed by EFA analysis. Both results could be related to secondary reactions leading to the formation of phenolic and arylamine methylene or arylamine Mannich bridges, in addition to the phenolic Mannich bridges, found in conventional benzoxazine resins. The significant change in the  $E_a$  observed in the isoconversional analysis is related to the different chemical situations and the fact that a new factor becomes significant at the threshold considered, as can be seen in Table 1 and EFA plots.

## Acknowledgements

The authors express their thanks to CICYT (Comisión Interministerial de Ciencia y Tecnología) (MAT2005-01593) (CTQ2007-6147/BQU) for financial support for this work.

## REFERENCES

- <sup>1</sup> Schreiber, H. Ger. Offen 2, 255, 504, 1973; (b) Ger Offen 2, 323, 936, 1973.
- <sup>2</sup> Riess, G.; Schowb, J. M.; Roche, M.; Laude, B. *Polym Prep (Am Chem Soc Div Polym Chem)* 1984, 25, 41-42.
- <sup>3</sup> Grosch, N.N.; Kiskan, B.; Yagsi, Y. *Prog Polym Sci* 2007, 32, 1344-1391.
- <sup>4</sup> Low H. I.; Ishida H. *Macromolecules*. 1997, 30, 1099-1106.
- <sup>5</sup> Wang, C.F.; Su, Y.C.; Kuo, S.W.; Huang, C.F.; Sheen, Y.C.; Chang, F.C. *Angew Chem Int Ed* 2006, 45, 2248-2251.
- <sup>6</sup> Takeichi, T.; Agag, T. *High Performance Polym* 2006, 18, 777-797.
- <sup>7</sup> Ishida H.; Allen D.J. *Polymer* 1996, 37, 4487-4495.
- <sup>8</sup> Agag, T.; Takeichi, T. *High Performance Polym* 2002, 14, 115-132.
- <sup>9</sup> Takeichi, T.; Agag, T. *J Polym Sci Part A: Polym Chem* 2001, 39, 2633-2641.
- <sup>10</sup> Agag, T.; Takeichi, T. *Polymer* 2000, 41, 7083-7090.
- <sup>11</sup> Agag T.; Takeichi T. *Macromolecules* 2001, 34, 7257-7263.
- <sup>12</sup> Agag, T.; Takeichi T. *Macromolecules* 2003, 36, 6010-6017.
- <sup>13</sup> Kim, H.J.; Brunovska, Z.; Ishida, H. *Polymer* 1999, 40, 6565-6573.
- <sup>14</sup> Ishida, H.; Ohba, S. *Polymer* 2005, 46, 5588-5595.
- <sup>15</sup> Brunovska, Z.; Ishida, H. *J. Appl Polym Sci* 1999, 73, 2937-2949.
- <sup>16</sup> Choi, S-W.; Ohba, S.; Brunovska, Z.; Hemvichian, K.; Ishida, H. *Polym Deg Stab* 2006, 91, 1166-1178.
- <sup>17</sup> Shen, S.B.; Ishida, H.; *J Appl Polym Sci* 1996, 61, 1595-1605.
- <sup>18</sup> Takeichi, T.; Kano, T.; Agag, T. *Polymer* 2005, 46, 12172-12180.
- <sup>19</sup> Men, W.; Lu, Z.; *J Appl Polym Sci* 2007, 106, 2769-2774.
- <sup>20</sup> Men, W.; Lu, Z.; *J Appl Polym Sci* 2008, 109, 2219-2223.
- <sup>21</sup> Subrayan, R.P.; Jones, F.N. *Chem Mater* 1998, 10, 3506-3512.
- <sup>22</sup> Lin, C.H.; Chang, S.L.; Hsieh, C.W.; Lee, H.H. *Polymer* 2008, 49, 1220-1229.
- <sup>23</sup> Lin, C. H.; Chang, S. L.; Lee, H. H.; Chang, H. C.; Hwang, K. Y.; Tu, A. P.; Su, W. C. *J Polym Sci Part A Polym Chem* 2008, 46, 4970-4983.
- <sup>24</sup> Lu, S-Y.; Hamerton, I. *Prog Polym Sci* 2002, 27, 1661-1712.
- <sup>25</sup> Gampp, H.; Maeder, M.; Meyer, C.J.; Zuberbuehler, A.D. *Anal Chim Acta* 1987, 193, 287-293.
- <sup>26</sup> Maeder, M., *Anal Chem* 1987, 59, 527-530.
- <sup>27</sup> Golub, G.H.; Van Loan, C.F. *Matrix Computations*, Johns Hopkins University Press, Baltimore, 1996.
- <sup>28</sup> Amrhein, M.; Srinivasan, B.; Bonvin, D.; Schumacher, M.M. *Chem Intell Lab Syst* 1996, 33, 17-33.
- <sup>29</sup> Ishida, H.; Rodríguez, Y. *Polymer* 1995, 36, 3151-3158.
- <sup>30</sup> Varma, I. K.; Gupta, U. J. *Macromol Sci Chem* 1986, A23, 19-36.
- <sup>31</sup> The Mathworks, MATLAB Version 7.0, Natick, MA, 2004.
- <sup>32</sup> Ning, X.; Ishida, H. *J Polym Sci Part A; Polym Chem* 1994, 32, 921-927.
- <sup>33</sup> Ning, X.; Ishida, H. *J Polym Sci Part A; Polym Chem* 1994, 32, 1121-1129.
- <sup>34</sup> Andreu, R.; Reina, J. A.; Ronda, J. C. *J Polym Sci Part A; Polym Chem* 2008, 46, 3353-3366.

<sup>35</sup> Ishida, H.; Sanders, D.P. *Macromolecules*, 2000, 33, 8149-8157.

<sup>36</sup> Jubsilp, Ch.; Damrongsakkul, S.; Takeichi, T.; Rimdusit S. *Thermochim Acta* 2006, 447, 131-140.

<sup>37</sup> Vyazovkin, S.; Sbirrazzuoli, N. *Macromolecules* 1996, 29, 1867-1873.

<sup>38</sup> Mijovic, J.; Fishbain, A.; Wijaya, J. *Macromolecules* 1992, 25, 979-985.



---

*3.7.2. STUDIES ON THERMAL AND FLAME RETARDANT BEHAVIOUR  
OF MIXTURES OF BIS (m-AMINOPHENYL)METHYLPHOSPHINE OXIDE  
BASED BENZOXAZINE AND GLYCIDYLETHER OR BENZOXAZINE OF  
BISPHENOL A*

---

UNIVERSITAT ROVIRA I VIRGILI  
RESINAS EPOXI Y BENZOXAZINAS FOSFORADAS Y SILILADAS RETARDANTES A LA LLAMA  
Marisa Elisabet Spontón  
ISBN:978-84-691-9480-5/DL:T-22-2009



**STUDIES ON THERMAL AND FLAME RETARDANT BEHAVIOUR OF MIXTURES OF BIS(*m*-AMINOPHENYL)METHYLPHOSPHINE OXIDE BASED BENZOXAZINE AND GLYCIDYLETHER OR BENZOXAZINE OF BISPHENOL A**

M. Spontón, J. C. Ronda, M. Galià, V. Cádiz

Departament de Química Analítica i Química Orgànica. Universitat Rovira i Virgili. Campus Sescelades Marcel·lí Domingo s/n. 43007 Tarragona. Spain.  
marina.galia@urv.cat

**ABSTRACT**

---

The curing of mixtures of bis(*m*-aminophenyl)methylphosphine oxide based benzoxazine and glycidylether or benzoxazine of Bisphenol A has been studied. In all samples the molar ratio of benzoxazine monomers or the benzoxazine-epoxy system was varied to achieve different phosphorus content. The phosphorus-containing polybenzoxazines have been characterized by dynamic mechanical and thermogravimetric analysis. Limiting oxygen index values indicate good flame retardant properties.

---

**Keyword:** Flame retardant, Benzoxazine, Epoxy Heteroatom-containing polymers.

## INTRODUCTION

Polybenzoxazine as a novel phenolic type thermoset has been developed to overcome the shortcomings associated with the use of traditional phenolics.<sup>1</sup> It can be prepared from benzoxazines via thermally-induced ring opening polymerisation. Benzoxazine are readily synthesized either in solution or by a melt-state reaction using a combination of a phenolic derivative, formaldehyde, and a primary amine.<sup>2</sup> Polybenzoxazines have not only the advantageous properties of conventional phenolic resins but also other interesting advantages such as excellent dimensional stability. The disadvantages of the typical polybenzoxazines are the high temperature needed for complete curing and the brittleness of the cured materials that can sometimes limit their potential applications. Polybenzoxazines with high flame retardant properties have attracted much attention owing to development demands for electronic materials. It is well known that organophosphorus compounds have been used as flame retardants for decades.<sup>3</sup> The presence of phosphorus compounds plays an important role in the high performance of thermally stable materials due to its ability to inhibit ignition and promote char formation. Therefore, incorporating a phosphorus-containing group into the benzoxazine monomer was thought to increase the char yield of benzoxazine.

The polyfunctionality required to form an infinite network structure upon benzoxazine polymerisation may be achieved through monomer synthesis utilizing either a multifunctional phenolic molecule with a monoamine or a multifunctional amine paired with a mono-phenol. Of these two approaches, the majority of polybenzoxazine research published today has focused on materials in which the multifunctional core is provided by the phenolic compound. Multifunctional amine based

polybenzoxazines have an enormous potential in tailoring molecule structure for specific applications and benzoxazines based on difunctional,<sup>4-7</sup> multifunctional aromatic diamines or their derivatives<sup>8</sup> have been discussed in the literature. Recently aromatic diamine-based benzoxazines, which could not easily be synthesized by traditional approaches, were prepared by a three-step procedure.<sup>9</sup> Moreover, in a previous work we incorporated a phosphorus-compound into the structure of the benzoxazine in the form of phenylphosphine oxide functional group in a diamine-based benzoxazine and synthesized bis(*m*-aminophenyl)methylphosphine oxide based benzoxazine (Bz-BAMPO), using this procedure.<sup>10</sup>

Together with the structure modification by designing new benzoxazine monomers, there are other approaches for improving the performance of polybenzoxazines, such as copolymerising two or more than two benzoxazine monomers or copolymerising with epoxy resins.<sup>11</sup> The crosslinking densities of benzoxazine resins are believed to be considerably lower than those of ordinary thermosetting resins.<sup>12</sup> The tightening of the network structure has been investigated by copolymerizing benzoxazine resin with epoxy resin.<sup>13-15</sup> The crosslinking density and glass transition temperature of these copolymers were higher than those of the polybenzoxazine homopolymer, and their heat resistance and mechanical properties were also better. In addition, the presence of the epoxy resins significantly improves the processability of benzoxazine resins but the resulting mixtures require higher curing temperatures than the pure benzoxazine resins.

In this work polybenzoxazines with different phosphorus content were prepared from copolymerisation of Bz-BAMPO either with the conventional Bisphenol A based benzoxazine or with diglycidylether of Bisphenol A.

The curing behaviour of these materials was investigated by differential scanning calorimetry (DSC). Finally, the properties of the materials were evaluated by termogravimetric analysis (TGA), dynamic mechanical analysis (DMTA) and the limiting oxygen index (LOI).

## EXPERIMENTAL

### Materials

The following chemicals were obtained from the sources indicated: aniline, Bisphenol A, diglycidylether of Bisphenol A (DGEBA), methyldiphenylphosphine oxide, hydrazine monohydrate, 2-hydroxybenzaldehyde, sodium borohydride ( $\text{NaBH}_4$ ) from Aldrich. Paraformaldehyde from Probus. Bisphenol A based benzoxazine (Bz-BA)<sup>16</sup> and bis(*m*-aminophenyl)methylphosphine oxide (BAMPO)<sup>17</sup> were synthesized as previously described.

All the solvents were purified with standard procedures.

### Synthesis of BAMPO based benzoxazine (Bz-BAMPO).

In a three-neck round-bottom flask equipped with a magnetic stirrer, BAMPO (20 g 81 mmol), 2-hydroxybenzaldehyde in excess (25 g 205 mmol) and ethanol (200 ml) were placed. The resultant mixture was stirred for 2 days at 60 °C under an argon atmosphere. The reaction was cooled at room temperature and  $\text{NaBH}_4$  (4 g 105 mmol) was added in portions maintaining stirring of the solution. After the solvent was removed under reduced pressure, the solid residue was dissolved in  $\text{CH}_2\text{Cl}_2$  and extracted with water. After the solvent was removed under reduced pressure, paraformaldehyde (6 g 0.2 mol) dissolved in dioxane was added. The mixture was stirred for 48 h at 100 °C. The reaction was followed by thin

layer chromatography using ethyl acetate as eluent. After evaporating the solvent, the resulting product was dissolved in  $\text{CH}_2\text{Cl}_2$  and extracted with  $\text{NaOH}$  2M solution three times and the organic phase was collected, dried over  $\text{MgSO}_4$  and concentrated under reduced pressure. Thus, 35 g (95% yield) of yellowish powder was afforded.

$\text{C}_{29}\text{H}_{27}\text{N}_2\text{O}_3\text{P}$  (482.5): Calcd. C 72.19%; H 5.64%; N 5.82%, O 9.95%, P 6.42%; Found: C 71.19%; H 5.64%; N 5.81%, P 6.38%.

$^1\text{H}$  NMR ( $\text{CDCl}_3/\text{TMS}$ ,  $\delta$  (ppm)): 7.50(2 H, d, 13.2 Hz), 7.29 (2H, d, 3.2 Hz); 7.12 (2H), 7.09 (2H), 6.97 (2H) 6.82 (2H, dd, 1.6 Hz, 12 Hz); 6.77 (2H, m); 5.25 (4H, s); 4.52 (4H, s), 1.91 (3H, d, 13.2 Hz).

$^{13}\text{C}$  NMR ( $\text{CDCl}_3$ ,  $\delta$  (ppm)): 154.26 (s), 148.67 (d), 135.47 (d); 129.77 (d); 128.05 (s), 126.87 (s), 122.75 (s), 121.11 (s), 120.71 (d), 120.63 (s), 120.00 (d) 117.07 (s), 78.78 (s), 50.36 (s), 17.01 (d).

$^{31}\text{P}$  NMR ( $\text{CDCl}_3/\text{H}_3\text{PO}_4$ ,  $\delta$  (ppm)): 30.99

FTIR :  $944\text{cm}^{-1}$  (N-C-O st),  $1035\text{cm}^{-1}$  (Ar-O-C st),  $1189\text{cm}^{-1}$  (P=O)  $1223\text{cm}^{-1}$  (Ar-O st)  $1425\text{cm}^{-1}$  (P-Ar st).

### Crosslinking reaction

Samples (Tables 1 and 3) were prepared by the dissolution of benzoxazine and epoxy monomers in  $\text{CH}_2\text{Cl}_2$ . Then, this solution was evaporated at room temperature under vacuum. About 10 mg of a known weight of the mixture was put into the aluminum pan, and the polymerization was monitored in a dynamic DSC experiment using a heating rate of  $10\text{ }^\circ\text{C}/\text{min}$ .

Molded, cured benzoxazine resins were prepared with a manual hydraulic press 15-ton sample pressing (SPECAC) equipped with a water cooled heated platens. The mixture was placed in a  $70 \times 6 \times 3\text{ mm}$  mold and compression molded at  $180\text{ }^\circ\text{C}$  for 2.5h,  $200\text{ }^\circ\text{C}$  for 1h and  $215\text{ }^\circ\text{C}$  for 2h. under 0.1 mPa.

### Instrumentation

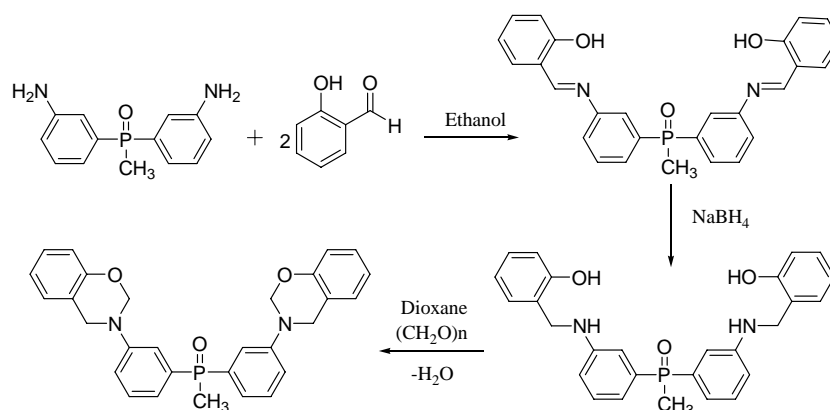
The quantitative analyses of C, N and H were carried out on a Perkin Elmer 2400 CHN microanalyzer. The FTIR spectra were recorded on a JASCO 680 FTIR spectrophotometer with a resolution of  $4\text{ cm}^{-1}$  in the absorbance mode. An attenuated total reflection (ATR) accessory with thermal control and a diamond crystal (Golden Gate heated single – reflection diamond ATR, Specac. Teknokroma) was used to determine FTIR spectra.  $^1\text{H}$  400 MHz,  $^{13}\text{C}$  100.5 MHz and  $^{31}\text{P}$  161,9 MHz NMR spectra were obtained using a Varian Gemini 400 spectrometer with Fourier transform,  $\text{CDCl}_3$  as solvent and TMS or phosphoric acid as internal standards.

Calorimetric studies were carried out on a Mettler DSC821e thermal analyzer using  $\text{N}_2$  as a purge gas (20 ml/min) at scanning rate of  $10\text{ }^\circ\text{C}/\text{min}$ . Thermal stability studies were carried out on a Mettler TGA/SDTA851e/LF/1100 with  $\text{N}_2$  or air as a purge gas at scan rates of  $10\text{ }^\circ\text{C}/\text{min}$ . Mechanical properties were measured using a dynamic mechanical thermal analysis (DMTA) apparatus (TA DMA 2928). Specimens ( $10 \times 6 \times 1.9\text{ mm}$ ) were tested in a single cantilever configuration. The thermal transitions were studied in the  $30\text{-}250\text{ }^\circ\text{C}$  at a heating rate of  $5\text{ }^\circ\text{C}/\text{min}$  and at a fixed frequency of 1 Hz.

LOI values were measured on a Stanton Redcroft, provided with an Oxygen Analyzer, on polymer bars that measured  $70 \times 6 \times 3\text{ mm}$  and which were prepared by molding.

## RESULTS AND DISCUSSION

As it is well known, benzoxazines are synthesized by the reaction via Mannich condensation of phenol, formaldehyde and diamines.<sup>18</sup> However, in an effort to minimize the generation of oligomers, the synthesis of Bz-BAMPO<sup>10</sup> was conducted by a different pathway, preventing the direct reaction between diamine and paraformaldehyde, using a three-step synthesis<sup>19</sup>, according the procedure presented in Scheme 1. In the first step, 2-hydroxybenzaldehyde was reacted with BAMPO. The resulting imine compound was reduced in situ with NaBH<sub>4</sub> at room temperature yielding the o-hydroxybenzylamine derivative. In the last step paraformaldehyde in dioxane was added and the benzoxazine derivative was obtained with 95% of yield.



Scheme 1.

Firstly, in this work polybenzoxazines with different phosphorus content were prepared from copolymerization of this phosphorus-containing based benzoxazine and the conventional Bisphenol A based benzoxazine. Table 1 summarizes the sample compositions, crosslinking data and  $T_g$ s of the final

materials. Bz-BAMPO and Bz-BA homopolimerizations were carried out to compare the crosslinking data and they were collected in the same table. The reaction enthalpy values decrease as the Bz-BAMPO amount increases. The  $T_g$  values for all systems could not be observed in a second dynamic run.

Fig. 1 shows the DSC plots of these systems. As can be seen from the crosslinking exotherms, the ring opening reaction starts, in all cases, about 210 °C. Bz-BA shows a typical polymerisation exotherm for difunctional benzoxazines centered at 245 °C. In contrast, Bz-BAMPO exhibit different curing behaviour, that can be seen also for sample 2. A shifting of the main polymerisation exotherm to lower temperatures and dual exotherm can be seen as the Bz-BAMPO amount increases.

**Table 1.** Curing conditions of bezoxazine systems.

| Sample | Resin           | Molar ratios resin | P % | $T_{\text{onset}}$ (°C) <sup>a</sup> | $T_{\text{max}}$ (°C) <sup>b</sup> | $\Delta H_0$ (KJ/mol) <sup>c</sup> | $T_g$ (°C)         |                                 |
|--------|-----------------|--------------------|-----|--------------------------------------|------------------------------------|------------------------------------|--------------------|---------------------------------|
|        |                 |                    |     |                                      |                                    |                                    | $E''_{\text{max}}$ | $\text{Tan}\delta_{\text{max}}$ |
| 1      | Bz-BAMPO        | -                  | 6.4 | 215                                  | 240                                | 125                                | 183                | 210                             |
| 2      | Bz-BAMPO /Bz-BA | 3:1                | 4.8 | 211                                  | 240                                | 128                                | 180                | 197                             |
| 3      | Bz-BAMPO /Bz-BA | 2:1                | 4.3 | 212                                  | 241                                | 131                                | 175                | 196                             |
| 4      | Bz-BAMPO /Bz-BA | 1:1                | 3.3 | 212                                  | 241                                | 142                                | 176                | 196                             |
| 5      | Bz-BAMPO /Bz-BA | 1:2                | 2.2 | 210                                  | 242                                | 142                                | 169                | 185                             |
| 6      | Bz-BA           | -                  | -   | 210                                  | 245                                | 146                                | 154                | 172                             |

<sup>a</sup> Initial temperature of the crosslinking exotherm.

<sup>b</sup> Temperature of the maximum heat release rate.

<sup>c</sup> Reaction enthalpy values extrapolated to zero heating rate.



Different polymerisation kinetics must be taking place in these two compounds. In a previous study of the Bz-BAMPO homopolymerization<sup>10</sup> we showed that the high temperature shoulder corresponds to the side reactions which generate the bisphenolic methylene linkages and possibly reaction to the *para*-position of the arylamine ring. Bz-BAMPO has *ortho*- and *para*-free phenolic positions, in addition to the *ortho* and *para* arylamine sites. Thus, a Mannich bridge network structure can develop. A network in which some oxazine rings cleave during cure could produce a phenolic network or alternately a network with arylamine methylene bridges.

The dynamic chemical and thermogravimetric properties of the polybenzoxazines were investigated. According to DSC data, the networks were prepared by heating samples at 180 °C for 2.5h, 200 °C for 1h and 220 °C for 2.5h. under 0.1 mPa.

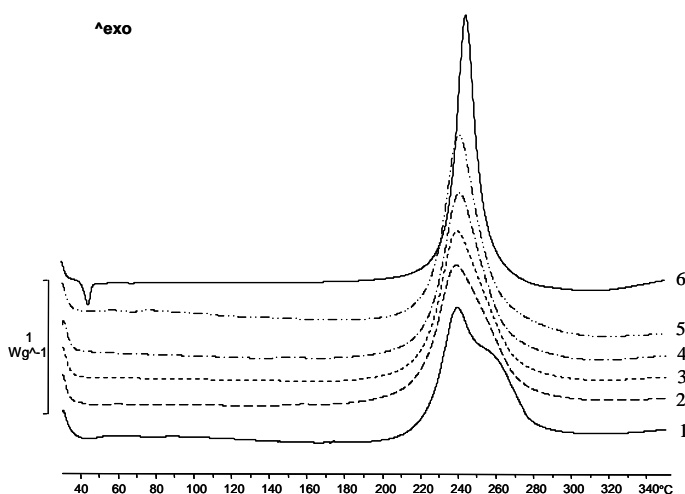


**Figure 1.** DSC plots of benzoxazine systems: 1 (Bz-BAMPO), 2 (Bz-BAMPO/Bz-BA 3:1), 3 (Bz-BAMPO/Bz-BA 2:1), 4 (Bz-BAMPO/Bz-BA 1:1), 5 (Bz-BAMPO/Bz-BA 1:2) and 6 (Bz-BA).

The dynamic mechanical behavior of the cured benzoxazine resins was obtained as a function of the temperature beginning in the glassy state of each composition to the rubbery plateau of each material (Fig. 2). The crosslinking density of a polymer can be estimated from the plateau of the elastic modulus in the rubbery state.<sup>20</sup> However, this theory is strictly valid only for lightly crosslinked materials, and was therefore used only to make qualitative comparisons of the level of crosslinking among the various polymers. As can be seen, crosslinking density results somewhat higher for Bz-BA derivative and somewhat lower for Bz-BAMPO derivative. For the mixture of benzoxazine systems intermediate values are observed. It seems that the diphenyl phosphine oxide moieties lead to looser networks.

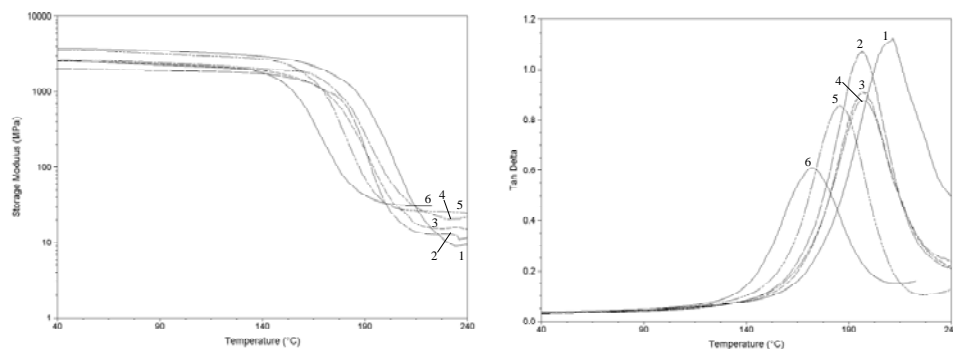


**Figure 2.** Storage modulus and loss factor of benzoxazine systems: 1 (Bz-BAMPO), 2 (Bz-BAMPO/Bz-BA 3:1), 3 (Bz-BAMPO/Bz-BA 2:1), 4 (Bz-BAMPO/Bz-BA 1:1), 5 (Bz-BAMPO/Bz-BA 1:2) and 6 (Bz-BA).

Fig. 2 shows the plots of loss factor ( $\tan \delta$ ) versus temperature. The  $T_g$ s of the crosslinked materials can be detected as the maximum of the loss modulus ( $E''$ ) or as the  $\alpha$  relaxation peak of the loss factor. Table 1 shows the  $T_g$  values of both measurements. From a practical point of view, the maximum  $E''$  is the most appropriate value since it corresponds to the

highest temperature of use. As can be seen,  $T_g$  values from DMTA follow the expected trend:  $T_g$ s increase as the content of Bz-BAMPO increases. This can be related to the chemical structure of Bz-BAMPO with a strong polar P=O group that causes restriction in the segmental mobility. Moreover, the analysis of the height and width of the  $\alpha$  relaxation peak shows trends in the crosslinking densities and network homogeneities as the composition of the material changes. The height of the Tan  $\delta$  peak, which is associated with the crosslinking density, increases as the Bz-BAMPO content increases. Because Tan  $\delta$  is the ratio of viscous components to elastic components, it can be assumed that the decreasing height is associated with lower segmental mobility and fewer relaxing species and is therefore indicative that the networks for the Bz-BA-rich samples are tighter. The peak width at half-height broadens as the number of branching modes increases, which produces a wider distribution of structures. The range of temperatures at which the different network segments gain mobility therefore increases. There were no significant differences among the samples, thus showing similar branching distribution for all of them.

To examine the effect of phosphorus content on thermal stability and the decomposition behavior, TGA data under nitrogen and air atmospheres were determined and analysed. Fig. 3 shows the weight loss with the temperature for the different compositions as well as the derivative curves. Table 2 summarizes the thermogravimetric data.

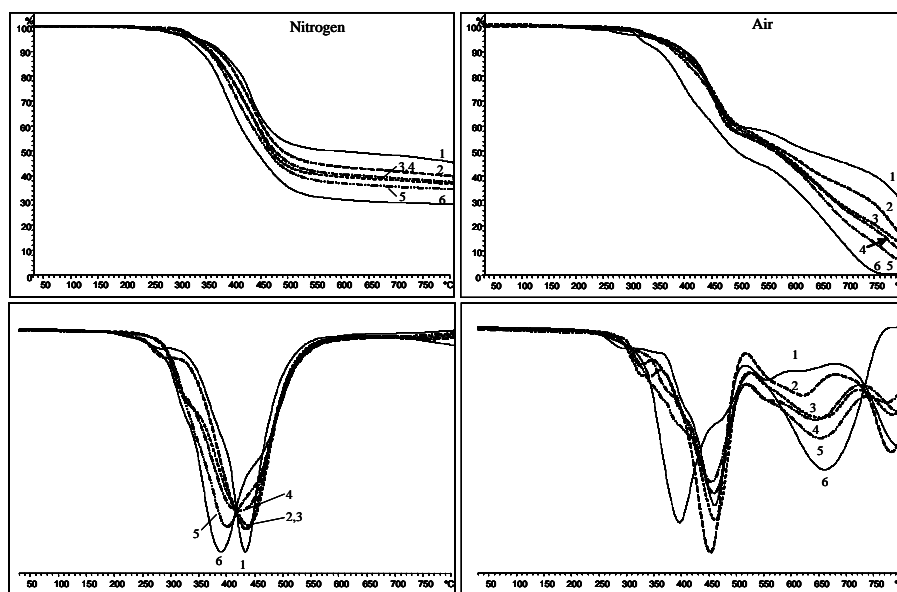


**Figure 3.** TGA plots in nitrogen and air of benzoxazine systems: 1 (Bz-BAMPO), 2 (Bz-BAMPO/Bz-BA 3:1), 3 (Bz-BAMPO/Bz-BA 2:1), 4 (Bz-BAMPO/Bz-BA 1:1), 5 (Bz-BAMPO/Bz-BA 1:2) and 6 (Bz-BA).

To examine the effect of phosphorus content on thermal stability and the decomposition behavior, TGA data under nitrogen and air atmospheres were determined and analysed. Fig. 3 shows the weight loss with the temperature for the different compositions as well as the derivative curves. Table 2 summarizes the thermogravimetric data. In nitrogen, a maximum weight loss rate appears in all cases. This behaviour indicates that there is a single decomposition mechanism which is similar for these resins. The decomposition temperature of the phosphorus-free resin is slightly lower than the phosphorus-containing resins. In air, a second stage of weight loss for the phosphorus free resin and a third stage for the resins with lower phosphorus content are observed at temperatures above 500 °C. Resin 1,

with the highest phosphorus content, shows only a second degradation stage 800 °C.

Table 2. Thermogravimetric and flame retardant properties of benzoxazine systems

| Resins | P%  | Nitrogen                          |                                    |                       | Air                               |                                    |                       | LOI,<br>% O <sub>2</sub> (V/V) |      |
|--------|-----|-----------------------------------|------------------------------------|-----------------------|-----------------------------------|------------------------------------|-----------------------|--------------------------------|------|
|        |     | T <sub>5%</sub> (°C) <sup>a</sup> | T <sub>max</sub> (°C) <sup>b</sup> | Char (%) <sup>c</sup> | T <sub>5%</sub> (°C) <sup>a</sup> | T <sub>max</sub> (°C) <sup>b</sup> | Char (%) <sup>c</sup> |                                |      |
| 1      | 6.4 | 333                               | 431                                | 46                    | 344                               | 455                                | >800                  | 32                             | 38.0 |
| 2      | 4.8 | 328                               | 430                                | 40                    | 342                               | 460                                | >800                  | 15                             | 37.0 |
| 3      | 4.3 | 330                               | 417                                | 37                    | 337                               | 460                                | 780                   | 13                             | 36.1 |
| 4      | 3.3 | 330                               | 433                                | 34                    | 335                               | 452                                | 770                   | 10                             | 35.8 |
| 5      | 2.2 | 331                               | 397                                | 32                    | 335                               | 454                                | 770                   | 7                              | 34.9 |
| 6      | -   | 313                               | 389                                | 32                    | 322                               | 397                                | -                     | 0                              | 31.8 |

<sup>a</sup> Temperature of 5% weight loss.

<sup>b</sup> Temperature of the maximum weight loss rate.

<sup>c</sup> Char yield at 800 °C.

Under an air atmosphere, a polymeric material at these temperatures loss weight because the char formed oxidized. It can be seen that the weight loss rate of phosphorus-containing resins is significantly lower than that of the phosphorus-free resin for the thermo-oxidative degradation. This

behavior is in accordance with the mechanism of improved fire performance via phosphorus modification. In this retarded-degradation phenomenon, the phosphorus groups form an insulating protective layer, which prevents the combustible gases from transferring to the surface of the materials, increases the thermal stability at higher temperatures and improves the fire resistance. Char yield under nitrogen is correlated to the polymer's flame retardancy.<sup>21</sup> In our case, the experimental char yields of the phosphorus-containing resins slightly increase with the phosphorus content. Under air, the char yield is low and increases significantly with the phosphorus content.

The LOI values, which can be taken as an indicator to evaluate the polymer's flame retardancy of the phosphorus-containing resins were also measured and shown in Table 2. As can be seen the presence of phosphorus increases the LOI values even when the phosphorus content is low, and slight differences can be observed when the phosphorus content increases.

In a second approach phosphorus-containing benzoxazine-epoxy resins have been prepared by curing Bz-BAMPO with different molar ratios of DGEBA as shown in Table 3. The reactions were monitored by DSC (Fig. 4) and showed dual exotherms in all cases except for the sample with the lowest Bz-BAMPO content (sample 10). As can be seen, adding epoxy monomer increases the temperature of the maximum heat release rate in the crosslinking exotherm. The retardation of the curing reaction increases with increasing amount of the epoxy resins and the exotherms shift to higher temperatures, according to the ring opening of benzoxazine and further reaction between the formed phenolic groups and epoxy resins. By DSC the  $T_g$  values of crosslinked materials are not detected.

**Table 3.** Curing condition of benzoxazine/epoxy systems.

| sample | Resin          | Molar ratios resin | P % | $T_{\text{onset}}$ (°C) <sup>a</sup> | $T_{\text{max}}$ (°C) <sup>b</sup> | $\Delta H_0$ (KJ/mol) <sup>c</sup> | $T_g$ (°C)         |                                 |
|--------|----------------|--------------------|-----|--------------------------------------|------------------------------------|------------------------------------|--------------------|---------------------------------|
|        |                |                    |     |                                      |                                    |                                    | $E''_{\text{max}}$ | $\text{Tan}\delta_{\text{max}}$ |
| 1      | Bz-BAMPO       | -                  | 6.4 | 215                                  | 240                                | 125                                | 183                | 210                             |
| 7      | Bz-BAMPO/DGEBA | 3:1                | 5.1 | 232                                  | 241                                | 136                                | 136                | 156                             |
| 8      | Bz-BAMPO/DGEBA | 2:1                | 4.6 | 233                                  | 246                                | 136                                | 136                | 155                             |
| 9      | Bz-BAMPO/DGEBA | 1:1                | 3.7 | 237                                  | 261                                | 135                                | 151                | 172                             |
| 10     | Bz-BAMPO/DGEBA | 1:2                | 2.6 | 241                                  | 274                                | 132                                | 169                | 178                             |

<sup>a</sup> Initial temperature of the crosslinking exotherm.

<sup>b</sup> Temperature of the maximum heat release rate.

<sup>c</sup> Reaction enthalpy values extrapolated to zero heating rate.

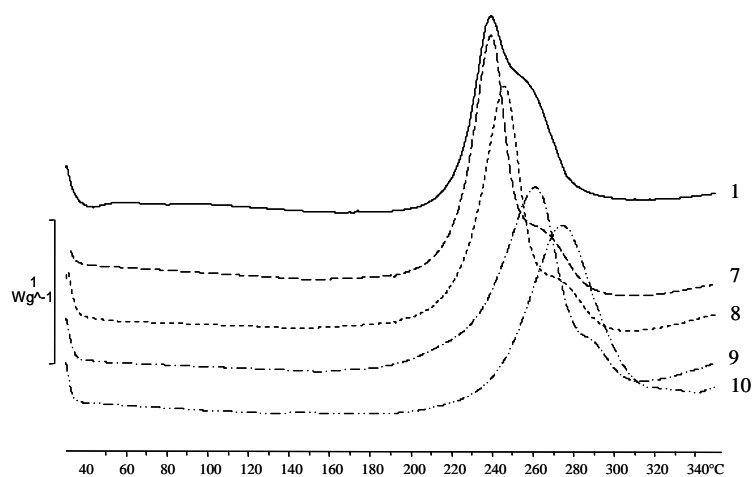


**Figure 4.** DSC plots of benzoxazine/epoxy systems: 1 (Bz-BAMPO), 7 (Bz-BAMPO/DGEBA 3:1), 8 (Bz-BAMPO/DGEBA 2:1), 9 (Bz-BAMPO/DGEBA 1:1) and 10 (Bz-BAMPO/DGEBA 1:2).

The dynamic mechanical behaviour of the benzoxazine-epoxy resin systems were obtained as function of temperature. As can be seen, in Fig. 5, the value of storage modulus in the rubber plateau increases with the epoxy content of the copolymers. Thus, the crosslink density of the copolymers appears to be increasing as epoxy is added to the benzoxazine matrix. DMTA allows to determine the  $T_g$  of the crosslinked materials. Table 3 shows the  $T_g$  values of both  $E''$  y  $\text{Tan } \delta$  and they follow the expected trend according to the crosslinking density:  $T_g$ 's increase as the epoxy content does. Moreover the height of the  $\text{Tan } \delta$  peak decreases as the epoxy content increases according to a lower segmental mobility and fewer relaxing species, indicating a higher degree of crosslinking. It should be pointed out that the Bz-BAMPO-epoxy systems exhibit a  $T_g$  lower than that pure polybenzoxazines what is associated not only with the inter and intramolecular hydrogen bonding but also with the chemical structure of Bz-BAMPO with a strong polar P=O group that also causes restriction in the segmental mobility.

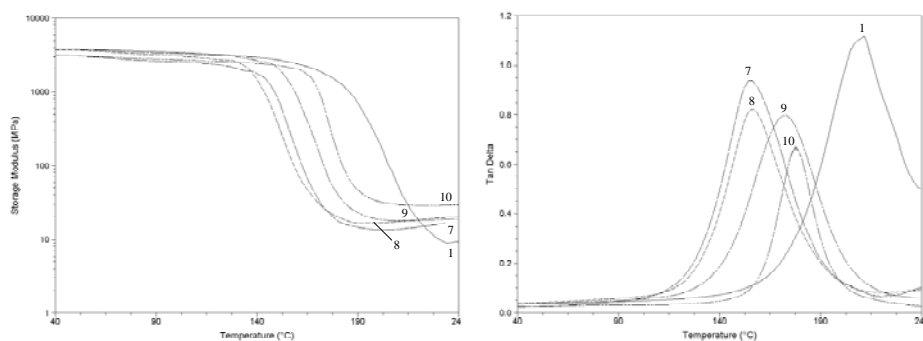


**Figure 5.** Storage modulus and loss factor of benzoxazine/epoxy systems: 1 (Bz-BAMPO), 7 (Bz-BAMPO/DGEBA 3:1), 8 (Bz-BAMPO/DGEBA 2:1), 9 (Bz-BAMPO/DGEBA 1:1) and 10 (Bz-BAMPO/DGEBA 1:2).



TGA data under nitrogen and air atmospheres of these materials were determined and analysed. Fig. 6 shows the weight loss with the temperature for the different compositions as well as the derivative curves. Table 4 summarizes the thermogravimetric data. Both in nitrogen and air the decomposition temperature increase with the epoxy content. In nitrogen, a maximum weight loss rate appears in all cases. This behaviour indicates that there is a single decomposition mechanism which is similar for these resins. In air, a second stage of weight loss for the lower phosphorus content benzoxazine-epoxy resins and a third stage for the rest of benzoxazine-epoxy resins are observed at temperatures above 600 °C. Char yields under air and nitrogen increases with the phosphorus content.

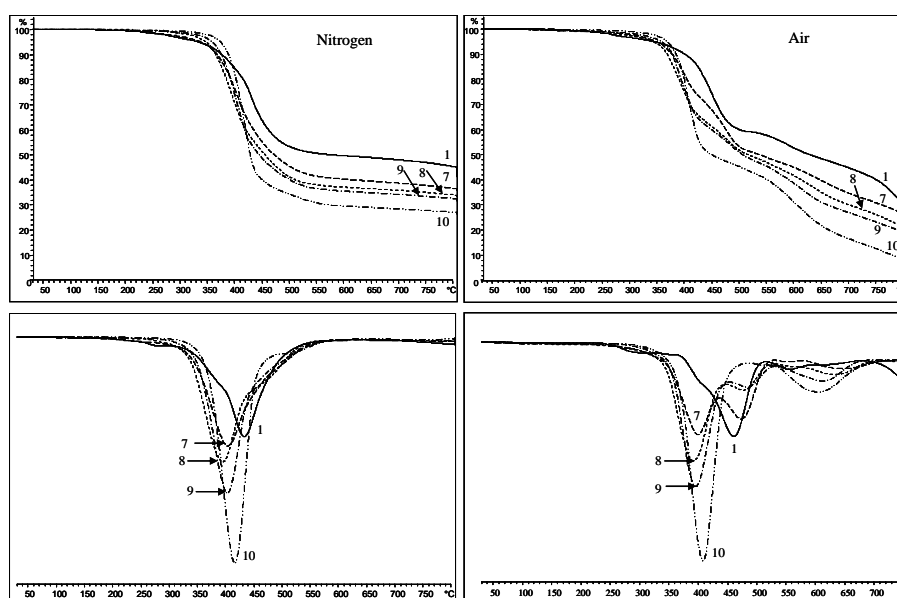


**Figure 6.** TGA plots in nitrogen and air of benzoxazine/epoxy systems: 1 (Bz-BAMPO), 7 (Bz-BAMPO/DGEBA 3:1), 8 (Bz-BAMPO/DGEBA 2:1), 9 (Bz-BAMPO/DGEBA 1:1) and 10 (Bz-BAMPO/DGEBA 1:2).

**Table 4.** Thermogravimetric and flame retardant properties of benzoxazine/epoxy systems

| Resins | P%  | Nitrogen                          |                                    |                       | Air                               |                                    |                       | LOI,<br>% O <sub>2</sub><br>(V/V) |    |      |
|--------|-----|-----------------------------------|------------------------------------|-----------------------|-----------------------------------|------------------------------------|-----------------------|-----------------------------------|----|------|
|        |     | T <sub>5%</sub> (°C) <sup>a</sup> | T <sub>max</sub> (°C) <sup>b</sup> | Char (%) <sup>c</sup> | T <sub>5%</sub> (°C) <sup>a</sup> | T <sub>max</sub> (°C) <sup>b</sup> | Char (%) <sup>c</sup> |                                   |    |      |
| 1      | 6.4 | 333                               | 431                                | 46                    | 344                               | 455                                | -                     | >800                              | 32 | 38.0 |
| 7      | 5.1 | 338                               | 401                                | 35                    | 348                               | 398                                | 476                   | 650                               | 27 | 43.0 |
| 8      | 4.6 | 347                               | 404                                | 33                    | 348                               | 397                                | 481                   | 630                               | 22 | 42.1 |
| 9      | 3.7 | 359                               | 404                                | 32                    | 358                               | 398                                | 483                   | 610                               | 20 | 42.0 |
| 10     | 2.6 | 374                               | 416                                | 27                    | 369                               | 407                                | -                     | 605                               | 9  | 41.1 |

<sup>a</sup> Temperature of 5% weight loss.

<sup>b</sup> Temperature of the maximum weight loss rate.

<sup>c</sup> Char yield at 800 °C.

The LOI values are shown in Table 4. As can be seen the introduction of epoxy in these systems increases the LOI values as high as 43.0 and no significant differences are observed with the phosphorus content, according to the reported results that indicate that about 2% phosphorus content is enough to confer flame retardance. It has to be pointed out the outstanding LOI values obtained, that are higher in the case of phosphorylated benzoxazine-epoxy systems than in phosphorylated polybenzoxazines.

## CONCLUSIONS

Phosphorus-containing polybenzoxazines can be prepared from mixtures of bis(*m*-aminophenyl)methylphosphine oxide based benzoxazine and glycidylether or benzoxazine of Bisphenol A. Higher curing temperatures for the benzoxazine-epoxy system are needed. All the obtained materials show high  $T_g$  values and higher crosslinking densities are observed for benzoxazine-epoxy systems. No significant differences are observed in the thermal degradation behaviour of the two series of samples. However LOI values are significantly higher for the benzoxazine-epoxy systems.

## Acknowledgements

The authors express their thanks to CICYT (Comisión Interministerial de Ciencia y Tecnología) (MAT2005-01593) for financial support for this work.

## REFERENCES

- <sup>1</sup> Ghosh NN, Kiskan B, Yagci Y. Polybenzoxazines-New high performance thermosetting resins: Synthesis and properties. *Prog Polym Sci* 2007;32:1344-1391.

- <sup>2</sup> Ning X, Ishida H. Phenolic Materials via Ring-Opening Polymerization of Benzoxazines: Effect of Molecular Structure on Mechanical and Dynamic Mechanical Properties. *J Polym Sci Part A Polym Chem Ed* 1994;32:1121-29
- <sup>3</sup> Lu S-Y, Hamerton I. Recent developments in the chemistry of halogen-free flame retardant polymers. *Prog Polym Sci* 2002;27:1661-712.
- <sup>4</sup> Shen SB, Ishida H. Synthesis and characterization of polyfunctional naphthoxazines and related polymers. *J Appl Polym Sci* 1996; 61:1595-605
- <sup>5</sup> Takeichi T, Kano T, Agag T. Synthesis and thermal cure of high molecular weight polybenzoxazine precursors and the properties of the thermosets. *Polymer* 2005, 46, 12172-80.
- <sup>6</sup> Men W, Lu Z. Synthesis and Characterization of 4,4-Diaminodiphenyl Methane-Based Benzoxazines and Their Polymers. *J Appl Polym Sci* 2007;106:2769-74.
- <sup>7</sup> Men W, Lu Z. Synthesis of a Novel Benzoxazine Precursor Containing Phenol Hydroxyl Group and Its Polymer. *J Appl Polym Sci* 2008;109:2218-23.
- <sup>8</sup> Subrayan RP, Jones FN. Condensation of Substituted Phenols with Hexakis (methoxymethyl)melamine: Synthesis, Characterization, and Properties of Substituted 2,4,6-Tris(3,4-dihydro-1,3-(2H)-benzoxazin-3yl)-s-triazine Derivatives. *Chem Mater* 1998;10:3506-12.
- <sup>9</sup> Lin CH, Chang SL, Hsieh CW, Lee HH. Aromatic Diamine-based benzoxazines and their high performance thermoset. *Polymer* 2008;49:1220-29.
- <sup>10</sup> Sponton M, Larrechi MS, Ronda JC, Galià M, Cádiz V. Synthesis of Bis(m-aminophenyl)methylphosphine Oxide Based Benzoxazine and study of thermal cross linking. *J Polym Sci Part A Polym Chem*, in press.
- <sup>11</sup> Agag T, Takeichi T. Synthesis, characterization and clay-reinforcement of epoxy cured benzoxazine. *High Performance Polym* 2002;14:115-32
- <sup>12</sup> Ishida H, Allen DJ. Mechanical characterization of copolymers based on benzoxazine and epoxy. *Polymer* 1996;37:4487-95.
- <sup>13</sup> Kimura H, Matsumoto A, Hasegawa K, Ohtsuka K, Fukuda A. Epoxy Resin Cured by Bisphenol A Based Benzoxazine. *J Appl Polym Sci* 1998;68:1903-10.
- <sup>14</sup> Jain R, Narula AK, Choudhary V. Studies on Curing and Thermal Behavior of Diglycidyl Ether of Bisphenol-A and Benzoxazine Mixtures. *J Appl Polym Sci* 2007;106:3327-34.
- <sup>15</sup> Kimura H, Matsumoto A, Ohtsuka K. Studies on New Type of Phenolic Resin – Curing Reaction of Bisphenol-A-Based Benzoxazine with Epoxy Resin Using Latent Curing Agent and the Properties of the Cured Resin. *J Appl Polym Sci* 2008;109:1248-56.
- <sup>16</sup> Ishida H, Rodríguez Y. Polymer Curing Kinetics of the new Benzoxazine-based phenolic resin by differential scanning calorimetry. *Polymer* 1995;36:3151-58.
- <sup>17</sup> Varma IK, Gupta U. Curing of Epoxy Resin with Phosphorylated Diamine. *J. Macromol Sci Chem* 1986;A23:19-36.
- <sup>18</sup> Ishida H, Low HI. A Study on the Volumetric Expansion of Benzoxazine-Based Phenolic Resin. *Macromolecules* 1997;30:1099-106.

<sup>19</sup> Andreu R, Reina JA, Ronda JC. Studies on the Thermal Polymerization of Substituted Benzoxazine Monomers: Electronic Effects. *J Polym Sci Part A Polym Chem* 2008;46:3353-66.

<sup>20</sup> Tobolsky AV, Carlson DW, Indictor NJ. Rubber elasticity and chain configuration. *J Polym Sci* 1961;54:175-92.

<sup>21</sup> Van Krevelen DW. Basic aspects of flame resistance of polymeric materials. *Polymer* 1975;16:615-20.

UNIVERSITAT ROVIRA I VIRGILI  
RESINAS EPOXI Y BENZOXAZINAS FOSFORADAS Y SILILADAS RETARDANTES A LA LLAMA  
Marisa Elisabet Spontón  
ISBN:978-84-691-9480-5/DL:T-22-2009

---

---

*3.7.3. DEVELOPMENT OF FLAME RETARDANT PHOSPHORUS- AND SILICON- CONTAINING POLYBENZOXAZINES*

---

---

UNIVERSITAT ROVIRA I VIRGILI  
RESINAS EPOXI Y BENZOXAZINAS FOSFORADAS Y SILILADAS RETARDANTES A LA LLAMA  
Marisa Elisabet Spontón  
ISBN:978-84-691-9480-5/DL:T-22-2009



## DEVELOPMENT OF FLAME RETARDANT PHOSPHORUS- AND SILICON- CONTAINING POLYBENZOXAZINES

M. Spontón, J.C. Ronda, M. Galià, V. Cádiz\*

Departament de Química Analítica i Química Orgànica. Universitat Rovira i Virgili. Campus Sescelades Marcel·lí Domingo s/n. 43007 Tarragona. Spain.  
virginia.cadiz@urv.cat

### ABSTRACT

The copolymerisation of benzoxazine of Bisphenol A and diglycidyl ether of (2,5-dihydroxyphenyl)diphenyl phosphine oxide or diglycidyloxy methyl phenyl silane has been studied. In all samples the molar ratio of the benzoxazine-epoxy system was varied to achieve different phosphorus or silicon content. Their thermal, dynamomechanical and flame retardant properties were evaluated. The high limiting oxygen index values confirmed that the phosphorus-containing benzoxazine-epoxy resins are effective flame retardants, but no efficiency of silicon on flame retardation was observed.

**Keywords:** benzoxazine; phosphorous-containing epoxy resin; silicon-containing epoxy resin; thermal stability; flame retardance.

## INTRODUCTION

Polybenzoxazines are a class of thermosetting phenolic resins that has been developed over the last decade as an attractive alternative to traditional phenolic resins.<sup>1</sup> These new materials overcome several shortcomings of conventional novolac and resol type phenolic resins while retaining their benefits. Benzoxazine resins are easily synthesized, either in solution or by a melt state reaction using a combination of a phenolic derivative, formaldehyde, and a primary amine. The unique chemistry of benzoxazines is responsible for several processing benefits as low melt viscosity, no volatile release upon cure and low overall shrinkage. Thermally activated ring opening polymerization results in a high modulus thermosetting material with excellent thermal, mechanical, and electrical properties. The molecular structure of benzoxazines offers superb design flexibility that allows properties of the cured materials to be controlled for specific requirements.<sup>2</sup>

In general, the approaches for improving the performance of polybenzoxazines can be classified into two ways. One is the structure modification by designing new benzoxazine monomers or copolymerizing with epoxy resins;<sup>3</sup> the other is the formation of composites or blends with other high temperature polymers like polyimide<sup>4</sup> as well as with inorganic fillers such as clay.<sup>5</sup>

However, the crosslinking densities of benzoxazine resins are believed to be considerably lower than those of ordinary thermosetting resins<sup>6</sup> Incorporation of another polymerizable groups such as ethynyl, phenylethynyl, allyl, propargyl, maleimide and epoxy have been reported to increase the crosslinking density and glass transition temperatures.<sup>7-11</sup>

The tightening of the network structure has been investigated copolymerising benzoxazine resin with epoxy resin.<sup>12,13</sup> The crosslinking density and glass transition temperature of these copolymers were higher than those of the polybenzoxazine homopolymer, and their heat resistance and mechanical properties were also better. In addition, the presence of the epoxy resins significantly improves the processability of benzoxazine resins but the resulting mixtures require higher curing temperatures than the pure benzoxazine resins.

To compensate for the flammability of the epoxy resins, brominated compounds are imparted into the formulation as a flame retardant. Halogenated compounds are harmful to the environment and human health and therefore there is a tendency to use halogen-free flame retardant in polymers.<sup>14,15</sup>

Besides the halogen based compounds, another way of retarding polymer combustion is to block the source of fuel by covering the outer layer of the material with a nonflammable coating, such as a phosphorous containing compound. Also, silicon-containing polymers are described that can degrade forming thermally stable silica, which have the tendency to migrate to the char surface serving as a protection layer to prevent further degradation of char at high temperatures.<sup>16</sup>

In our search for new phosphorus- and silicon-containing glycidyls with high thermal and chemical stability, we synthesized diglycidyl ether of (2,5-dihydroxyphenyl)diphenyl phosphine oxide (Gly-P)<sup>17</sup> and diglycidylloxymethylphenyl silane (Gly-Si).<sup>18</sup> This paper focuses on developing high performance flame retardant thermosetting resins through the copolymerization of the benzoxazine of Bisfenol A (Bz-BA) and the

above phosphorus- and silicon containing glycidyl derivatives (Scheme 1). The copolymerization reaction and the copolymer properties were examined and discussed.

## EXPERIMENTAL

### Materials

The following chemicals were obtained from the sources indicated: methylphenyl silane, triphenylphosphine, Wilkinson catalyst and diglycidylether of bisphenol A (DGEBA) from Aldrich, epichlorhydrin (EPC), benzoquinone and benzyltrimethylammonium chloride (BTMA) from Fluka, bisphenol A based benzoxazine (Bz-BA) from Shikoku Chemicals and were used as received. Glycidol (Aldrich) was vacuum distilled over  $\text{CaH}_2$  prior to use. All solvents were purified by standard procedures. Diglycidyl ether of (2,5-dihydroxyphenyl)diphenyl phosphine oxide (Gly-P) was obtained from (2,5-dihydroxyphenyl)diphenyl phosphine oxide by reaction with epichlorohydrin and BTMA as catalyst as has been previously described.<sup>17</sup>

### Synthesis of diglycidyloxy methyl phenyl silane (Gly-Si)

Into a three-necked round bottom flask equipped with a magnetic stirrer, a dropping funnel and a reflux condenser, 30 mL of anhydrous toluene, 12.0 g (0.162 mol) of freshly distilled glycidol and  $6.7 \times 10^{-2}$  g ( $7.2 \times 10^{-2}$  mol, 0.05 mol% per Si-H) of Wilkinson catalyst were placed. The red solution was degassed with argon and heated at 60 °C for 30 min., after which 8.8 g (0.072 mol) of methylphenyl silane was added dropwise over 1h. Vigorous  $\text{H}_2$  evolution was observed immediately and the reaction mixture was kept under positive argon pressure during the entire course of the reaction in

order to flush the H<sub>2</sub> gas from the reaction mixture. The solution was stirred at 60 °C for 1h to ensure complete conversion and was allowed to reach ambient temperature overnight. The reaction mixture was washed with water and phosphate buffer and the organic layer was dried over MgSO<sub>4</sub>, filtered and then the solvent was evaporated at reduced pressure. The product obtained was dissolved in hexane/ethylacetate (8:2) mixture and filtered through a short column of silicagel to remove traces of catalyst and other polar impurities. The obtained colorless solution was concentrated under vacuum to give a clear oil (74% yield) essentially pure by <sup>1</sup>H NMR.

<sup>1</sup>H NMR (CDCl<sub>3</sub>/TMS, δ (ppm)): 7.65 (2H, m); 7.42 (3H, m); 4.03 (2H, dd, 12.0, 3.2 Hz); 3.75 (2H, dd, 12.0, 5.2 Hz); 3.15 (2H, m); 2.78 (2H, dd, 4.4, 2.8 Hz); 2.65 (2H, dd, 4.4, 2.8 Hz); 0.42 (3H, s).

<sup>13</sup>C NMR (CDCl<sub>3</sub>/TMS, δ (ppm)): 134.0 (d); 132.2 (s); 130.4 (d); 127.9 (d); 63.6 (t); 52.0 (d); 44.5 (t); -4.4 (q).

### Curing reactions

Samples (Table 1) were prepared by the dissolution of benzoxazine and epoxy monomers in CH<sub>2</sub>Cl<sub>2</sub>. Then this solution was evaporated at room temperature in vacuum. About 10 mg of a known weight of the mixture was put into the aluminum pan, and the polymerization was monitored in a dynamic DSC experiment using a heating rate of 10 °C /min.

Molded cured benzoxazine-epoxy resins were prepared with a manual hydraulic press 15-ton sample pressing (SPECAC) equipped with a water cooled heated platens. The mixture was placed in a (70 x 6 x 3) mm mold and compression molded at 180 °C for 3h under 0.1 mPa. Postcuring was carried out at 220 °C for 3h under the same pressure conditions.

### Instrumentation

$^1\text{H}$  400 MHz,  $^{13}\text{C}$  100.5 MHz and NMR spectra were obtained using a Varian Gemini 400 spectrometer with Fourier transform,  $\text{CDCl}_3$  as solvent and TMS as internal standard.

Calorimetric studies were carried out on a Mettler DSC821e thermal analyzer using  $\text{N}_2$  as a purge gas (20 ml/min) at scan rates between 5 and 20  $^\circ\text{C}$  /min. Thermal stability studies were carried out on a Mettler TGA/SDTA851e/LF/1100 with  $\text{N}_2$  or air as a purge gas at scan rates of 10  $^\circ\text{C}$  /min.

Mechanical properties were measured using a dynamic mechanical thermal analysis (DMTA) apparatus (TA DMA 2928). Specimens (10 x 6 x 2) mm were tested in a single cantilever configuration. The thermal transitions were studied in the 30-250  $^\circ\text{C}$  range at a heating rate of 2 or 5  $^\circ\text{C}$  /min and at a fixed frequency of 1 Hz.

LOI values were measured on a Stanton Redcroft, provided with an Oxygen Analyzer, on polymer bars that measured (70 x 6 x 3) mm and which were prepared by molding. The char produced by the samples was characterized by  $^{31}\text{P}$  MAS NMR spectroscopy.

Degradation studies were carried out in a Carbolite TZF 12/38/400 oven connected to a condenser cooled by liquid nitrogen. GC-MS measurements were carried out using an HP 6890 gas chromatograph with an Ultra 2 capillary column (crosslinked 5 % PH ME siloxane) and an HP 5973 mass detector.

## RESULTS AND DISCUSSION

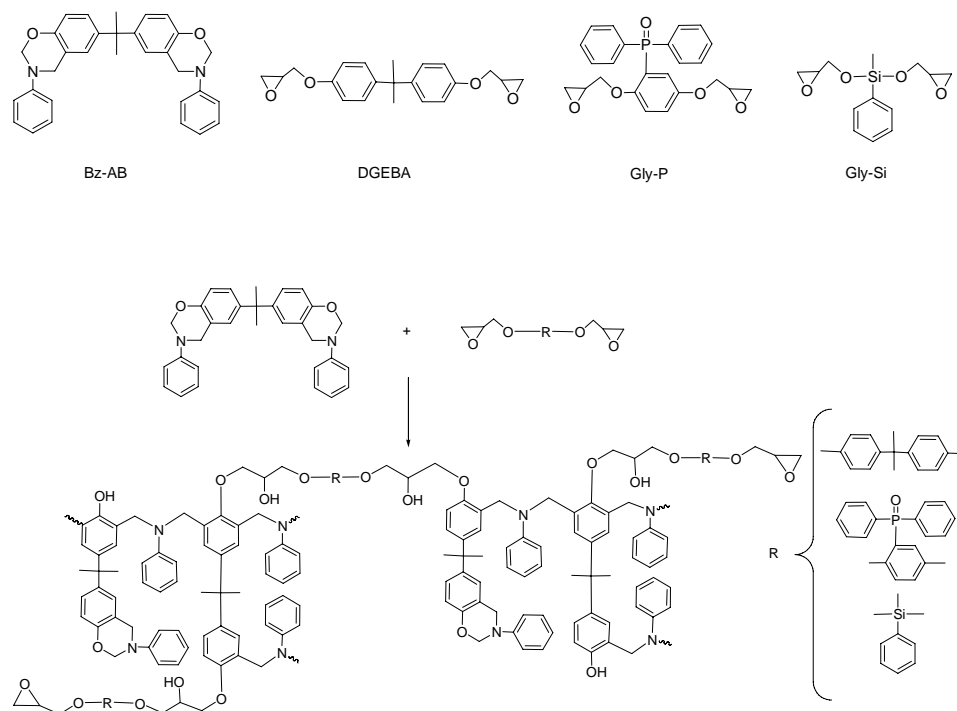
Several authors have reported the reaction between an epoxy resin and a benzoxazine resin. The oxirane ring opens when reacted with the hydroxyl group that results from the ring opening of benzoxazine, affording a network structure. Agag et al. reported that a single exotherm was present in DSC measurements for blends with equal functionality of oxirane to oxazine at temperatures of about 240 °C, because of the ring opening of benzoxazine and the partial cure of epoxy with hydroxyl functionalities.<sup>7</sup> When the blends contain a higher molar ratio of epoxy, a second exotherm appears at 300 °C on the DSC plot, which is attributed to the homopolymerization of the residual epoxy resin with secondary hydroxyl groups resulting from the ring opening of the epoxy.<sup>19</sup> The curing reaction of the mixture of benzoxazine and epoxy resins has also been studied by Ishida et al.<sup>20</sup> DSC plots show two exotherms, according to the existence of at least two reactions. The first exotherm in the temperature range of about 240-250 °C is attributed to the curing reaction among benzoxazine monomers. The second exotherm is attributed to the reaction between benzoxazine and epoxy resins, which occurs at temperatures of about 290-300 °C.<sup>21</sup> We have previously investigated the reaction of a phosphorus-containing glycidyl compound with the benzoxazine resin.<sup>22,23</sup> To elucidate the reaction mechanism, we used model compounds to show that benzoxazine homopolymerizes and the phenolic hydroxyl groups attack the oxirane rings. According to the above mentioned results from Agag, we observed a second exotherm in the DSC plots when the amount of the epoxy increased due to the homopolymerization of the remaining epoxy groups.

In this study we used the two diglycidyl compounds that we have used previously diglycidyl ether of (2,5-dihydroxyphenyl)diphenyl phosphine oxide (Gly-P)<sup>17</sup> and diglycidylloximethylphenylsilane (Gly-Si)<sup>18</sup> to prepare networks with bisphenol A based benzoxazine (Bz-BA). The incorporation of phosphorilated diglycidylether could have a twofold benefit. First, it contains no phosphorus-oxygen-carbon bonds that are susceptible to decomposition and higher char yields are expected with the addition of phosphorus. Second, a phosphine oxide group yields networks with increased glass transition temperatures and water absorptions as well as improved adhesive and thermal performances, because of the polar nature and strongly hydrogen bonding capability of this moiety. On the other hand, incorporation of silicon groups may also have a twofold benefit: increasing polybenzoxazine toughness<sup>24</sup> and flame retardancy. To compare we have also synthesized benzoxazine epoxy resins from Bz-BA and the heteroatom-free diglycidylether of bisphenol A (DGEBA).

Benzoxazine-epoxy resins have been prepared by curing Bz-BA with different molar ratios of glycidyl compounds as shown in Table 1. In this way, heteroatom-free resins and phosphorus- and silicon-containing resins with different heteroatom contents have been synthesized (Scheme 1).

The reactions were monitored by DSC and showed a single exotherm in all cases, regardless of the chemical structure of the diglycidyl compound or of its molar ratio in the initial mixture. Figure 1 depicts the DSC plots for all systems grouped in function of the glycidyl compounds used in the reaction with Bz-BA. As can be seen in the three cases adding epoxy monomer increases the temperature of the maximum heat release rate in the crosslinking exotherm.





Scheme 1

The retardation of the curing reaction increases with increasing amount of the epoxy resins and the exotherms shift to higher temperatures, according to the ring opening of benzoxazine and further reaction between the phenolic groups and epoxy resins. Among the different diglycidyl compounds this retardation is most significant for silicon-containing Gly-Si.

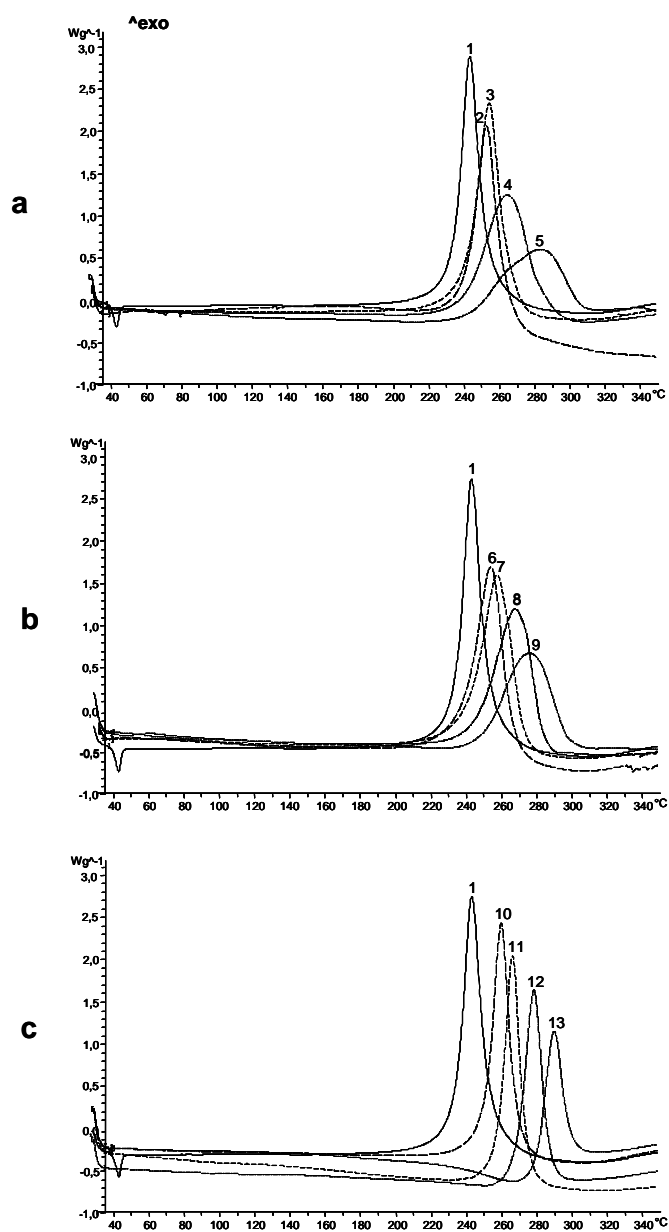


**Figure 1.** DSC curves of the epoxy-benzoxazine resins with different molar ratios for the systems: **a.** DGEBA/Bz-BA, **b.** Gly-P/ Bz-BA and **c** Gly-Si/Bz-BA.

The materials obtained after isothermal curing do not show any significant change of baseline in DSC plots, which could be associated to  $T_g$ . However dynamic-mechanical analysis makes it possible to determine the  $T_g$  of the crosslinked materials, detected as the maximum of the loss modulus ( $E''$ ) or as the  $\alpha$ -relaxation peak of the loss factor ( $\tan \delta$ ) (Fig. 2).

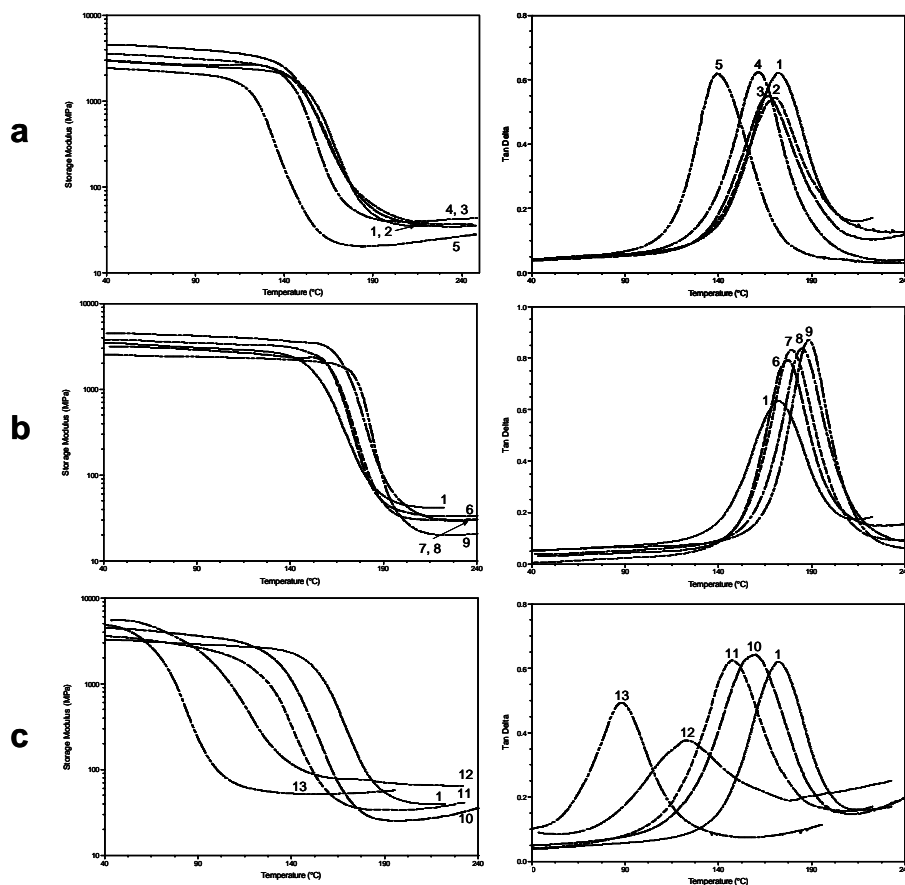


**Figure 2.** Storage modulus and  $\tan \delta$  as a function of the temperature of the epoxy-benzoxazine resins with different molar ratios for the systems: **a.** DGEBA/Bz-BA, **b.** Gly-P/Bz-BA, and **c.** Gly-Si/Bz-BA.

The  $T_g$  values from both measurements are shown in Table 1. From a practical point of view, the maximum  $E''$  is the most appropriate value. It corresponds to the initial drop from the glassy state into the transitions and to the highest use temperature.  $T_g$  values for DGEBA/Bz-BA and silicon-containing Gly-Si/Bz-BA decrease when the glycidyl content increases.

**Table 1.** Characteristics of the crosslinking and datas of  $T_g$  of the systems epoxy-benzoxazine obtained curing 180 °C for 3h and post-curing 220 °C for 3h.

| Resin | epoxy  | Molar ratios<br>Epoxy/DGEBA | P,% | Si,% | $T_{onset}^{\circ C^a}$ | $T_{Max}^{\circ C^b}$ | $T_g$ (°C)  |                   |
|-------|--------|-----------------------------|-----|------|-------------------------|-----------------------|-------------|-------------------|
|       |        |                             |     |      |                         |                       | $E''_{Max}$ | $Tan\delta_{max}$ |
| 1     | Bz-BA  | -                           | -   | -    | 235                     | 240                   | 154         | 172               |
| 2     | DGEBA  | 1:3                         | -   | -    | 241                     | 254                   | 152         | 171               |
| 3     | DGEBA  | 1:2                         | -   | -    | 242                     | 256                   | 149         | 170               |
| 4     | DGEBA  | 1:1                         | -   | -    | 242                     | 266                   | 143         | 161               |
| 5     | DGEBA  | 2:1                         | -   | -    | 242                     | 284                   | 124         | 139               |
| 6     | Gly-P  | 1:3                         | 1.7 | -    | 238                     | 256                   | 161         | 176               |
| 7     | Gly-P  | 1:2                         | 2.3 | -    | 242                     | 259                   | 161         | 179               |
| 8     | Gly-P  | 1:1                         | 3.5 | -    | 246                     | 269                   | 166         | 184               |
| 9     | Gly-P  | 2:1                         | 4.7 | -    | 250                     | 278                   | 174         | 189               |
| 10    | Gly-Si | 1:3                         | -   | 1.7  | 251                     | 261                   | 131         | 159               |
| 11    | Gly-Si | 1:2                         | -   | 2.3  | 259                     | 268                   | 124         | 147               |
| 12    | Gly-Si | 1:1                         | -   | 3.9  | 269                     | 280                   | 88          | 122               |
| 13    | Gly-Si | 2:1                         | -   | 5.6  | 281                     | 291                   | 64          | 88                |

<sup>a</sup> Initial temperature of the crooslinking exotherm.

<sup>b</sup> Temperature of the maximum heat release rate.

The opposite trend occurs for phosphorus-containing Gly-P/Bz-BA. These last materials have higher  $T_g$ s because of the presence of the strong polar group P=O. Moreover, the  $T_g$  values decrease as the Gly-Si content

increases and the  $T_g$  values for silicon-containing materials are lower than phosphorus-containing and heteroatom-free systems, due to the presence of the larger Si-O and Si-C units and the lower proportion of aromatic moieties.

The dynamic mechanical behaviour of the benzoxazine/epoxy systems were obtained as function of temperature. The crosslinking density of a polymer can be estimated from the plateau of the elastic modulus in the rubbery state with the statistical theory of the rubber elasticity. However, this theory is strictly valid only for lightly crosslinked materials, and was therefore used only to make qualitative comparisons of the level of crosslinking among the various polymers. As far as the chemical structures of these networks are concerned it can be predicted that the crosslink densities should decrease as the epoxy content increase. This is observed for DGEBA/Bz-BA and Gly-P/Bz-BA. However, the silicon-containing Gly-Si/Bz-BA do not follow this trend (Fig. 2).

To examine the effect of heteroatom content on thermal stability and the decomposition behavior, TGA data under nitrogen and air atmospheres are determined and analyzed. Figure 3 shows the derivative curves of the weight loss with the temperature in air for the epoxy compositions.

Table 2 summarizes thermogravimetric data. In nitrogen, when the DGEBA or Gly-P content increases the decomposition temperature increases while the addition of Gly-Si has the opposite effect. A similar trend can be observed under air although not so significant.

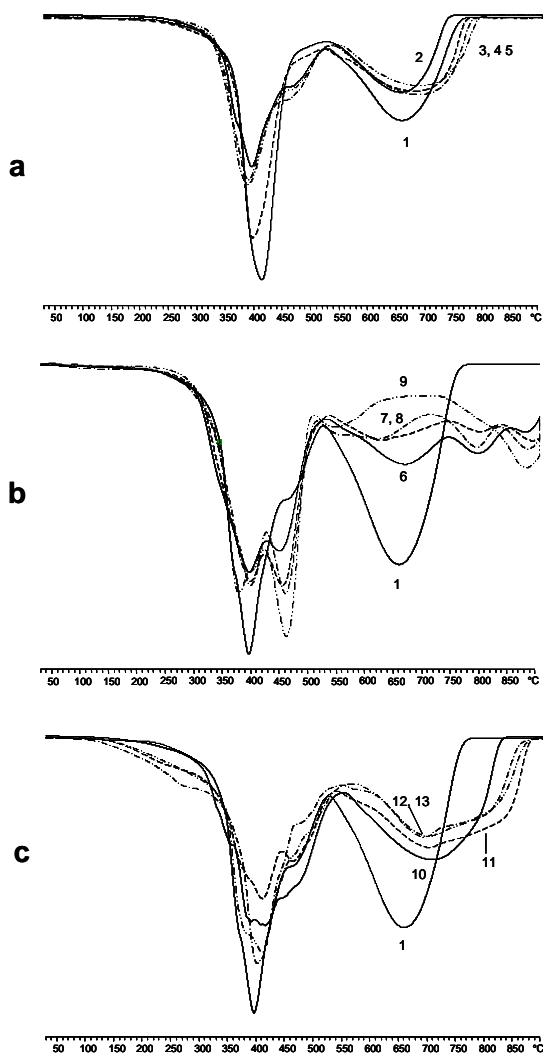


**Figure 3.** TGA derivative curves of the epoxy-benzoxazine resins with different molar ratios for the systems: **a.** DGEBA/Bz-BA, **b.** Gly-P/ Bz-BA, and **c.** Gly-Si/Bz-BA.

Table 2. Thermogravimetric data in N<sub>2</sub> and Air and LOIs of the polymers

| Resins | P, % | Si, % | Nitrogen                          |                                   |                       |                                   |                                   | Air                               |                                   |                                   |                                   |                                   | LOI,<br>% O <sub>2</sub> (V/V) |
|--------|------|-------|-----------------------------------|-----------------------------------|-----------------------|-----------------------------------|-----------------------------------|-----------------------------------|-----------------------------------|-----------------------------------|-----------------------------------|-----------------------------------|--------------------------------|
|        |      |       | T <sub>5%</sub> <sup>a</sup> , °C | T <sub>mt</sub> <sup>b</sup> , °C | Char <sup>c</sup> (%) | T <sub>5%</sub> <sup>a</sup> , °C | T <sub>mt</sub> <sup>b</sup> , °C | T <sub>5%</sub> <sup>a</sup> , °C | T <sub>mt</sub> <sup>b</sup> , °C | T <sub>5%</sub> <sup>a</sup> , °C | T <sub>mt</sub> <sup>b</sup> , °C | T <sub>5%</sub> <sup>a</sup> , °C |                                |
| 1      | -    | -     | 313                               | 391                               | 30                    | 322                               | 396                               | -                                 | 740                               | 0                                 | 31.8                              |                                   |                                |
| 2      | -    | -     | 330                               | 387                               | 31                    | 345                               | 390                               | -                                 | 698                               | 0                                 | 32.2                              |                                   |                                |
| 3      | -    | -     | 331                               | 387                               | 30                    | 346                               | 388                               | -                                 | 690                               | 0                                 | 32.2                              |                                   |                                |
| 4      | -    | -     | 341                               | 397                               | 26                    | 340                               | 397                               | -                                 | 388                               | 0                                 | 32.0                              |                                   |                                |
| 5      | -    | -     | 354                               | 411                               | 23                    | 341                               | 412                               | -                                 | 661                               | 0                                 | 31.6                              |                                   |                                |
| 6      | 1.7  | -     | 328                               | 400                               | 32                    | 335                               | 394                               | 451                               | 667                               | 14                                | 43.7                              |                                   |                                |
| 7      | 2.3  | -     | 329                               | 400                               | 32                    | 338                               | 398                               | 457                               | 629                               | 20                                | 46.0                              |                                   |                                |
| 8      | 3.5  | -     | 339                               | 404                               | 30                    | 338                               | 405                               | 459                               | 624                               | 20                                | 48.0                              |                                   |                                |
| 9      | 4.7  | -     | 346                               | 405                               | 26                    | 349                               | 400                               | 463                               | -                                 | 27                                | 45.5                              |                                   |                                |
| 10     | -    | 1.7   | 303                               | 400                               | 33                    | 330                               | 404                               | -                                 | 708                               | 5                                 | 32.1                              |                                   |                                |
| 11     | -    | 2.3   | 295                               | 397                               | 35                    | 292                               | 412                               | -                                 | 708                               | 15                                | 32.0                              |                                   |                                |
| 12     | -    | 3.9   | 261                               | 404                               | 36                    | 291                               | 410                               | -                                 | 708                               | 14                                | 32.4                              |                                   |                                |
| 13     | -    | 5.6   | 251                               | 405                               | 36                    | 267                               | 402                               | -                                 | 700                               | 16                                | 31.9                              |                                   |                                |

<sup>a</sup>Temperature of 5 % weight loss.

<sup>b</sup>Temperature of the maximum weight loss rate.

<sup>c</sup>Char yield at 800 °C.

In nitrogen all the samples have a single major break in their decomposition curve before their major weight losses level off. This behavior indicates that there is a single decomposition mechanism for these resins. In air, a second maximum weight loss appears for the heteroatom-free resins at temperatures above 500 °C. Under an air atmosphere, a polymeric material at these temperatures loss weight because the char formed oxidized. Phosphorus-containing resins show a two-step break in the decomposition curves at temperatures below 500 °C. It can be seen that the weight loss rate of phosphorus-containing resins is significantly lower than that of the phosphorus-free resins and decreases when the phosphorus content increases for the thermoxidative degradation.

This behaviour is in accordance with the mechanism of improved fire performance via phosphorus modification. In this retarded-degradation phenomenon, the phosphorus groups form an insulating protective layer, which prevents the combustible gases from transferring to the surface of the materials, increases the thermal stability at higher temperatures and improves the fire resistance. Silicon-containing resins show a decomposition behavior similar to heteroatom-free resins with only a step break before the thermoxidative degradation. Incorporating silicon results in a higher oxidation temperature. The Si-O unit can decompose at low temperatures and lead to the formation of the silicone-containing group which will participate in the crosslinked carbonization in the second stage of decomposition, and effectively retard the decomposition at higher temperatures.

Char yields under nitrogen is correlated to the polymer's flame retardance<sup>25</sup> but it should be pointed out that, in our case, the experimental char yields of the heteroatom-containing resins and the heteroatom-free



resins are not significantly different. Under air, the char yield is low and increases with the phosphorus or silicon content.

To further investigate the thermal degradation mechanism, samples were heated in an oven at 350 °C for 5h with air as purge gas. The degradation temperature was selected from dynamic TGA data and the time at which no weight loss was detected at 350 °C in an isothermal TGA experiment was selected as the degradation time. Volatile products were trapped at the liquid nitrogen temperature and subsequently analysed by GC/MS. At first, the thermal degradation of Bz-BA was carried out to compare to the phosphorus- and silicon-containing resins. The analysis of the evolved gases shows that various aromatic species are detected from this polybenzoxazine. As is known, from a covalent bond energy point of view, a C-N bond is weaker than a C-C bond. Due to the more stable C-C bond, degradation would occur being the major cleavage the Mannich base and giving different aromatic amines: aniline, N-methylaniline, o-toluidine, N,N-dimethylaniline and phenol and substituted phenols: 2-methylphenol, 4-methylphenol, 2,6-dimethylphenol.<sup>26,27</sup> On the other hand, the analysis of the evolved gases of the benzoxazine-epoxy resins shows moreover the dehydration of secondary alcohol groups which is the first step of degradation in epoxy resins, as has been previously described<sup>28,29</sup>. C-C double bonds formed in this step induce the  $\beta$ -scission of weakened C-O bonds. Thus, GC/MS analysis identified aromatic compounds as phenol, 4-isopropylphenol, bisphenol A for DGEBA-containing samples. Samples containing Gly-P and Gly-Si were studied in a similar way heating at 350 °C for 4h. The analysis of evolved gases resulted completely similar to the one previously described for the P-containing resins<sup>17</sup>. Solid residues were extracted with methanol and <sup>31</sup>P NMR spectroscopy allowed to identify phosphorus-containing compounds as triphenylphosphine oxide, (2,5-

dihydroxyphenyl) diphenylphosphine oxide and diphenylphosphinic acid. When they were heated at 600 °C the characterization of the solid residues by  $^{31}\text{P}$  MAS NMR spectroscopy show a broad peak at 0 ppm typical of phosphoric acid. However, the analysis of the evolved gases for Si-containing resins resulted similar to the above described but moreover 1,3,5-triphenyl-1,3,5-trimethylcyclotrisiloxane was detected.<sup>30</sup>

The LOI values, which can be taken as an indicator to evaluate the polymer's flame retardancy of the resins were also measured and shown in Table 2. As can be seen the presence of phosphorus increases the LOI values even when the phosphorus content is low, and no significant differences with the phosphorus content are observed. It has to be pointed out the outstanding LOI values obtained. However, the presence of silicon in the studied percentages has no effect in the flame retardant behaviour and the LOI values of silicon-containing resins are similar to those of heteroatom-free resins. This behaviour may be explained taking into account the loss of silicon as a volatile fraction thus decreasing the char silicon content.

## CONCLUSIONS

Phosphorus- or silicon-containing benzoxazine-epoxy resins with different phosphorus or silicon contents were obtained from Gly-P or Gly-Si and Bz-BA. A retardation of the crosslinking reaction with increasing amount of the epoxy resin has been observed, being the most significant for the silicon-containing epoxy.  $T_g$  values of thermosets increase with the epoxy content for the phosphorus-containing benzoxazine-epoxy while the opposite trend is observed for the silicon-containing benzoxazine-epoxy. Phosphorus-containing materials with outstanding LOI values were

obtained, even when the phosphorus content is low, with the corresponding excellent flame retardant properties. A flame retardant effect could not be observed for silicon-containing resins for the studied silicon percentages.

### Acknowledgements

The authors express their thanks to CICYT (Comisión Interministerial de Ciencia y Tecnología) (MAT2005-01593) for financial support for this work.

### REFERENCES

- <sup>1</sup> Reghunadham Nair CP. Advances in addition-cure phenolic resins. *Prog Polym Sci* 2004;29:401-498.
- <sup>2</sup> Ghosh NN, Kiskan B, Yagci Y. Polybenzoxazines-New high performance thermosetting resins: Synthesis and properties. *Prog Polym Sci* 2007;32:1344-1391, and references therein.
- <sup>3</sup> Jain R, Narula AK, Choudhary V. Studies on Curing and Thermal Behavior of Diglycidyl Ether of Bisphenol-A and Benzoxazine Mixtures. *J Appl Polym Sci* 2007;106:3327-34.
- <sup>4</sup> Takeichi T, Agag T. Preparation and properties of polybenzoxazine/poly(imide-siloxane) alloys: In situ ring-opening polymerization of benzoxazine in the presence of soluble poly(imide-siloxane)s. *J Polym Sci Part A: Polym Chem* 2001, 39, 2633-41
- <sup>5</sup> Agag T, Takeichi T. Polybenzoxazine-montmorillonite hybrid nanocomposites: synthesis and characterization. *Polymer*. 2000;41:7083-90.
- <sup>6</sup> Ishida H, Allen DJ. Mechanical characterization of copolymers based on benzoxazine and epoxy. *Polymer* 1996;37:4487-95.
- <sup>7</sup> Kim HJ, Brunovska Z, Ishida H. Synthesis and thermal characterization of polybenzoxazines based on acetylene-functional monomers. *Polymer*. 1999;40:6565-73.
- <sup>8</sup> Agag T, Takeichi T. Novel Benzoxazine Monomers Containing *p*-Phenyl Propargyl Ether: Polymerization of Monomers and Properties of Polybenzoxazines. *Macromolecules*. 2001;34:7257-63.
- <sup>9</sup> Agag T, Takeichi T. Synthesis and Characterization of Novel Benzoxazine Monomers Containing Allyl Groups and Their High Performance Thermosets. *Macromolecules*. 2003;36:6010-17.
- <sup>10</sup> Liu YL, Yu JM, Chou CI. Preparation and properties of novel benzoxazine and polybenzoxazine with maleimide groups. *J Polym Sci Part A: Polym Chem* 2004;42:5954-63
- <sup>11</sup> Andreu R, Espinosa MA, Galià M, Cádiz V, Ronda JC, Reina JA. Synthesis of Novel Benzoxazines Containing Glycidyl Groups: A Study of the Crosslinking Behavior. *J Polym Sci Part A: Polym Chem* 2006, 44, 1529-40.

- <sup>12</sup> Kimura H, Matsumoto A, Ohtsuka K. Studies on New Type of Phenolic Resin – Curing Reaction of Bisphenol-A-Based Benzoxazine with Epoxy Resin Using Latent Curing Agent and the Properties of the Cured Resin. *J Appl Polym Sci* 2008;109:1248-56.
- <sup>13</sup> Kimura H, Matsumoto A, Hasegawa K, Ohtsuka K, Fukuda A. Epoxy Resin Cured by Bisphenol A Based Benzoxazine. *J Appl Polym Sci* 1998;68:1903-10.
- <sup>14</sup> Green J. A Review of Phosphorus-Containing Flame Retardants. *J Fire Sci* 1992;10:470-87.
- <sup>15</sup> Lu S-Y, Hamerton I. Recent developments in the chemistry of halogen-free flame retardant polymers. *Prog Polym Sci* 2002;27:1661-712.
- <sup>16</sup> Kashiwagi T, Gilman JW. Fire retardancy of polymeric materials. Grand AF, Wilkie CA. Eds. New York, Marcel Dekker, 2000.
- <sup>17</sup> Spontón M, Ronda JC, Galià M, Cádiz V. Flame Retardant Epoxy Resins Based on Diglycidyl Ether of (2,5-Dihydroxyphenyl)diphenyl Phosphine Oxide. *J Polym Sci Part A Polym Chem*. 2007;45:2142-51.
- <sup>18</sup> Mercado LA, Reina JA, Galià M. Flame retardant epoxy resins based on diglycidylloxymethylphenylsilane. *J Polym Sci Part A Polym Chem* 2006;44: 5580-87.
- <sup>19</sup> Agag T, Takeichi T. Synthesis and characterization of epoxy film cured with reactive polyimide. *Polymer* 1999;40:6557-63.
- <sup>20</sup> Rimdusit, S.; Ishida, H. Development of new class of electronic packaging materials based on ternary systems of benzoxazine, epoxy, and phenolic resins *Polymer* 2000;41:7941-49.
- <sup>21</sup> Rimdusit S, Ishida H. Synergism and multiple mechanical relaxations observed in ternary systems of benzoxazine, epoxy and phenolic resin composites. *J Polym Sci Part B: Polym Phys* 2000;38:1687-98.
- <sup>22</sup> Espinosa MA, Galià M, Cádiz, V. Novel phosphorilated flame retardant thermosets: epoxy-benzoxazine-novolac systems. *Polymer* 2004;45:6103-09.
- <sup>23</sup> Espinosa MA, Cádiz V, Galià M. Development of novel flame-retardant thermosets based on benzoxazine-phenolic resins and a glycidyl phosphinate. *J Polym Sci Part A Polym Chem* 2004;42:279-89.
- <sup>24</sup> Liu Y-L, Hsu C-W, Chou C-I. Silicon-containing benzoxazines and their polymers: Copolymerization and copolymer properties. *J Polym Sci Part A Polym Chem* 2007;45:1007-15 .
- <sup>25</sup> Van Krevelen DW. Some basic aspect of flame resistance of polymeric materials. *Polymer*. 1975;16:615-20.
- <sup>26</sup> Hemvichian K, Kim HD, Ishida H. Identification of volatile products and determination of thermal degradation mechanisms of polybenzoxazine model oligomers by GC-MS. *Polym Deg Stab*. 2005;87:213-24.
- <sup>27</sup> Hemvichian K, Ishida H. Thermal descomposition processes in aromatic amine-based polybenzoxazines investigated by TGA-FTIR and GC-MS. *Polymer* 2002;43:4391-402.
- <sup>28</sup> Levchik SV, Camino G; Luda MP, Costa L, Muller G, Costes B. Epoxy resins cured with aminophenylmethylphophine oxide-II. Mechanism of thermal decomposition. *Polym Deg Stab*. 1998;60:169-83.

<sup>29</sup> Grassie N, Guy MJ. Degradation of Epoxy Polymers: 2-Mechanism of Thermal Degradation of Bisphenol-A Diglycidyl Ether. *Polym Deg Stab* 1985;13:1-20.

<sup>30</sup> Moronkov MC. The third route to the formation of the Si-O-Si group and siloxane structures. To siloxanes through to silanones. *J. Organometal. Chem.* 1998;557:143-55.

UNIVERSITAT ROVIRA I VIRGILI  
RESINAS EPOXI Y BENZOXAZINAS FOSFORADAS Y SILILADAS RETARDANTES A LA LLAMA  
Marisa Elisabet Spontón  
ISBN:978-84-691-9480-5/DL:T-22-2009

# CAPÍTULO 4

## **Estudio de retardancia a la llama de sistemas benzoxazina-epoxi fosforados y sililados mediante calorimetría de cono**

---

*El calorímetro de cono representa uno de los avances mas importantes a escala de laboratorio para estudiar el comportamiento de una serie de propiedades de materiales en un escenario de fuego bien definido. Así, en este capítulo se describe la aplicación de esta técnica a algunas de las resinas benzoxazina-epoxi fosforadas o sililadas descritas en el capítulo anterior.*

---

### 4.1 Introducción

### 4.2 Objetivos

### 4.3 Parte experimental y resultados

#### 4.3.1 Cone calorimetry studies of benzoxazine-epoxy systems flame retarded by chemically bonded phosphorus or silicon

UNIVERSITAT ROVIRA I VIRGILI  
RESINAS EPOXI Y BENZOXAZINAS FOSFORADAS Y SILILADAS RETARDANTES A LA LLAMA  
Marisa Elisabet Spontón  
ISBN:978-84-691-9480-5/DL:T-22-2009



## 4.1

### Introducción

Todos los incendios son diferentes y un único escenario de fuego o un único test de retardancia a la llama nunca abarcará todas las situaciones posibles y los correspondientes comportamientos frente al fuego. A consecuencia de la naturaleza compleja y la poca reproducibilidad de un incendio, en los últimos años se han desarrollado diferentes técnicas para estimar la inflamabilidad de los materiales poliméricos, concentrándose cada una de ellas en ciertas características del proceso de combustión. La valoración del retardo a la llama generalmente se realiza utilizando distintos procedimientos que han sido estandarizados previamente por organismos nacionales e internacionales.

El comportamiento de un incendio comprende tres etapas: la ignición, el desarrollo del fuego y la completa combustión. En cada uno de estos escenarios de fuego pueden evaluarse distintas propiedades aunque casi todos los tests tienen como objetivo el desarrollo de medidas de protección, como impedir la ignición continuada, limitar la contribución al desarrollo del fuego o crear una barrera protectora. La mayoría de tests bien establecidos tratan de crear un escenario realista del fuego y registrar un peligro específico para una determinada muestra en esas condiciones, más que de investigar las propiedades del material. Además, la forma en que una muestra responde al fuego, o a un determinado test puede contribuir de forma significativa al desarrollo del propio fuego. Así, comparar el comportamiento al fuego en distintos tests es difícil y las predicciones generalmente fallan porque las propiedades del material que determinan el comportamiento en los distintos tests son diferentes. Aún así se pueden establecer ciertas correlaciones limitadas a algunas clases de materiales

específicos. Por otra parte, el escalado se convierte en un tema clave en la ciencia del fuego y constituye un reto extender las conclusiones de los tests a pequeña escala a un incendio real.

El calorímetro de cono (ASTM E-1354/ISO/5660) es actualmente el método más avanzado para valorar la reacción de los materiales frente al fuego. Aunque se viene utilizando desde hace mucho tiempo como una de las herramientas más útiles en el análisis cuantitativo de la inflamabilidad de un material a nivel de ingeniería, sigue siendo uno de los tests más interesantes a escala de laboratorio ya que las condiciones de simulación del fuego son las que más se ajustan a un fuego real<sup>1</sup>.

El equipo consiste básicamente en una resistencia calefactora por radiación de forma cónica, un ambiente de ignición y un sistema colector de gases, como se muestra en la figura 4.1<sup>2</sup>. La superficie de la muestra se expone a una radiación de calor constante en el calefactor cónico y los volátiles desprendidos se encienden con una chispa eléctrica. Los gases que se generan en la combustión se recogen para su análisis posterior. Así se puede medir el tiempo de ignición, la velocidad de calor liberado, el calor total liberado, el área de extinción específica, la velocidad de pérdida de masa, la formación de CO, CO<sub>2</sub> y otros productos de combustión y la formación de humos.

---

<sup>1</sup> Schartel B, Hull TR. Fire Mater. 2007;31:327.

<sup>2</sup> Babrauskas V. Fire Mater. 1984;8:81.

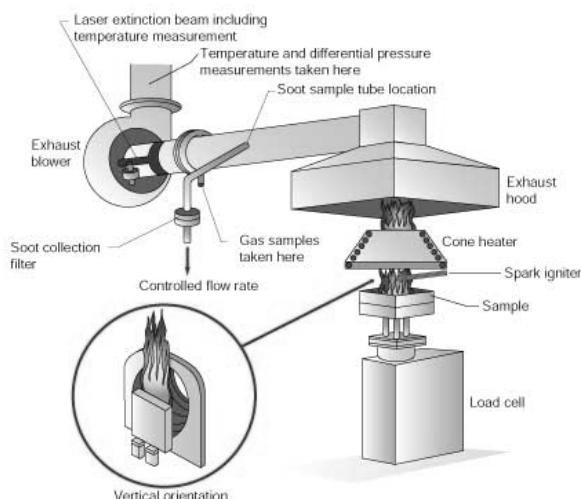


**Figura 4.1** Esquema del calorímetro de cono.

Estos parámetros medidos con el calorímetro de cono presentan distintas utilidades:

- Comparar la respuesta al fuego de los materiales para determinar su comportamiento o en vistas al desarrollo de nuevos materiales.
- Utilizar estos datos para simulaciones o predicciones del comportamiento al fuego a gran escala.
- Determinar parámetros característicos tales como el máximo de flujo de calor liberado o el total de calor liberado para comprobar si el material se ajusta a una determinada norma.

Durante el experimento del calorímetro de cono se determina la velocidad de desprendimiento de calor (HRR). Pueden distinguirse distintos comportamientos que dan lugar a curvas características de HRR

frente al tiempo (Figura 4.2)<sup>3</sup>. Las curvas del tipo a) corresponden a materiales que muestran un aumento inicial después de la ignición para llegar a un valor casi constante de HRR. Este “plateau” se mantiene prácticamente hasta el final del test cuando se alcanza el máximo de HRR. Para muestras del tipo b) este “plateau” disminuye y el pico de liberación de calor aumenta. Las muestras que forman residuo muestran un incremento inicial de HRR hasta que la formación de la capa protectora es efectiva (curva tipo c). Algunos de estos materiales muestran un segundo pico de HRR al final del experimento que puede ser debido a la rotura de la capa protectora (curva tipo d). Los materiales del tipo e) se caracterizan por un pico estrecho ya que toda la muestra se piroliza al mismo tiempo. Finalmente algunas muestras se caracterizan por un desarrollo discontinuo de la combustión (curva tipo f), debido a que se produce la ignición y autoextinción antes de que se establezca la llama o a que la muestra se deforma durante el quemado y cambia su área superficial y la distancia al punto de radiación calorífica.

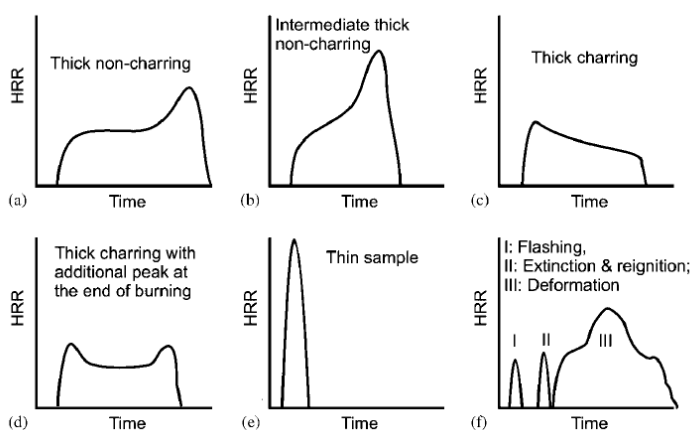


**Figura 4.2** Curvas de HRR para distintos comportamientos de quemado.

<sup>3</sup> Lyon RE. Ignition Resistance of Plastics in Recent Advances in Flame Retardance of Polymers. Vol 13, p 14. Ed: Lewin M. BCO 2002.

En general se observa una falta de correlación entre los resultados del índice limitante de oxígeno (LOI) o el test UL-94 y los resultados del calorímetro de cono. Si se considera como el calorímetro de cono mide la inflamabilidad y se compara con estos tests, esto no resulta sorprendente. El LOI es un test a pequeña escala que utiliza una atmósfera con un porcentaje variable de oxígeno para mantener la llama y el UL-94 aplica una pequeña llama dos veces bajo la muestra y mide el tiempo de extinción. Por otro lado, el calorímetro de cono utiliza un escenario de combustión forzada en el que el calor irradiado se proyecta en la muestra antes de la ignición y durante la combustión.

## 4.2 Objetivos

El objetivo del trabajo que se describe en este capítulo es estudiar el comportamiento de retardancia a la llama de algunos sistemas benzoxazina-epoxi utilizando la técnica del calorímetro de cono.

## 4.3

### Parte experimental y resultados

En este capítulo se expondrá la parte experimental y los resultados obtenidos al estudiar con el calorímetro de cono algunos de los sistemas termoestables obtenidos por copolimerización de la benzoxazina del bisfenol A y diglicidilos que contienen fósforo y silicio. El trabajo descrito en este capítulo ha sido aceptado para su publicación en *Polymer Degradation and Stability*. Los parámetros obtenidos mediante la calorimetría de cono han permitido correlacionar la influencia de la

estructura química sobre el comportamiento de retardancia a la llama del material.

---

---

*4.3.1. CONE CALORIMETRY STUDIES OF BENZOXAZINE-EPOXY  
SYSTEMS FLAME RETARDED BY CHEMICALLY BONDED  
PHOSPHORUS OR SILICON*

---

---

UNIVERSITAT ROVIRA I VIRGILI  
RESINAS EPOXI Y BENZOXAZINAS FOSFORADAS Y SILILADAS RETARDANTES A LA LLAMA  
Marisa Elisabet Spontón  
ISBN:978-84-691-9480-5/DL:T-22-2009



**CONE CALORIMETRY STUDIES OF BENZOXAZINE-EPOXY  
SYSTEMS FLAME RETARDED BY CHEMICALLY BONDED  
PHOSPHORUS OR SILICON.**

**M. Spontón, J.C. Ronda, M. Galià, V. Cádiz**

Departament de Química Analítica i Química Orgànica. Universitat Rovira I  
Virgili. Campus Sescelades Marcel·lí Domingo s/n. 43007 Tarragona. Spain.  
marina.galia@urv.cat

**ABSTRACT**

The combustion behaviour of phosphorus- and silicon-containing benzoxazine-epoxy systems has been studied by LOI and cone calorimetry giving a clear evidence that incorporation of 3.5% P into the benzoxazine-epoxy systems resulted in flame retardation while the silicon-containing copolymer was found to have no improvement in the LOI and cone calorimeter data, with values similar to the polymers without heteroatom, thus indicating that the 3.9% silicon content has no flame retarding effect. The peak of heat release rate value is reduced significantly for the phosphorus-containing benzoxazine as a result of a combination of condensed-phase and gas-phase mechanisms. The incorporation of phosphorus or silicon into the modified benzoxazine-epoxy system increases the smoke hazard and the CO emissions compared to the heteroatom-free system.

**Keywords:** Flame retardance, Cone calorimetry, LOI, Benzoxazine, Epoxy

Polymer Degradation and Stability 2008, In press.

## INTRODUCTION

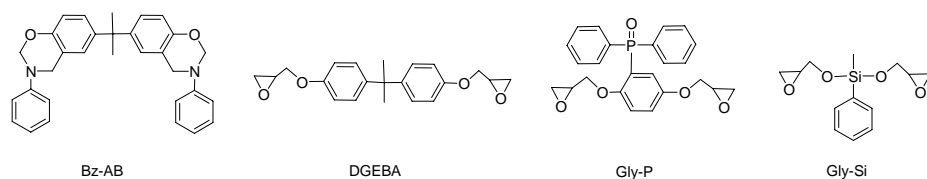
During the last decades much work has been concentrated on developing new flame-retardant materials with high performance for applications such as, electronic and aerospace industries. These must exhibit high glass transition temperature, low internal stress, good adhesion, low constant dielectric, low toxicity and high flame retardancy. The bromine-containing epoxy, are found among the most used polymers in the manufacture of electronic devices. However, the bromine-containing advanced epoxy resin release hydrogen bromide, dibenzo-*p*-dioxin and dibenzo-furan during combustion, which cause corrosion and toxicity. The concept of sustainable development requires fire retardant technologies to be developed, which have minimum impact on health and the environment through out the life cycle of the fire-retardant materials: that is to say, its synthesis, fabrication, use recycling, and disposal. The incorporation of phosphorus or silicon functionality in the polymeric structure is recognized as one of the most efficient ways to obtain an environmentally friendly flame retardant system.<sup>1</sup>

We have published a number of papers concerned with the behaviour of flame-retardant phosphorus<sup>2</sup>-, silicon<sup>3</sup>-, and phosphorus/silicon<sup>4</sup>-containing resins. These resins were obtained by copolymerisation of a variety of monomers containing covalently bonded phosphorus and silicon. The organophosphorus fire retardants mainly act as intumescent flame retardants resulting in a char layer in the condensed phase, which can produce less toxic gas and smoke compared with halogen-containing FRs.<sup>5,6</sup> Besides, phosphorus can also act in the gas phase as a catalytic radical scavenger.<sup>7</sup> Silicon-containing polymers were described to degrade forming thermally stable silica, which has the tendency to migrate to the char surface

serving as a protection layer to prevent further degradation of char at high temperatures.<sup>8</sup>

As a consequence of the complex nature and poor reproducibility of fire, there are many techniques for estimating the flammability of polymeric materials. Each technique concentrates on certain characteristic of the complex combustion process, for example, the ease of ignition of the material, the flame propagation, and heat release rate. Different tests have been developed and standardised by the International Standards Organisation. The most widely used laboratory test is the limiting oxygen index (LOI) ASTM-D-2683 technique. In recent years, also one of the most important instruments in this field is the cone calorimeter,<sup>9</sup> to measure the ignitability, heat release rate, total heat released, effective heat of combustion, specific extinction area, mass loss rate, and evolution of CO<sub>2</sub>, CO, and other combustion products with controlled-atmosphere.

In this paper we investigate the combustion behaviour of thermosetting resins obtained by copolymerizing benzoxazine of Bisfenol A and the previously reported phosphorus- and silicon-containing glycidyl derivatives (Scheme 1).<sup>2,3,10</sup> The phosphorus-containing systems investigated by us showed very good results of flame retardance, even when the phosphorus content was low, and no significant differences with the phosphorous content were observed. It has to be pointed out the outstanding LOI values obtained. However, the presence of silicon had no significant effect in the flame retardant behaviour, and the LOI values of silicon-containing resins were similar to those of heteroatom-free resins. This paper reports the results of cone calorimetry studies of these phosphorus- and silicon-containing benzoxazine-epoxy systems.



Scheme 1.

## EXPERIMENTAL

### Materials

Diglycidyl ether of bisphenol A (DGEBA) Eq. Epoxy (E.E= 192 g/eq) and diaminodiphenylmethane (DDM) were purchased from Aldrich. Benzoxazine derivative of bisphenol A was obtained from Shikoku Chemicals. Diglycidyl ether of (2,5-dihydroxyphenyl)diphenyl phosphine oxide (Gly-P) was obtained from (2,5-dihydroxyphenyl)diphenyl phosphine oxide by reaction with epichlorohydrin and BTMA as catalyst as has been previously described.<sup>2</sup>

Diglycidyl ether of methylphenyl silane (Gly-Si) was obtained from methylphenyl silane by reaction with glycidol and the Wilkinson catalyst.<sup>10</sup> Solvents were purified by standard procedures.

### Crosslinking reaction

Samples were prepared by the dissolution of benzoxazine and epoxy monomers in  $\text{CH}_2\text{Cl}_2$ . Then solution was evaporated at room temperature in vacuum. Moulded cured benzoxazine-epoxy resins (table 1) were prepared with a manual hydraulic press 15-ton sample pressing (SPECAC) equipped with a water cooled heated platens. The mixture was placed in a  $50 \times 50 \times 1.9 \text{ mm}^3$  or  $70 \times 6 \times 3 \text{ mm}^3$  moulds and compression moulded at  $180 \text{ }^\circ\text{C}$  for

3h under 0.1 mPa. Post-curing was carried out at 220 °C for 3h under the same pressure conditions.

#### **LOI measurements (LOI-ASTM-D-2863)**

These were performed on a Stanton Redcroft FTA flammability unit provided with an Oxygen Analyzer. Sample sizes measured 70 x 6 x 3 mm<sup>3</sup> and were prepared by moulding.

#### **Cone calorimetry**

The combustion behaviour was investigated using Fire Testing Technology cone calorimeter (according to ISO 5660) with specimen. Cone calorimeter was used under ventilated conditions including time to ignition (TTI), rate of heat release (HRR), the maximum rate of heat release (PHRR), smoke density, carbon monoxide and carbon dioxide evolution. The heat flux used was 50 kW/m<sup>2</sup> on the specimen, which had an exposed surface area of 50 mm × 50 mm. Edge burning effects were reduced by covering the non-exposed sample surface in heavy duty aluminium foil. The device consisted of a radiant electric heater in a trunk-conic shape, an exhaust gas system with oxygen monitoring and instrument to measure the gas flux, an electric spark for ignition, and a load cell to measure the weight loss. All tests were terminated after 600 s of exposure. TTI measures the time to achieve sustained flaming combustion for a given cone irradiance. Smoke density was measured by the decrease in transmitted light intensity of a helium–neon laser beam photometer, and expressed in terms of specific extinction area (SEA), with units of m<sup>2</sup>/kg. The experiments were repeated three times.

### **Thermogravimetric Analysis (TGA)**

Dynamic thermogravimetric studies was used to investigate the behaviour in an oxidative and non-oxidative environment using a Mettler TGA/SDTA851e/LF/1100 instrument. For both air and nitrogen atmospheres a flow rate of 50ml/min was used. Samples of 15-20 mg were placed in the crucible and heated from 50 °C to 800 °C at a constant heating rate of 10 °C /min.

## **RESULTS AND DISCUSSION**

Benzoxazine-epoxy systems have been prepared by curing DGEBA, phosphorus- and silicon-containing glycidyl compounds in equimolar amounts with Bz-BA.<sup>10</sup> Conventional epoxy resin has been prepared by curing DGEBA with stoichiometric amount of DDM with the purpose of comparison (Table 1). The flammability of these new benzoxazine-epoxy systems has been assessed by the LOI test and the results are given in Table 1. As can be seen the pure benzoxazine system Bz-BA exhibits a higher LOI value than epoxy system, as an indicator of its higher flame retardance. When benzoxazine is copolymerised with DGEBA the LOI value results similar without detriment to the polymer flammability and with an improvement of the physical and mechanical properties. The results show that the incorporation of just 3.5% phosphorus significantly increases the LOI value to 48. However, the silicon-containing copolymer was found to have no improvement in the LOI, with a value similar to the polymers without heteroatom, thus indicating that the 3.9% silicon content has no flame retarding effect.

Whilst the LOI is a useful small-scale test for flame retardance polymer the cone calorimeter provides a wealth of information on the combustion behaviour under ventilation conditions. The cone calorimeter is one of the most effective bench-scale methods for studying the flammability of materials. Typically, the subject material is irradiated with a heat intensity similar to that experienced in a fire situation (25-75kW/m<sup>2</sup>). This method enables investigations with respect to heat release rate (HRR), total heat release (THR), mass loss rate (MLR), time to ignition (TTI), specific extinction area (SEA), maximum average rate of heat emission (MARHE), CO and CO<sub>2</sub> emissions and mass loss during combustions.<sup>11</sup> These parameters are reported in table 1, 2 and 3 for different samples at an external heat flux of 50 K Wm<sup>-2</sup>.

Time to ignition TTI is used to determine the influence on ignitability, which can be measured from the onset on an HRR curve. The time to ignition shows clear differences in the ignition behaviour of the different samples. Ignition occurs when the mass loss rate produces sufficient volatiles whose effective heat of combustion make a gas mixture capable of being ignited by a spark. Ignition does not directly correspond to flammability measured by LOI since this is an extinction test and good correlations between both measurements are not expected. DGEBA-containing polymers (samples 1 and 3) have improved times to sustained ignition, as compared to the other benzoxazine systems which ignited at about 23 s. The presence of DGEBA appears to be a significant factor in the ignition time.

**Table 1.** Cone calorimeter data.

| Samples | Resins       | LOI  | TTi (s) | HRR <sub>peak</sub> (kW/m <sup>2</sup> ) | THR (MJ/m <sup>2</sup> ) | THR/TML (MJ/m <sup>2</sup> ) | MAHRE (kW/m <sup>2</sup> ) | FIGRA (kW/m <sup>2</sup> s) |
|---------|--------------|------|---------|--|--------------------------|------------------------------|----------------------------|-----------------------------|
| 1       | DGEBA/DDM    | 24.4 | 33      | 732                                      | 66                       | 6.0                          | 301                        | 6.9                         |
| 2       | Bz-BA        | 31.8 | 23      | 628                                      | 56                       | 6.3                          | 258                        | 7.5                         |
| 3       | BzBA/DGEBA   | 32.2 | 31      | 556                                      | 47                       | 5.5                          | 213                        | 6.4                         |
| 4       | Bz-BA/Gly-P  | 48.0 | 23      | 370                                      | 36                       | 4.1                          | 174                        | 4.2                         |
| 5       | Bz-BA/Gly-Si | 32.4 | 21      | 536                                      | 49                       | 6.5                          | 232                        | 6.5                         |

The heat release rate (HRR) versus time curves for the different systems are presented in Fig. 1. Practically, the heat release rate for low applied heat flux corresponds roughly with LOI results. In our case the LOI values increase as the heat release rates decrease.

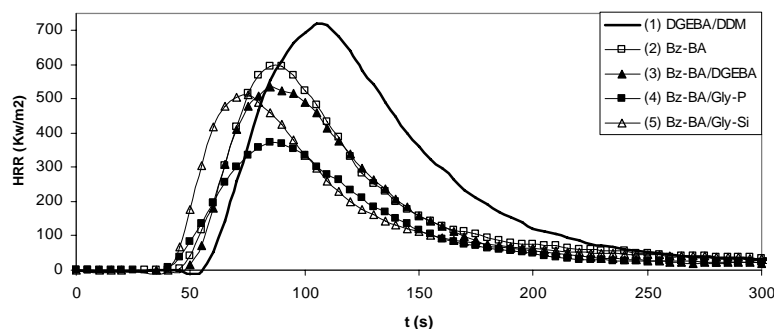


**Figure 1.** Heat Release Rate (HRR) versus time curves for the benzoxazine-epoxy systems.

The HRR curves showed a shape that is normally rather typical for non-charring samples of intermediate thickness. There is an initial increase in HRR up to a shoulder, followed by a dominant peak of HRR at the end of burning. The HRR of the DGEBA/DDM system is characterized by an intense peak, whereas the HRR of Bz-BA containing systems was reduced strongly. The HRR results provide a much better indication than do the LOI



values that benzoxazine copolymers show flame retardant behaviour. Their  $HRR_{peak}$  values are reduced, more significantly in the phosphorus-containing benzoxazine compared to the other resins. Further confirmation is provided for the total heat evolved (THR) by each polymer as given in Table 1.

The behaviour of the HRR for the phosphorus-containing systems arises from a combination of condensed-phase and gas-phase mechanisms as a result on the increased residue and the reduction in total heat evolved per total mass loss (THR/TML), respectively.<sup>12</sup> This last parameter is a measure for the effective heat of combustion of the volatiles, multiplied by the combustion efficiency during the cone calorimeter test. The THR/TML for our phosphorus-containing sample showed a reduction of around 40% in comparison to epoxy or heteroatom free benzoxazine system, which indicated a flame inhibition effect as a fire retardancy mechanism.

The Average Rate of Heat Emission (AHRE) curve is reported in Fig. 2. This parameter is defined as the cumulative heat emission divided by time and its peak value (Maximum Average Rate of Heat Emission, MAHRE) has recently been proposed as a good measure of the propensity for fire development under real scale conditions.<sup>13</sup> MAHRE for phosphorus-containing benzoxazine system (sample 4) (table 1) shows a notable reduction (about 40-50%) with respect to epoxy (sample 1) and heteroatom free benzoxazine system (sample 2). Similar behaviour can be found for benzoxazine-epoxy systems (samples 3 and 5) showing that the addition of epoxy to the benzoxazine does not exert a great influence in the MAHRE value and that the presence of silicon does not diminishes the propensity for fire development.

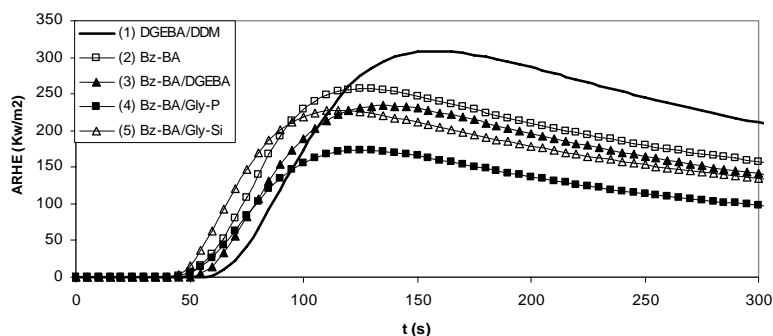


**Figure 2.** Average Rate of Heat Emission (AHRE) versus time curves for the benzoxazine-epoxy systems.

The Fire Growth Rate Index (FIGRA)<sup>14</sup> (Table 1) is calculated by dividing the peak heat release rate by time to peak heat release (TTPH), giving a unit of  $\text{kW}/\text{m}^2\text{s}$ , which can estimate both the predicted fire spread rate and the size of a fire. The higher the FIGRA, the faster the flame spread and flame growth are assumed to be.<sup>15,16</sup> The FIGRA of the materials ranges between 6 and 7  $\text{kW}/\text{m}^2\text{s}$  while that of the phosphorus-containing benzoxazine-epoxy system decreases to 4.2  $\text{kW}/\text{m}^2\text{s}$ , meaning that this system performs much better than the other studied systems.

Percentage mass loss curves obtained as a function of time from cone calorimeter test and thermogravimetry in air and nitrogen for the resins are presented in Fig. 3. The residual mass remaining after complete combustion in the cone calorimeter of DGEBA/DDM (sample 1) is negligible (Table 2). The benzoxazine-containing samples left a residual mass at the end of their test around 4% except the phosphorus-containing sample with a significant residual mass higher than 10%. This is due to the formation of carbonaceous char indicating a condensed phase mode as a flame retardant mechanism. This further supports the role of the mechanism being related to the

formation of a char layer, as these values correlate well with improvement in the peak heat release rate determined by cone calorimetry<sup>17</sup>.

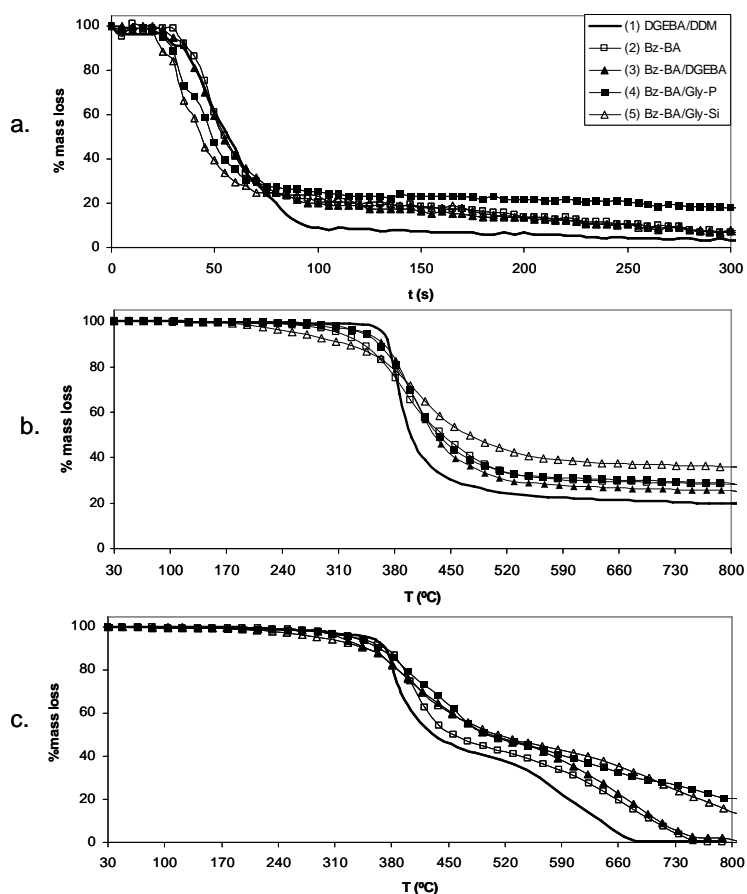


**Figure 3.** Percentage of mass loss curves for the benzoxazine-epoxy systems. **a.** Cone calorimeter, **b.** TGA data in nitrogen, **c.** TGA data in air.

Table 2 compares the char yields in nitrogen and air atmospheres obtained by thermogravimetric analysis with the residual masses after combustion in cone calorimetry for all the samples. The char yields at 800 °C both in nitrogen and air follow a different trend than cone calorimeter residues. While in nitrogen benzoxazine-containing systems showed an

enhanced char formation, in air this is true only for those heteroatom-containing systems. These results do not correlate with a previous described work which demonstrated a close relationship between cone calorimeter and TGA char yields in nitrogen atmosphere highlighting the anaerobic environment during combustion and the role of char formation in improving fire performance.<sup>18</sup>

**Table 2.** Residue from cone calorimeter and thermogravimetric tests.

| Samples | Resins       | Cone calorimeter (g/g) | Nitrogen                          |                         | Air                               |                         |
|---------|--------------|------------------------|-----------------------------------|-------------------------|-----------------------------------|-------------------------|
|         |              |                        | T <sub>5%</sub> <sup>a</sup> , °C | Char <sup>b</sup> , (%) | T <sub>5%</sub> <sup>a</sup> , °C | Char <sup>b</sup> , (%) |
| 1       | DGEBA/DDM    | 0                      | 351                               | 20                      | 341                               | 0                       |
| 2       | Bz-BA        | 4                      | 313                               | 30                      | 322                               | 0                       |
| 3       | BzBA/DGEBA   | 5                      | 341                               | 26                      | 340                               | 0                       |
| 4       | Bz-BA/Gly-P  | 11                     | 338                               | 30                      | 338                               | 20                      |
| 5       | Bz-BA/Gly-Si | 4                      | 291                               | 36                      | 291                               | 14                      |

<sup>a</sup>Temperature of 5 % weight loss.

<sup>b</sup>Char yield at 800 °C.

The weight loss curves obtained from cone calorimeter test are similar to those obtained from thermogravimetry in nitrogen but show differences with those obtained from thermogravimetry in air. On heating in a thermobalance at 10 °C /min in air, the resins present a two-step weight loss corresponding to two different degradation mechanisms whereas a single step is observed during the combustion test. This can be due to the different heating conditions during cone calorimeter test where a high heating rate and a high temperatures are reached.

Apart from the heat release characteristics the smoke and CO and CO<sub>2</sub> releases are important fire hazards. Smoke emission is caused by the evolution of the products of incomplete oxidation. Due to their aromatic

structure, benzoxazine-epoxy systems evolve large amounts of smoke. The rate of smoke emission, indicated by the specific extinction area (SEA) is similar for epoxy and benzoxazine systems and decrease for the benzoxazine-epoxy system (Table 3). The incorporation of phosphorus or silicon into the modified benzoxazine-epoxy system increases the smoke hazard compared to the heteroatom-free system resulting the presence of phosphorus in a very significant increase in smoke production during combustion.

**Table 3.** Smoke, CO and CO<sub>2</sub> releases.

| Samples | Total smoke release (m <sup>2</sup> /m <sup>2</sup> ) | SEA <sub>Av</sub> (m <sup>2</sup> /Kg) | CO (Kg/Kg) | CO <sub>2</sub> (Kg/Kg) |
|---------|---|--|------------|-------------------------|
| 1       | 3003  | 1051                                   | 0.14       | 2.4                     |
| 2       | 2307  | 1021                                   | 0.22       | 3.8                     |
| 3       | 1929  | 858                                    | 0.17       | 3.0                     |
| 4       | 2790  | 1276                                   | 0.29       | 2.1                     |
| 5       | 1844  | 920                                    | 0.19       | 3.64                    |

Both CO and CO<sub>2</sub> production often indicate the fire retardancy mechanism. Flame inhibition results in an increase in combustion products typical for incomplete combustion, in particular CO, whereas increased charring bears the potential decrease of the absolute CO production due to an unchanged yield and a reduced mass loss. The temporal behaviour of the CO evolution rate during the cone calorimetry experiments is shown in Fig. 4. Heteroatom-free samples evolved similar CO amounts at a similar rates and the phosphorus-containing sample evolved more CO amount at a faster rate. This could indicate that the chemical incorporation of phosphine oxide into the resins has a more effective flame retardant effect in the vapour phase. The silicon-containing sample evolved less CO amount at a lower

rate, according a condensed phase action. The charring induced in this silicon-containing sample seems not influence HRR and THR.

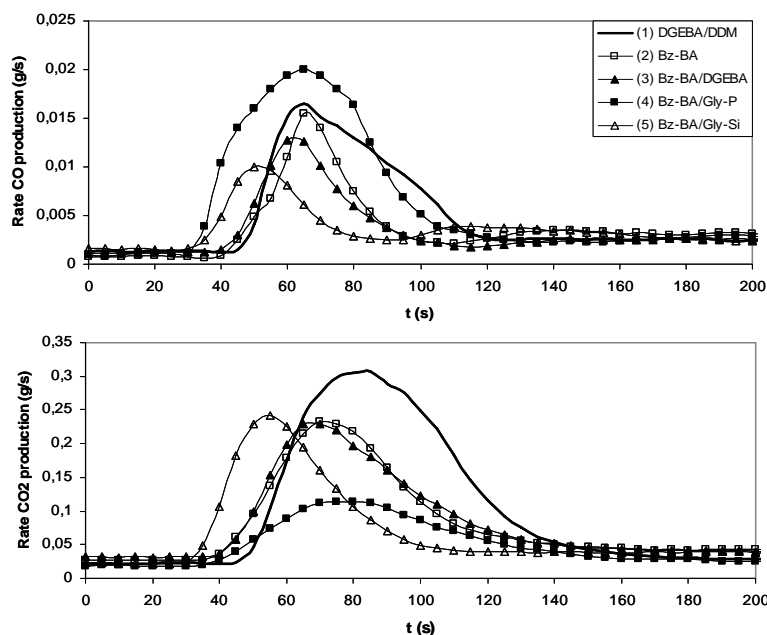


Figure 4. CO and CO<sub>2</sub> evolution versus time for the benzoxazine-epoxy systems.

## CONCLUSIONS

Within this work we presented a detailed study on the fire behaviour of the phosphorus- and silicon-containing benzoxazine-epoxy systems. Cone calorimetry experiments gave much clearer evidence than did the LOI measurements that incorporation of 3.5% P into the benzoxazine-epoxy systems resulted in flame retardation. DGEBA-containing polymers have improved times to sustained ignition as compared to the benzoxazine systems. The peak of heat release rate value is reduced significantly for the phosphorus-containing benzoxazine. This behaviour arises from a

combination of condensed-phase and gas-phase mechanisms as a result on the increased residue and the reduction of around 40% in total heat evolved per total mass loss (THR/TML), respectively. According to these results, MAHRE and FIGRA show a notable reduction meaning that this phosphorus-containing system perform much better than the other studied systems. The formation of carbonaceous char in cone calorimeter test and thermogravimetry indicates a condensed phase mode as a flame retardant mechanism, according to the formation of a char layer.

The incorporation of phosphorus or silicon into the modified benzoxazine-epoxy system increases the smoke hazard and the CO emissions compared to the heteroatom-free system, resulting the presence of phosphorus in a very significant increase in smoke production during combustion. This could indicate that the chemical incorporation of phosphine oxide into the resins has a more effective flame retardant effect in the vapour phase. The silicon-containing sample evolved less CO amount at a lower rate, according a condensed phase action. The charring induced in this silicon-containing sample seems not influence HRR and THR.

## REFERENCES

- <sup>1</sup> Lu SY, Hamerton Y. Recent developments in the chemistry of halogen-free flame retardant polymers. *Prog Polym Sci* 2002;27:1661-712
- <sup>2</sup> Spontón M, Ronda JC, Galià M, Cádiz V. Flame retardant epoxy resins based on diglycidyl ether of (2,5-dihydroxyphenyl) diphenyl phosphine oxide. *J Polym Sci Part A: Polym Chem* 2007;45:2142-51.
- <sup>3</sup> Mercado LA, Reina JA, Galià M. Flame retardant epoxy resins based on diglycidyl oxymethyl phenylsilane. *J Polym Sci Part A: Polym Chem* 2006;44:5580-7.
- <sup>4</sup> Spontón M, Mercado LA, Ronda JC, Galià M, Cádiz V. Preparation, thermal properties and flame retardancy of phosphorus- and silicon-containing epoxy resins. *Polym Degrad Stab* 2008;in press.
- <sup>5</sup> Levchik SV, Weil ED. Thermal decomposition, combustion and flame-retardancy of epoxy resins – a review of the recent literature. *Polym Int* 2004;53:1901-29.

- <sup>6</sup> Levchik SV, Piotrowski A, Weil ED, Yao Q. New developments in flame retardancy of epoxy resins. *Polym Degrad Stab* 2005;88:57-62.
- <sup>7</sup> Braun U, Balabanovich AI, Scharrel B, Knoll U, Artner J, Ciesielski M, Döring M, Perez R, Sandler JKW, Altstädt V, Hoffmann T, Pospiech D. Influence of the oxidation state of phosphorus on the decomposition and fire behaviour of flame-retarded epoxy resin composites. *Polymer* 2006;47:8495-508.
- <sup>8</sup> Kashiwagi T, Gilman JW. In: Grand AF, Wilkie CA, editors. *Fire retardancy of polymeric materials*. New York: Marcel Dekker Inc.; 2000. p. 353-89
- <sup>9</sup> Scharrel B, Hull TR. Development of fire-retarded materials - Interpretation of cone calorimeter data. *Fire Mater* 2007;31:327-54.
- <sup>10</sup> Spontón M, Ronda JC, Galià M, Cádiz V. Development of flame retardant phosphorus-silicon-containing polybenzoxazine-epoxy systems. *Eur Polym J*. Submitted.
- <sup>11</sup> Price D, Bullett KJ, Cunliffe LK, Hull TR, Milnes GJ, Ebdon JR, Hunt BJ, Joseph P. Cone calorimetry studies of polymer systems flame retarded by chemically bonded phosphorus. *Polym Degrad Stab* 2005;88:74-9.
- <sup>12</sup> Scharrel B, Braun U, Balabanovich AI, Artner J, Ciesielski M, Döring M, Perez RM, Sandler JKW, Altstädt V. Pyrolysis and fire behaviour of epoxy systems containing a novel 9,10-dihydro-9-oxa-10-phosphaphenanthrene-10-oxide- (DOPO)-based diamino hardener. *Eur Polym J* 2008;44:704-15.
- <sup>13</sup> Duggan GJ, Grayson SJ, Kumar S. *New fire classifications and fire test methods for the European railway industry, Flame retardants 2004*. London: Interscience Communications; 2004.
- <sup>14</sup> Gao L-P, Wang D-Y, Wang Y-Z, Wang J.S, Yang B. A flame-retardant epoxy resin based on a reactive phosphorus-containing monomer of DODPP and its thermal and flame-retardant properties. *Polym Degrad Stab* 2008;93:1308-15.
- <sup>15</sup> Messerschmidt B, Hees PV. Influence of delay times and response times on heat release measurements. *Fire Mater* 2000;24:121-30.
- <sup>16</sup> Nazaré S, Kandola B, Horrocks RA. Use of cone calorimetry to quantify the burning hazard of apparel fabrics. *Fire Mater* 2002;26:191-9.
- <sup>17</sup> Liu W, Varley RJ, Simon GP. Understanding the decomposition and fire performance processes in phosphorus and nanomodified high performance epoxy resins and composites. *Polymer* 2007;48:2345-54.
- <sup>18</sup> Lyon RE. Heat release kinetics. *Fire Mater* 2000;24:179-86.



## CONCLUSIONES

- Se ha obtenido un nuevo diglicidilo fosforado: el diglicidiléter del óxido de (2,5-dihidroxifenil) difenil fosfina (Gly-P), dos diglicidilos sililados: el diglicidiloxifenilmetilsilano (Gly-Si) y el 1,4-bis(glicidiloxidimetil silil) benceno, una amina fosforada: el óxido de bis(3-aminofenil)metil fosfina (BAMPO) y otra sililada: la bis(4-aminofenoxi)dimetil silano.
- A partir de los monómeros anteriores se han desarrollado nuevos sistemas epoxi-amina con diferentes proporciones de fósforo y/o silicio. Todos ellos mostraron buenas propiedades térmicas y de retardancia a la llama sin que en esta última se observara efecto sinérgico para las resinas con fósforo y silicio.
- Se ha obtenido una nueva benzoxazina derivada de la diamina aromática fosforada BAMPO siguiendo un método sintético en tres etapas, a través de un intermedio imina, como alternativa al método convencional. Mediante técnicas calorimétricas y espectroscópicas se ha detectado la formación de puentes metileno fenólicos y arilamina y puentes de Manich arilamina como reacciones secundarias en el entrecruzamiento térmico.
- La benzoxazina derivada del BAMPO fue copolimerizada con la benzoxazina derivada del bisfenol A y con diglicidiléter de bisfenol A obteniendo distintos sistemas benzoxazina y benzoxazina-epoxi

con diferentes proporciones de fósforo. La presencia del fósforo, incluso en proporciones bajas (alrededor de un 2%), condujo a una mejora en la retardancia a la llama, significativamente más importante para los sistemas benzoxazina-epoxi.

- Se han desarrollado nuevos sistemas benzoxazina-epoxi con diferentes proporciones de fósforo y silicio, que fueron obtenidos por copolimerización de la benzoxazina de bisfenol A con Gly-P y Gly-Si. Todos los sistemas mostraron buenas propiedades retardantes a la llama si bien para los que contienen fósforo se obtuvieron valores del índice limitante de oxígeno excepcionalmente elevados, demostrando el efecto beneficioso de este heteroátomo en la retardancia a la llama.
- La técnica de calorimetría de cono permitió observar el importante efecto que supone la incorporación de fósforo en sistemas benzoxazina-epoxi sobre la retardancia a la llama, de acuerdo con la combinación de un mecanismo de actuación en fase condensada y en fase gas. La presencia de silicio no ejerce la misma influencia en este tipo de sistemas.
- La incorporación de fósforo o silicio en el sistema benzoxazina-epoxi incrementa las emisiones de CO y humos durante la combustión, especialmente en el caso del fósforo, comparado con los sistemas libres de heteroátomos.

# APÉNDICE A

## LISTA DE ABREVIATURAS:

**APDS:** Bis(4-aminofenoxi) dimetilsilano

**BAMPO:** Óxido de bis(*m*-aminofenil)metilfosfina.

**BGDMSB:** 1,4-Bis(glicidiloxidimetilsilil)benceno

**BTMA:** Cloruro de benciltrimetilamonio

**Bz-BA:** Benzoxazina derivada de bisfenol A

**Bz-BAMPO:** Benzoxazina derivada del óxido de bis(*m*-aminofenil)metilfosfina

**DDM:** 4,4' diaminodifenilmetano

**DGEBA:** Diglicidiléter de bisfenol A.

**DGMPS o Gly-Si:** Diglicidiloxifenilmetilsilano

**DOPO:** Óxido de 10(9,10-dihidro-9-oxa-10-fosfafenantreno)

**Gly-HPO o Gly-P:** Diglicidiléter del óxido de (2,5-dihidroxifenil) difenil fosfina

**HPO:** Óxido de (2,5-dihidroxifenil)difenil fosfina

**IHPO:** Óxido de isobutil bis(hidroxipropil)fosfina

**IHPO Gly:** Óxido de isobutil bis(glicidilpropil éter)fosfina

**LOI:** Índice de Oxígeno Limitante

UNIVERSITAT ROVIRA I VIRGILI  
RESINAS EPOXI Y BENZOXAZINAS FOSFORADAS Y SILILADAS RETARDANTES A LA LLAMA  
Marisa Elisabet Spontón  
ISBN:978-84-691-9480-5/DL:T-22-2009

## APÉNDICE B

### LISTA DE PUBLICACIONES.

- Flame retardant epoxy resins based on diglycidyl ether of (2,5-dihydroxyphenyl)diphenyl phosphine oxide  
M. Spontón, J.C. Ronda, M. Galià, V. Cádiz  
J Polym Sci: Part A: Polym Chem. 2007: 45: 2142
- Preparation, thermal properties and flame retardancy of phosphorus- and silicon-containing epoxy resins  
M. Spontón, L. A. Mercado, J.C. Ronda, M. Galià, V. Cádiz  
Polym Degrad Stab. DOI 10.1016/j.polymdegradstab.2008.02.014
- Synthesis and study of the thermal crosslinking of bis(*m*-aminophenyl) methylphosphine oxide based benzoxazine.  
M. Spontón, M. S. Larrechi, J.C. Ronda, M. Galià, V. Cádiz  
J Polym Sci: Part A: Polym Chem. 2008: 46: 7162
- Studies on thermal and flame retardant behaviour of mixtures of bis(*m*-aminophenyl)methylphosphine oxide based benzoxazine and glycidylether or benzoxazine of bisphenol A.  
M. Spontón, M. J. C. Ronda, M. Galià, V. Cádiz  
Polym Degrad Stab. DOI:10.1016/j.polymdegradstab.2008.08.004

- Development of flame retardant phosphorus- and silicon-containing polybenzoxazines.  
M. Spontón, J.C. Ronda, M. Galià, V. Cádiz  
European Polymer Journal, 2008, Submitted for publication.
  
- Cone calorimetry studies of benzoxazine-epoxy systems flame retarded by chemically bonded phosphorus or silicon.  
M. Spontón, J.C. Ronda, M. Galià, V. Cádiz  
Polym Degrad Stab. 2008, In press.